



# Particle Detectors

*Lecture at the African School for Fundamental Physics and Applications,  
July 2024  
Marrakesh, Morocco*

*Lecture IV*

**Advanced detectors and  
some new developments**

(c) CERN. All rights reserved.

# Particle Detectors

*Lecture at the African School for Fundamental Physics  
Marrakesh, Morocco, July 2024*

**Goal this lecture:**

**to discuss some examples**

**Looking at recent technological developments**

**infinite number of ideas for new detectors**

## Lecture IV

- LHC detectors
- Recent developments of CMOS pixel detectors
- Fast detectors for time of flight measurements
- High granularity calorimeters
- High purity segmented Ge-detectors for Nuclear physics
- A glimpse at cryogenic detectors for particle and astrophysics

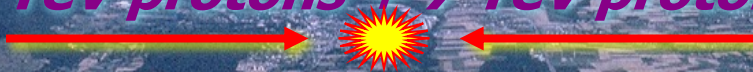
***Don't forget the Exercises!!!!***



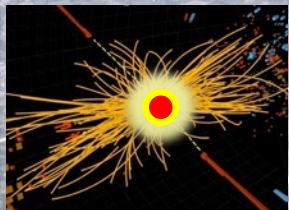
# The LHC

Large Hadron Collider

7 TeV protons + 7 TeV protons



CMS



Large Hadron Collider

- Proton beams circulate 11,245 times/sec
- 100's of millions of proton-proton collisions/second
- 65 pp collisions every 25 ns
- new particles are created ( $E = mc^2$ )



# The LHC

Large Hadron Collider

7 TeV protons + 7 TeV protons

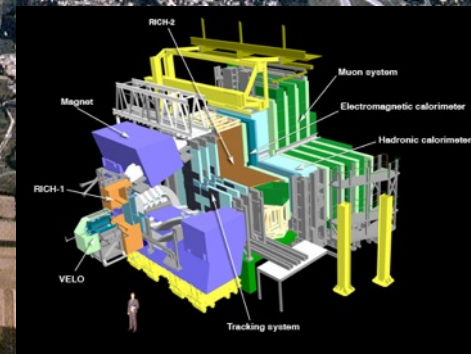


**CMS**

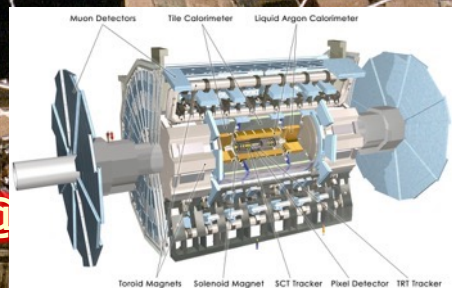


Large Hadron Collider

- Protons circulate 11,245 times/sec
- 100's of millions of proton-proton collisions/second
- 65 pp collisions every 25 ns
- new particles are created ( $E = mc^2$ )



**ALICE**



Center

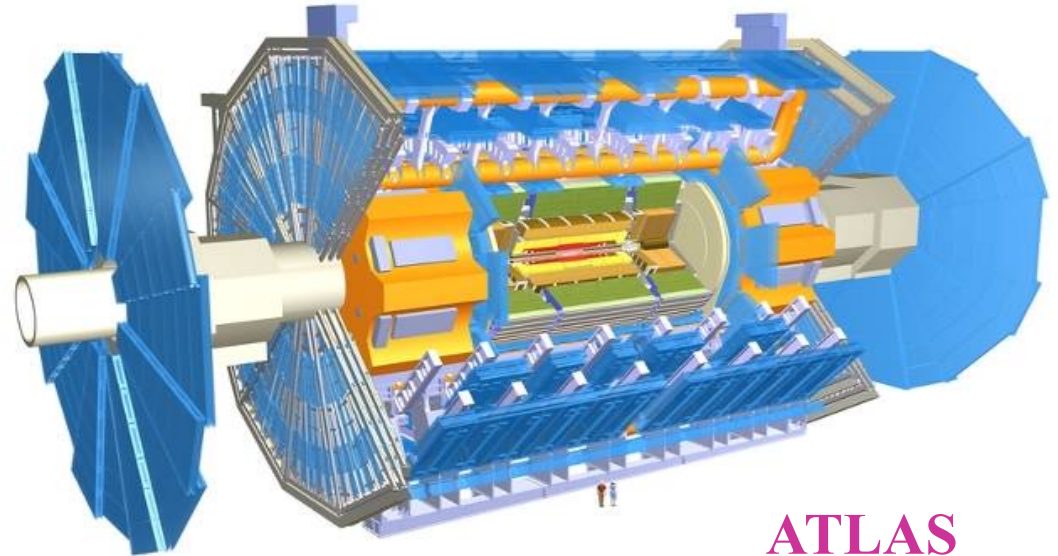
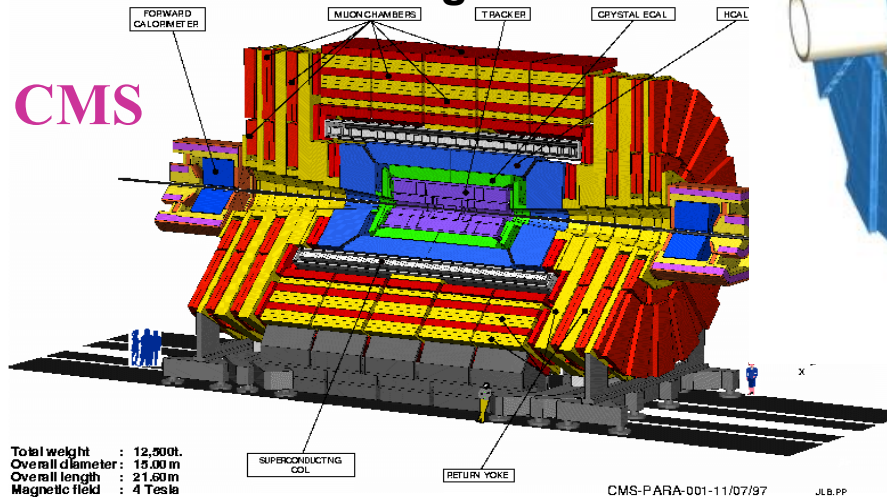
CMS Centre @





## How huge are ATLAS and CMS?

ATLAS superimposed to  
the 5 floors of building 40

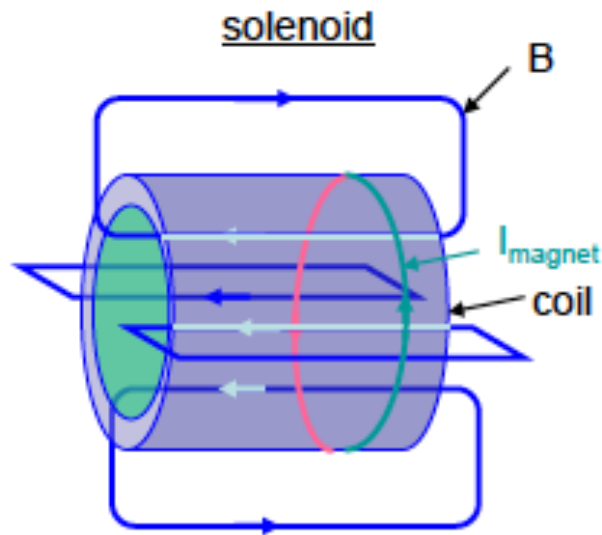


ATLAS

	<u>ATLAS</u>	<u>CMS</u>
Overall weight (tons)	7000	12500
Diameter	22 m	15 m
Length	46 m	22 m
Solenoid field	2 T	4 T



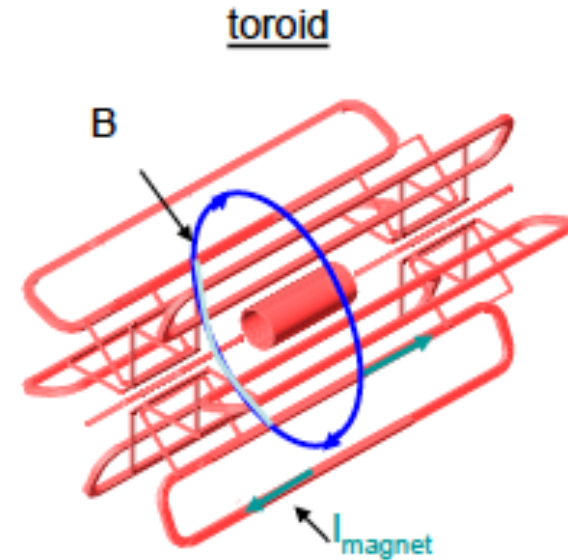
## Magnetic field configurations:



- + Large homogenous field inside coil
- weak opposite field in return yoke
- Size limited (cost)
- rel. high material budget

## Examples:

- DELPHI (SC, 1.2T)
- L3 (NC, 0.5T)
- CMS (SC, 4T)

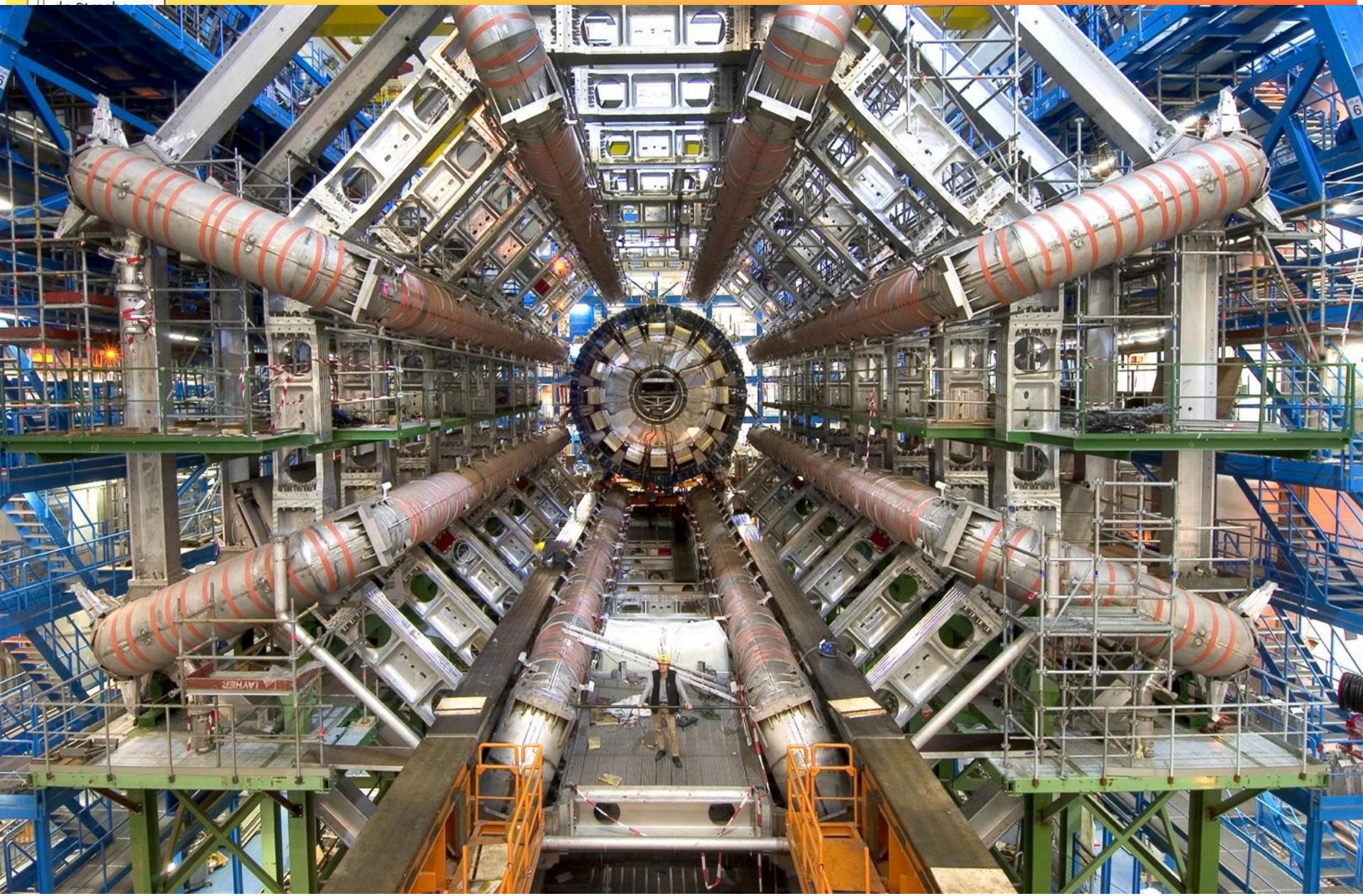


- + Rel. large fields over large volume
- + Rel. low material budget
- non-uniform field
- complex structure

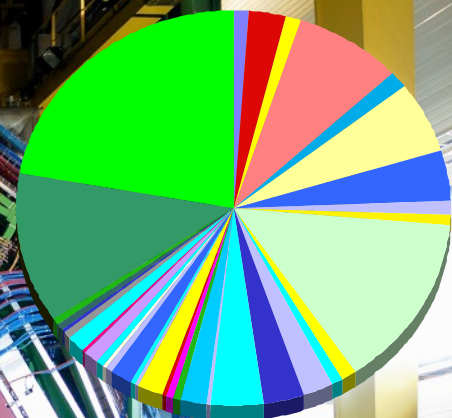
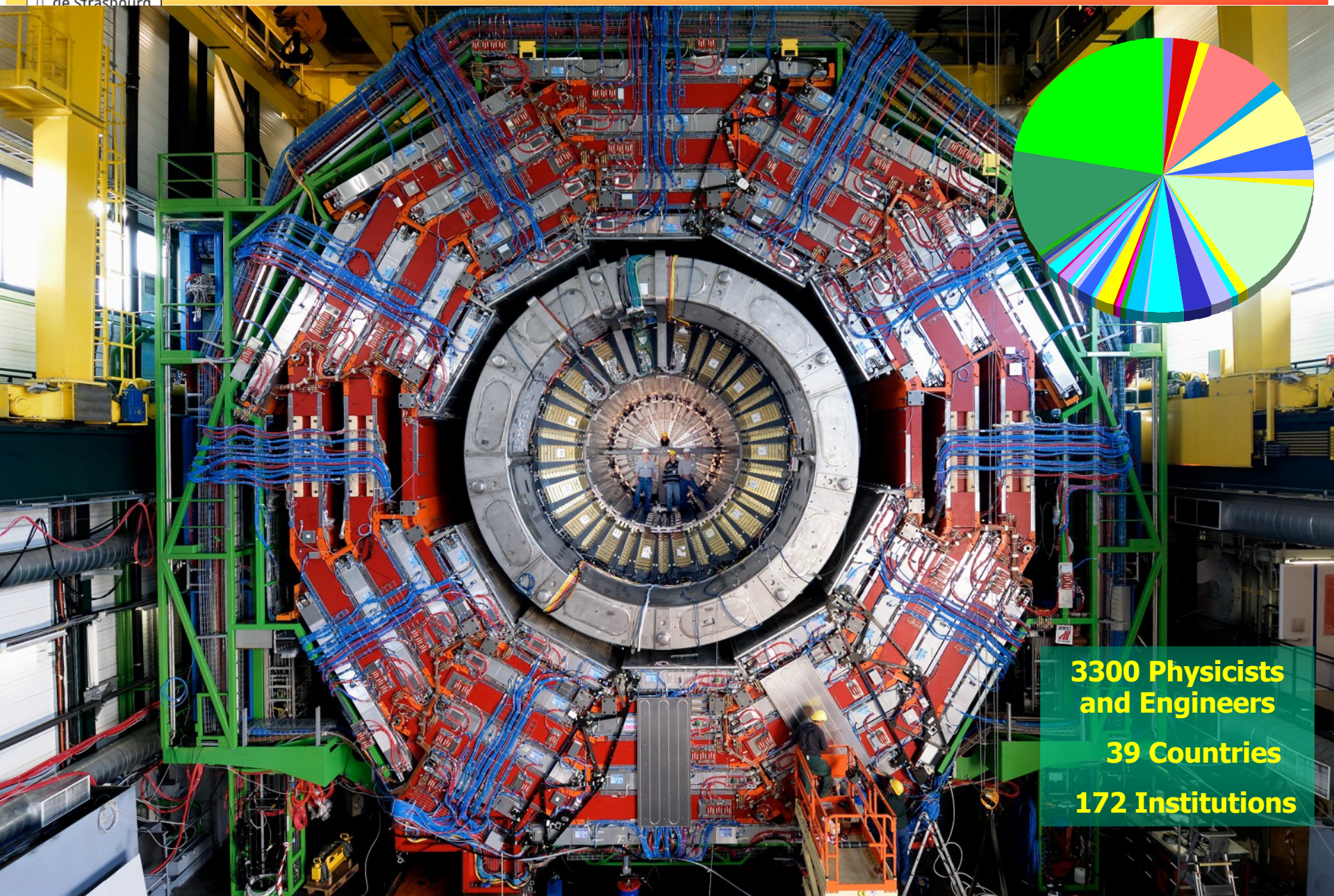
## Example:

- ATLAS (Barrel air toroid, SC, 0.6T)





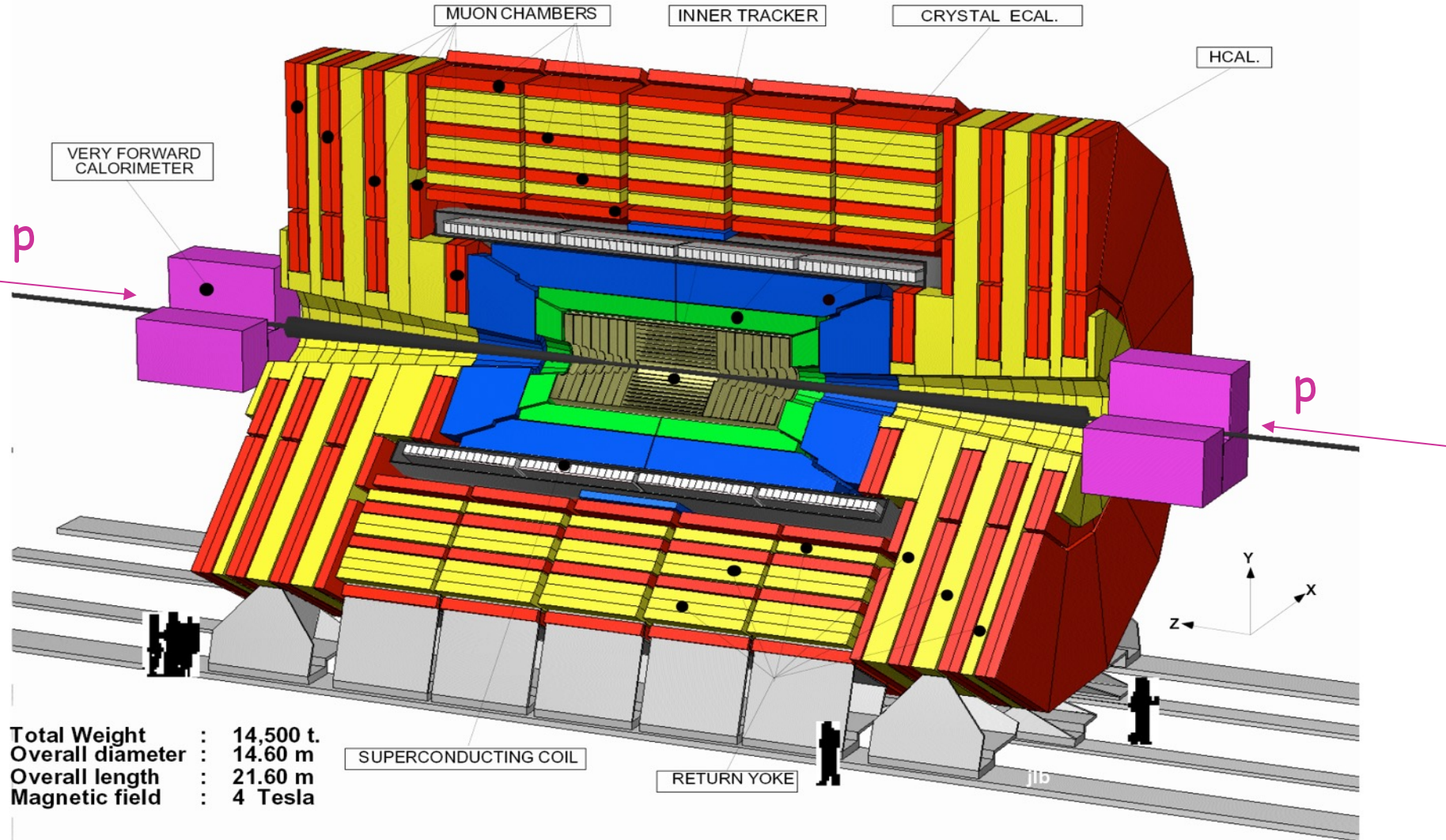




**3300 Physicists  
and Engineers**  
**39 Countries**  
**172 Institutions**



# Compact Muon Solenoid





# CMS

## MUON ENDCAPS

473 Cathode Strip Chambers (CSC)  
 432 Resistive Plate Chambers (RPC)

## IRONYOKE

**Preshower**  
 Si Strips  $\sim 16 \text{ m}^2$   
 $\sim 137\text{k}$  ch

**Forward Cal**  
 Steel + quartz  
 Fibers  $2\sim\text{k}$  ch

## 3.8T Solenoid

**HCAL** Scintillator/brass  
 Interleaved  $\sim 7\text{k}$  ch

**ECAL** 76k scintillating  
 $\text{PbWO}_4$  crystals

YBO

YB1-2

YE1-3

## MUON BARREL

250 Drift Tubes (DT) and  
 480 Resistive Plate Chambers (RPC)

## Pixels & Tracker

- Pixels ( $100 \times 150 \mu\text{m}^2$ )  
 $\sim 1 \text{ m}^2 \sim 66\text{M}$  ch
- Si Strips ( $80\text{-}180 \mu\text{m}$ )  
 $\sim 200 \text{ m}^2 \sim 9.6\text{M}$  ch

Pixel  
 Tracker

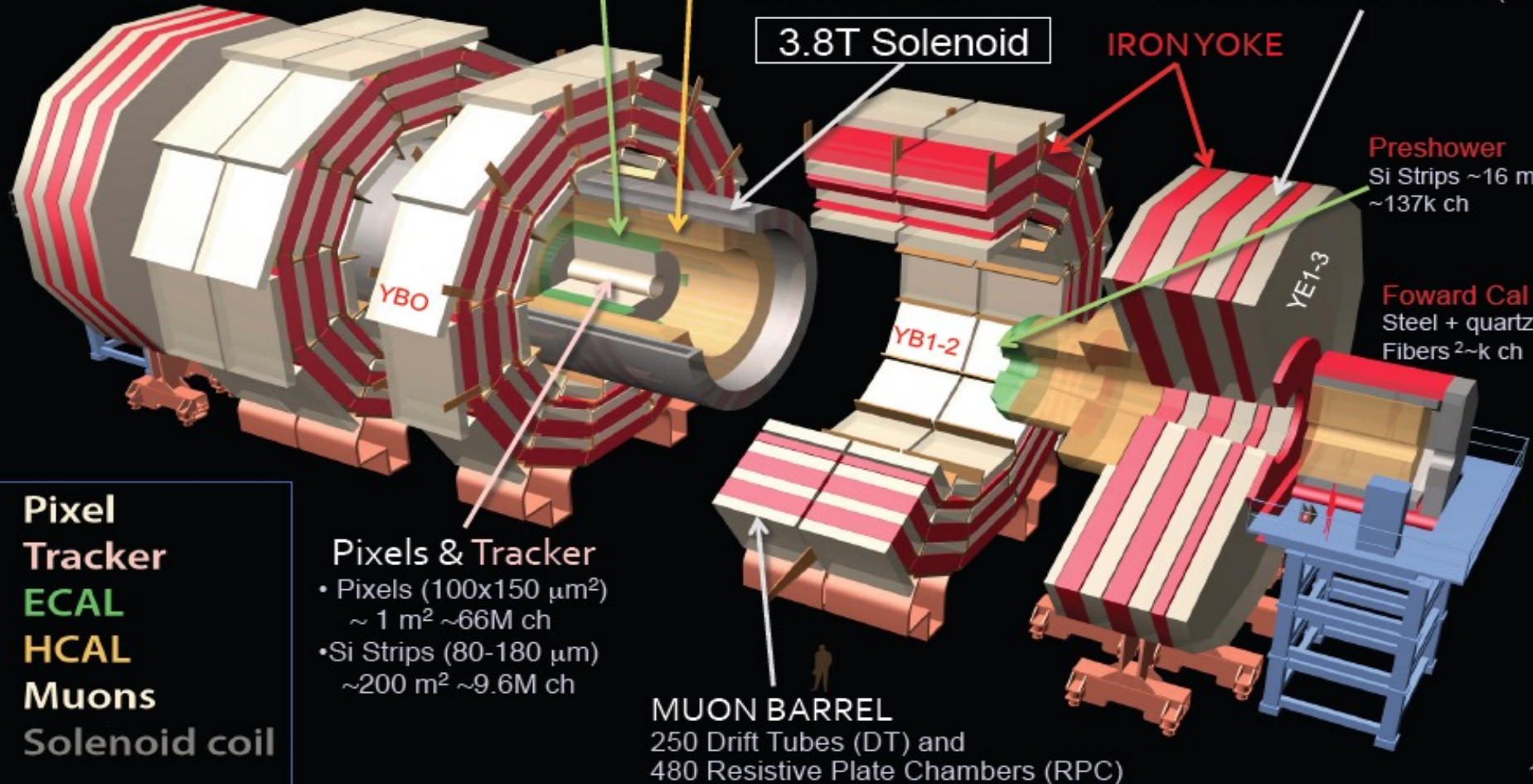
ECAL

HCAL

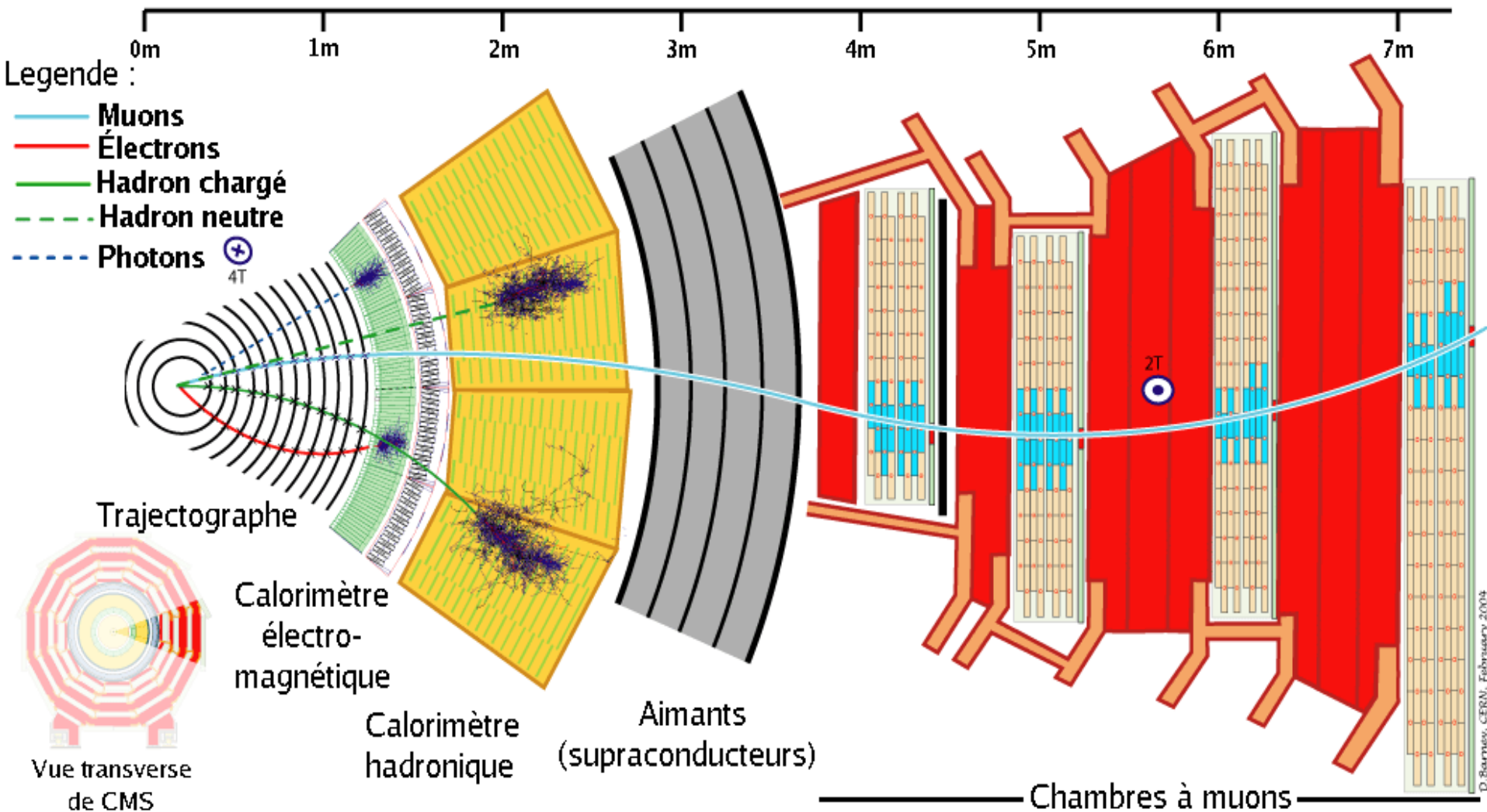
Muons

Solenoid coil

Total weight 14000 t  
 Overall diameter 15 m  
 Overall length 28.7 m

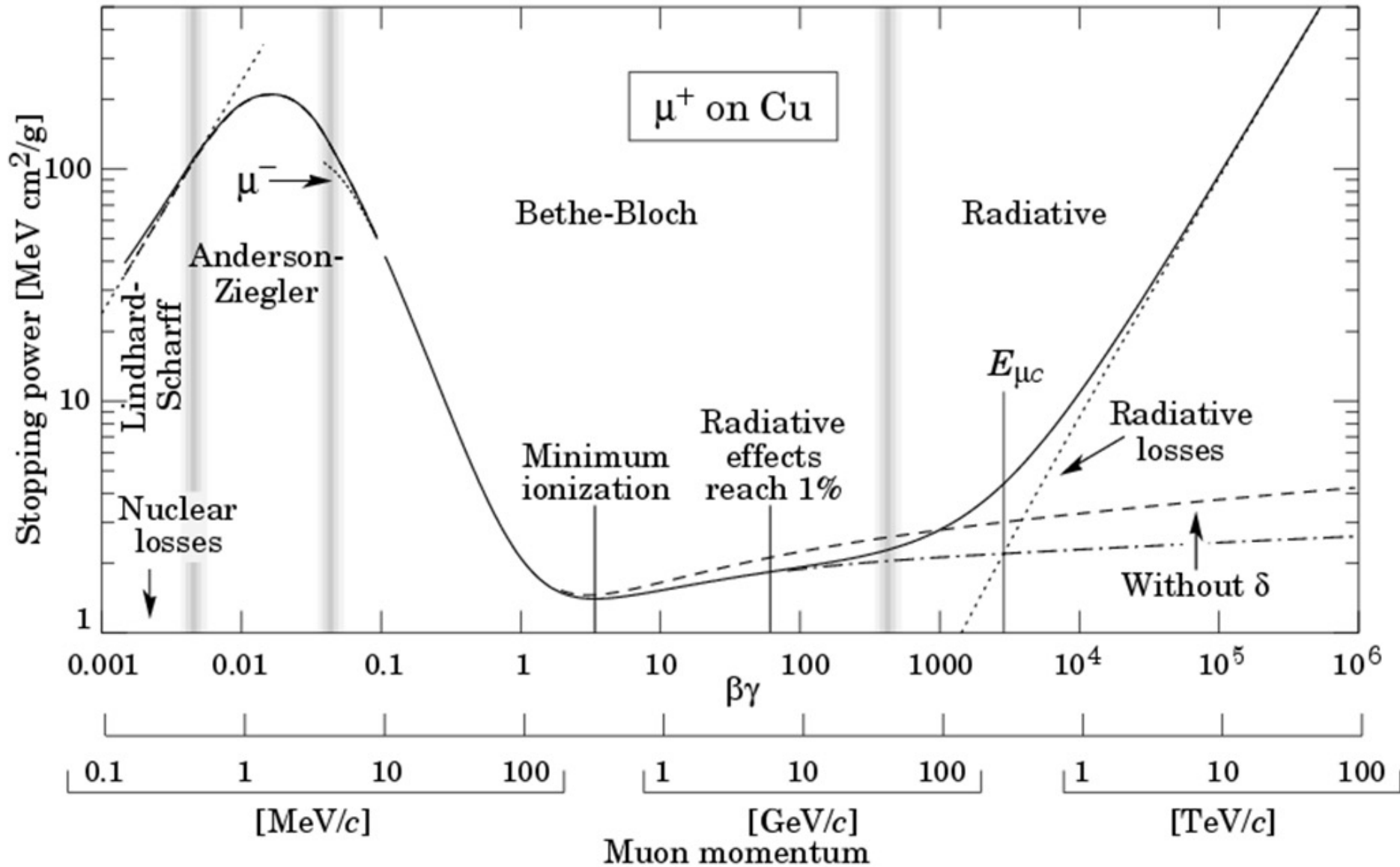






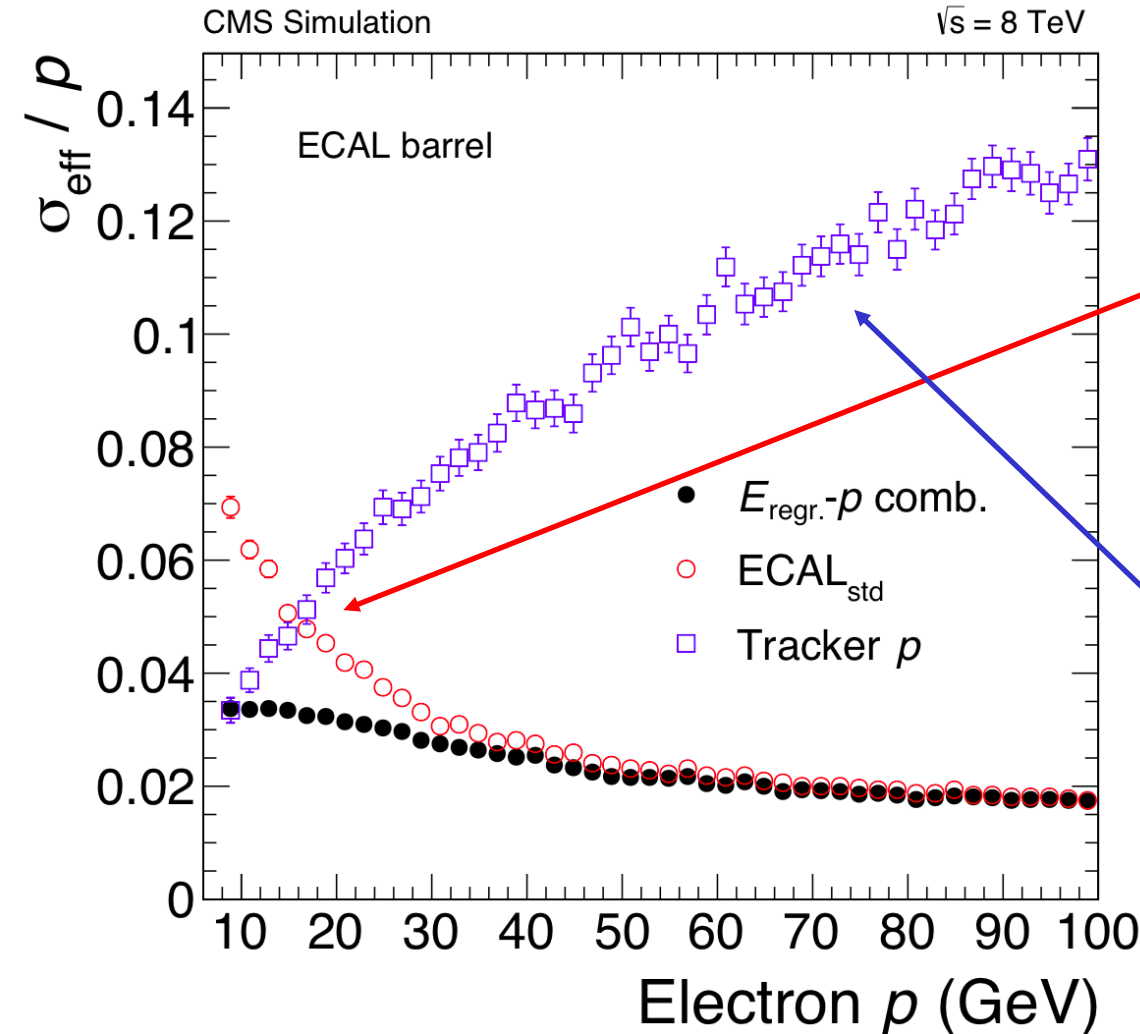
## Transverse slice through CMS detector







# Energy / momentum resolution



## Calorimetry

$$\frac{dE}{E} \sim \frac{1}{\sqrt{E}};$$

## Tracking

$$\frac{dp_T}{p_T} \sim \frac{\Delta S}{BL^2} p_T$$

The number of created secondary particles is proportional to the energy

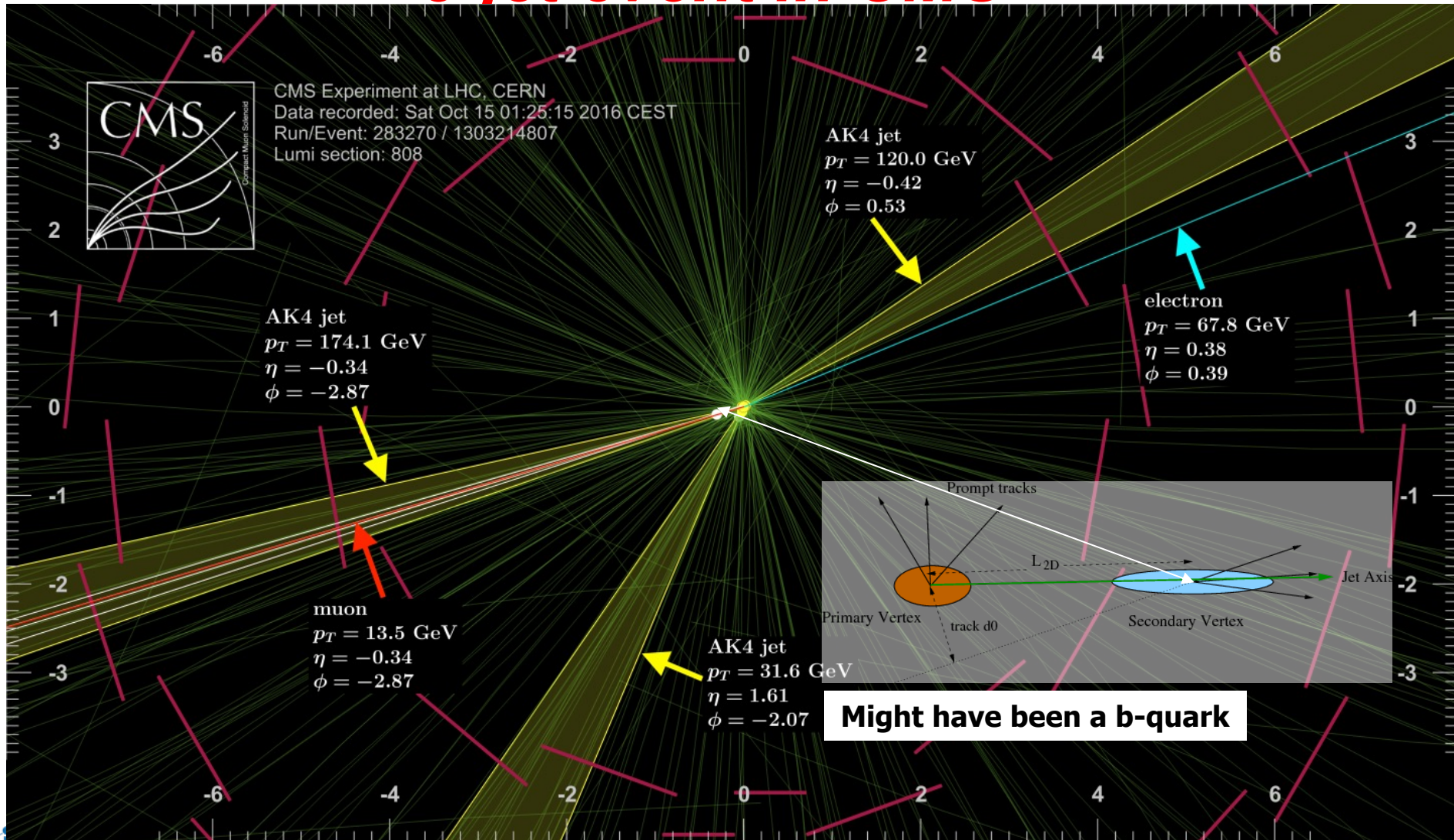
$$E \sim N, \quad \sigma_{\text{RMS}} \sim \sqrt{N} \sim \sqrt{E}$$

$$\left. \frac{\sigma(p_T)}{p_T} \right|^{meas.} = \frac{\sigma(x) \cdot p_T}{0.3 \cdot BL^2} \sqrt{720 / (N + 4)}$$

(for  $N \geq \sim 10$ )



# 3-jet event in CMS



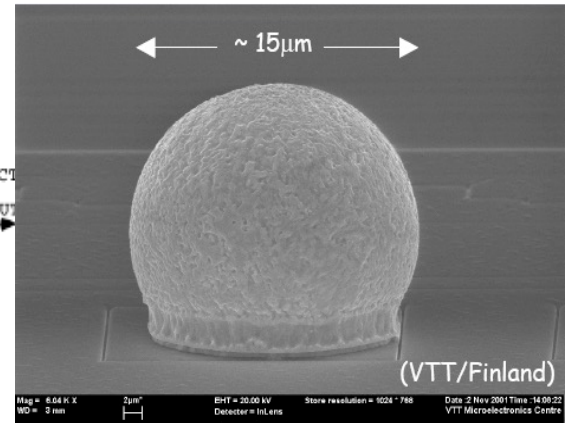
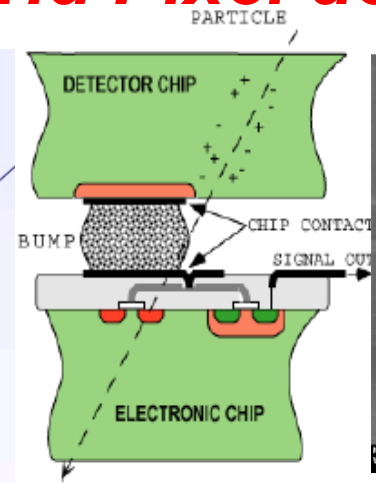
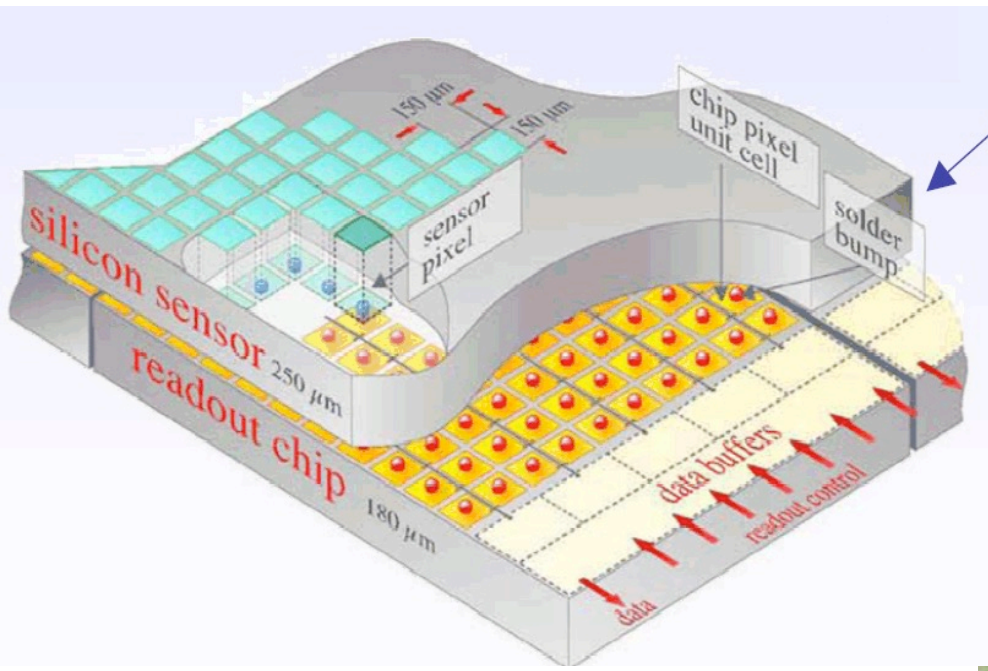


## **CMOS Pixel detectors**

- **Powerful vertex detectors**
- **For high resolution tracking**
- **Industrial processes**
- **Very small material budget (thin detectors)**
  - „ Remember multiple scattering !
  - „ Photon conversion to  $e^+ e^-$
  - „ Bremsstrahlung of electrons
- **MAPS = Monolithic Active Pixel Sensors**

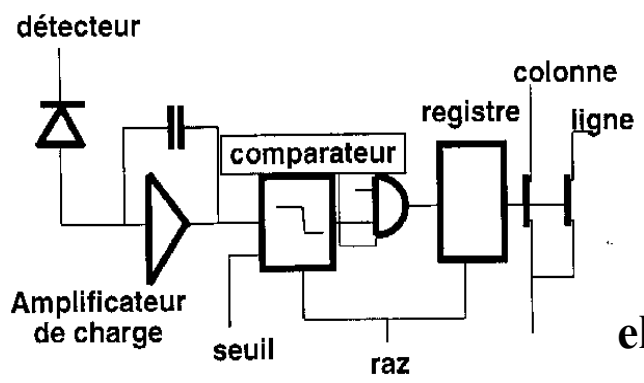


# Classical Hybrid Pixel detector

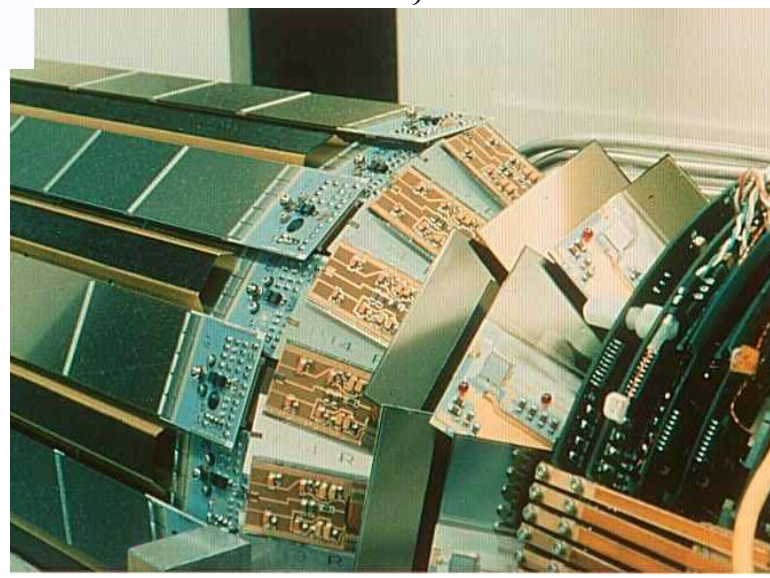


**DELPHI-LEP-CERN**

**Pixels : 330x330 μm  
152 modules, 1.22 M channels**

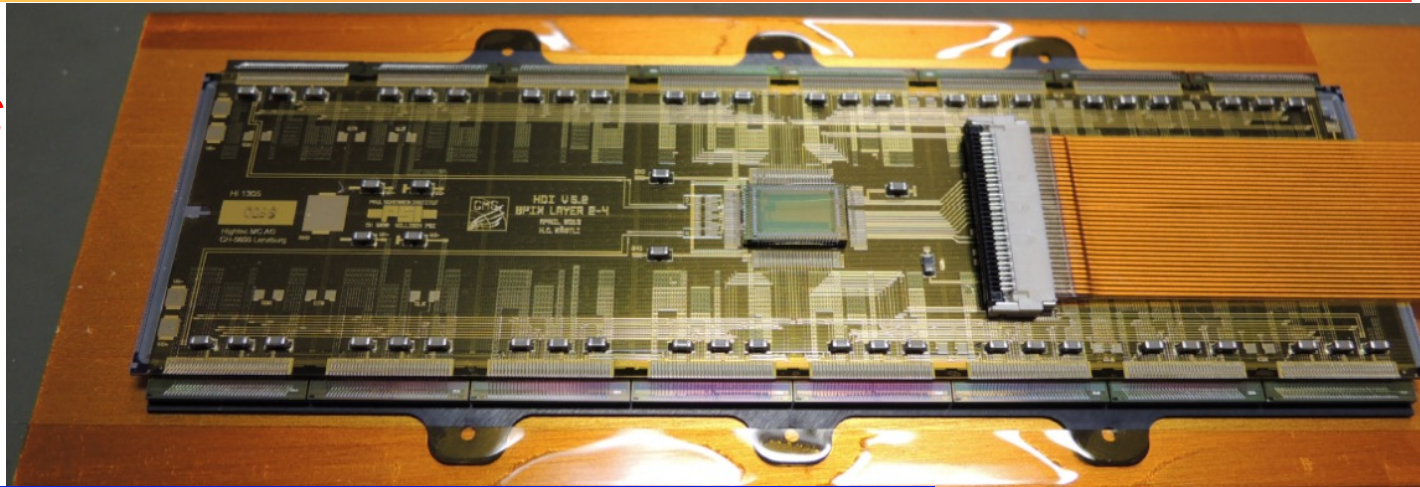


**Pixel electronics: complex!**

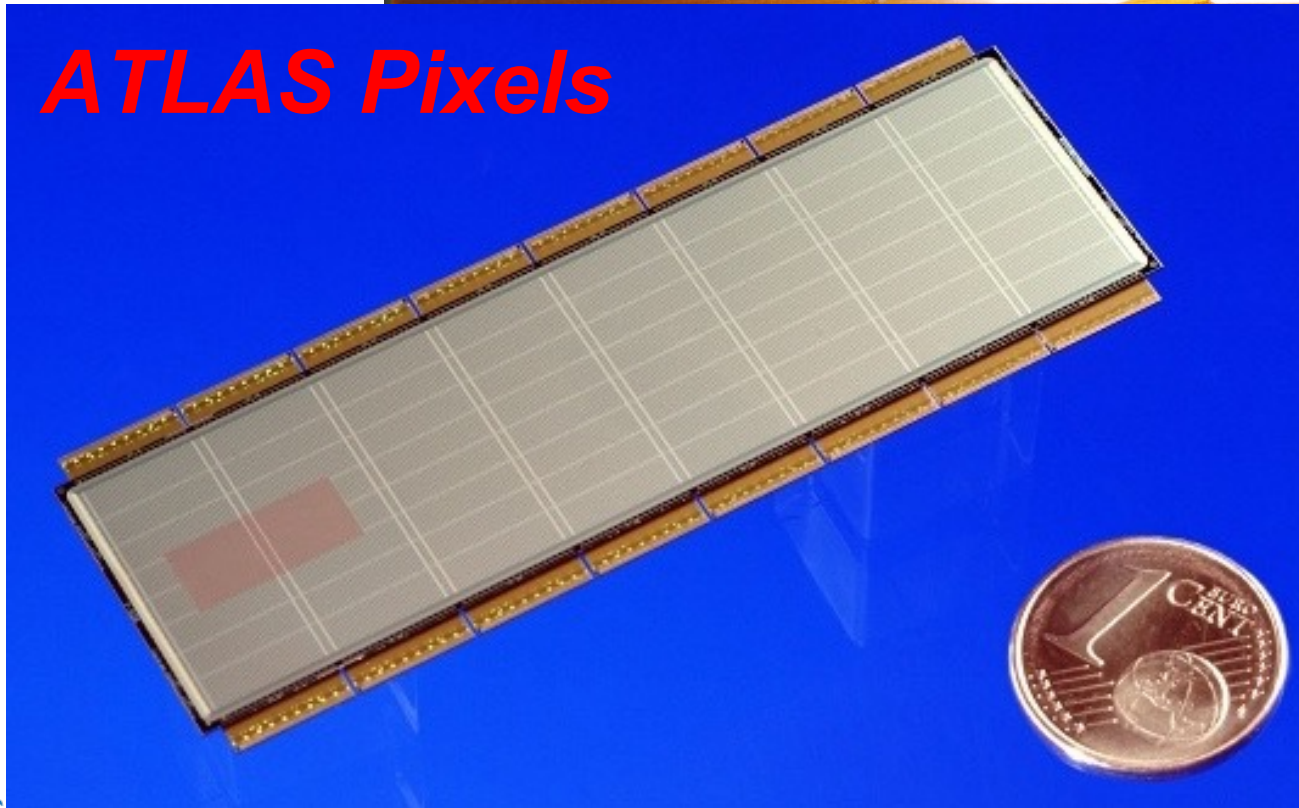




# CMS Pixels

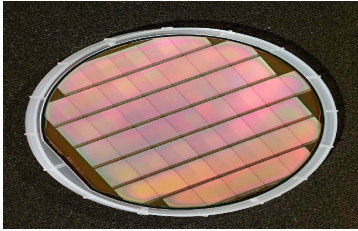


# ATLAS Pixels



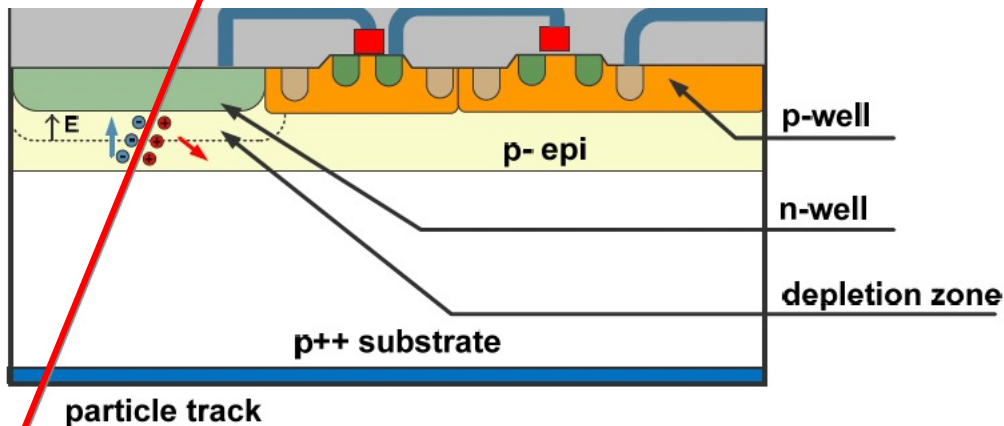


# CMOS (Complementary metal-oxide-semiconductor) Detectors



Avantages of CMOS VLSI technology:

- $\mu$ -circuits integrated but still
- 100% fill factor
- Small sensitive volume ( $\approx$  épitaxial layer)  $\approx 10 \mu\text{m}$  thick detectors can be very thin
- Industrial production standards  $\Rightarrow$  « modestes » costs,



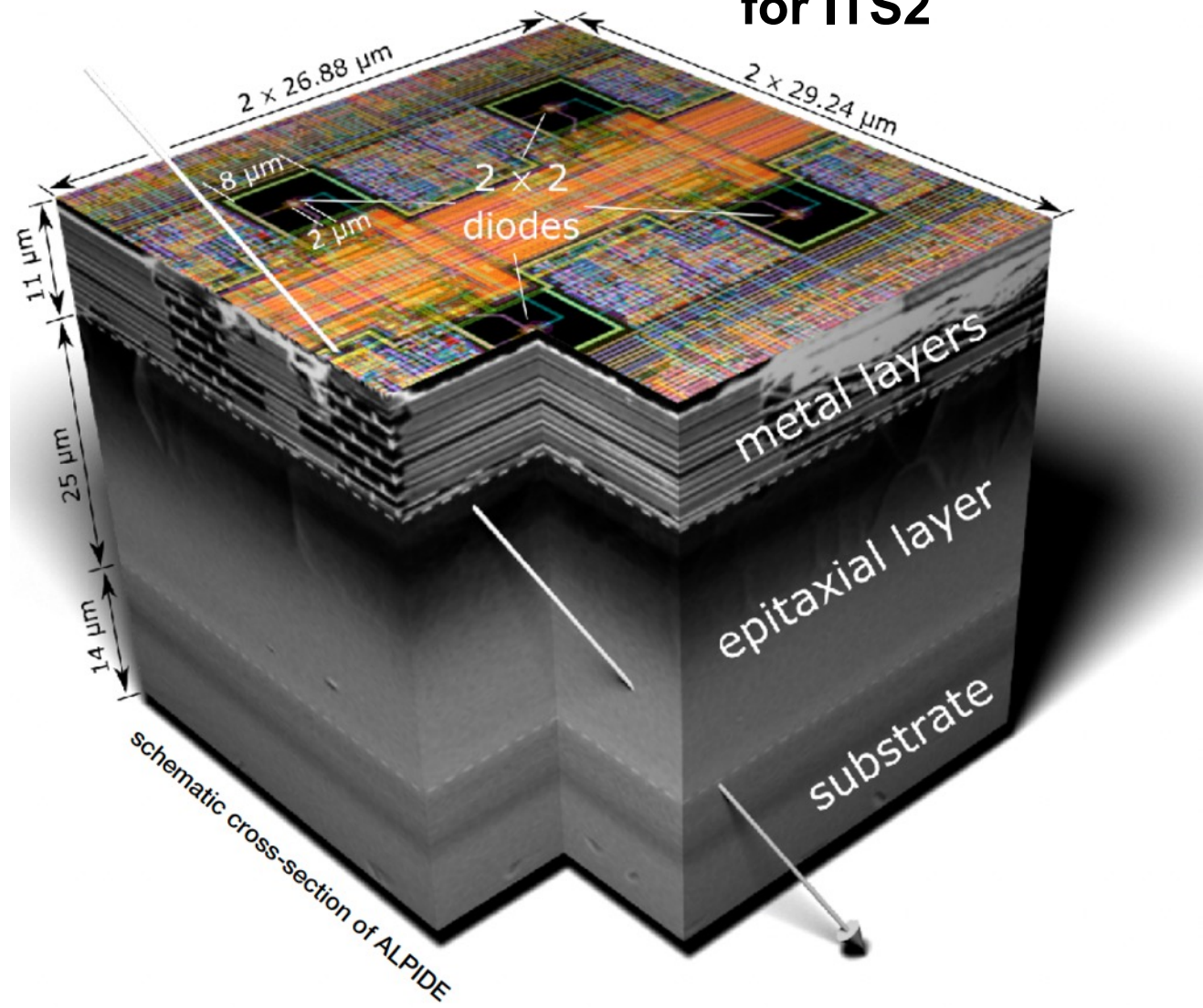
- Signal is created in p-epitaxial layer (lower doping):  
 $Q \approx 80 \text{ e-h} / \mu\text{m} \Rightarrow \text{signal} < 1000 \text{ e}^-$
- $\text{e}^-$  diffusent (thermiquement) to the jonction helped by reflexions at the boundaries formed by the p-well and the substrat (higher doping)
- Diffusion time  $< 100\text{ns}$
- Charge is collected by the diode formed by the jonction n-well/p-epitaxial layer

**Short coming:**

Circuitry of the electronic circuit is limited to only NMOS transistors.

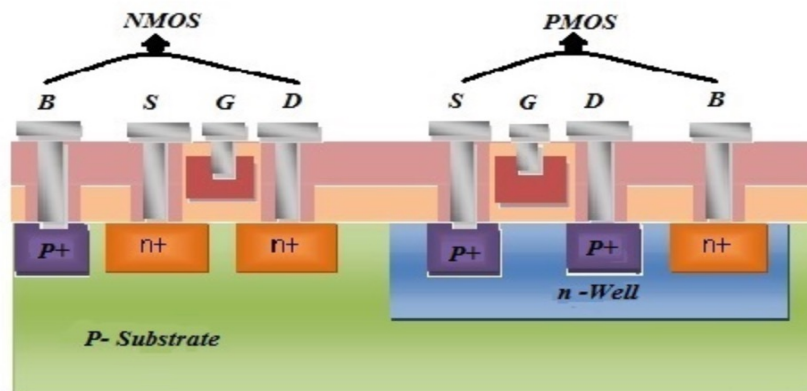


# ALPIDE — the Monolithic Active Pixel Sensor (MAPS) for ITS2



# Characteristics:

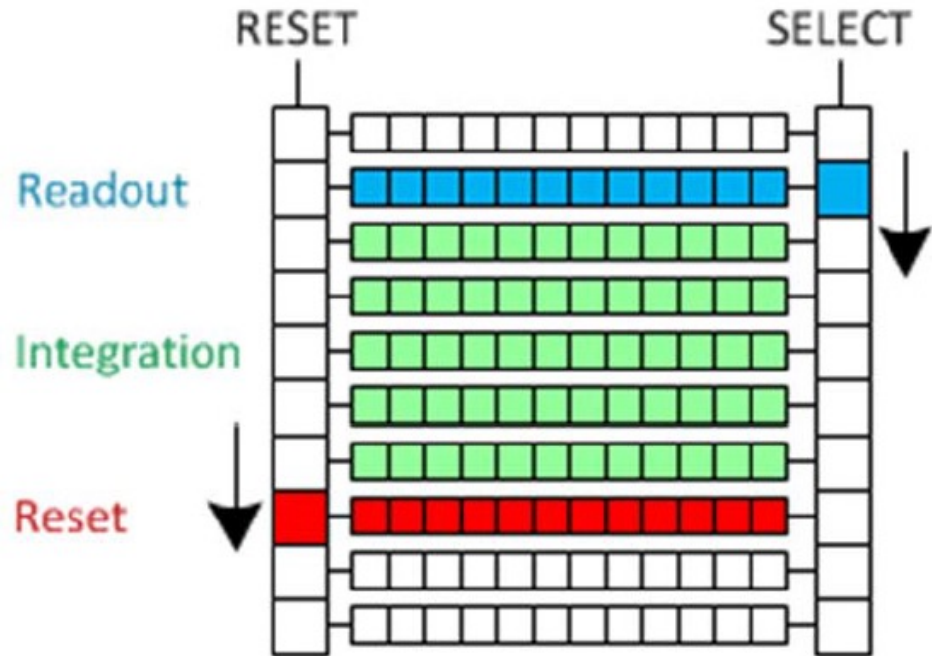
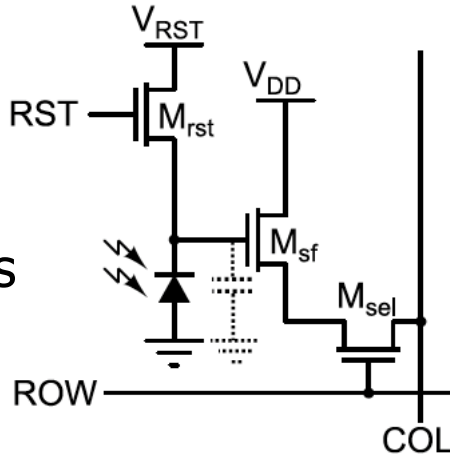
- Pixel detector **could be made very thin**, low material budget!
- Thin epitaxial layer → **Small signals**
- Small pixel size possible ( $10 \times 10 \mu\text{m}^2$ ) to obtain very good spatial resolution, but then limited space for electronic circuit available
- (Only n-well Transistors)
- **Simple on pixel-cell electronics** → slow Read Out (next slide)





# Overview of Rolling Shutter Architecture

On chip electronics



**Rolling shutter readout concept where the integrated signal is read out and reset row by row:**

- In this case all pixel outputs in the column are connected.
- Only one row of pixels is selected at a time for readout and/or reset.
- The column outputs can be multiplexed at the periphery in case of limited analog outputs.
- The recorded values can be digitized by external or internal components

# Typical layout of a MAPS chip

CMOS 0.35  $\mu\text{m}$  OPTO technology  
 Chip size : 13.7 x 21.5  $\text{mm}^2$

- Pixel array: 576 x 1152, pitch: 18.4  $\mu\text{m}$
- Active area:  $\sim 10.6 \times 21.2 \text{ mm}^2$
- In each pixel:
  - Amplification
  - CDS (Correlated Double Sampling)

- Testability: several test points implemented all along readout path
  - Pixels out (analogue)
  - Discriminators
  - Zero suppression
  - Data transmission

- Row sequencer
- Width:  $\sim 350 \mu\text{m}$

- 1152 column-level discriminators
  - offset compensated high gain preamplifier followed by latch

- Zero suppression logic

- Reference Voltages Buffering for 1152 discriminators

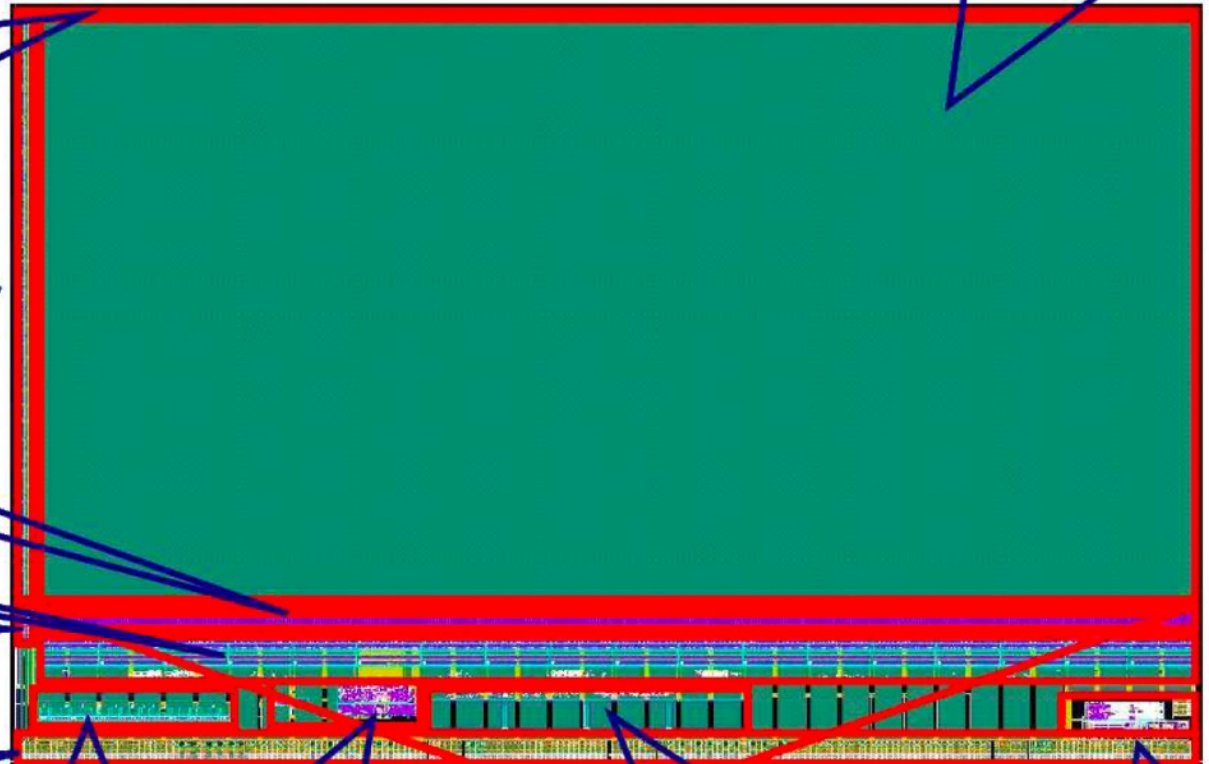
- I/O Pads
- Power supply Pads
- Circuit control Pads
- LVDS Tx & Rx

- Current Ref.
- Bias DACs

- Readout controller
- JTAG controller

- Memory management
- Memory IP blocks

- PLL, 8b/10b optional





## ***Developments to improve performance for different experiments***

- **Several labs develop CMOS pixel sensors : Italy (INFN, Univ.), UK (RAL), CERN, France (IPHC, Saclay), USA, ...**
- **Increase and speed up collected charge by drift in depleted silicon**
- **Use of high resistivity silicon wafers**
- **Use of different (more complicated) CMOS processes**
- **Change layout to use the complete design potential (use of p-MOS transistors)**
- **Speed up Read Out architecture**
- **Large area (wafer size) devices (stitching)**
- **Curved thin detector layers without additional support material**
- **....**

# Depleted Monolithic Active Pixels (HV-MAPS or D-MAPS)

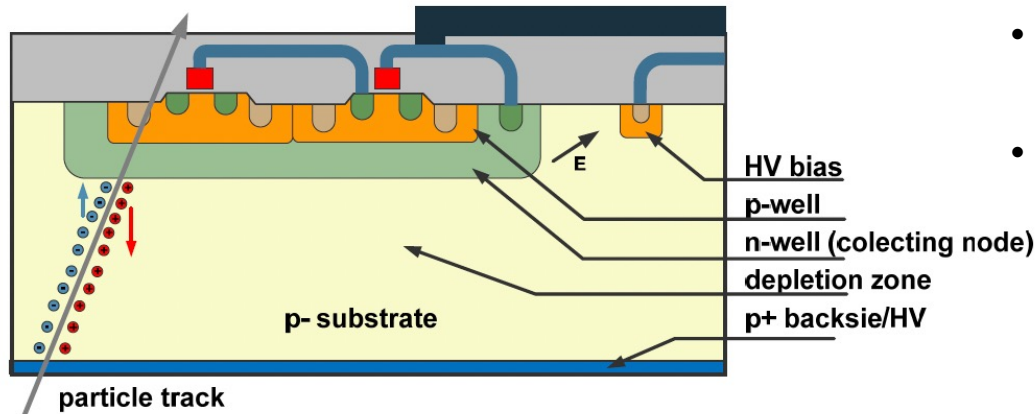
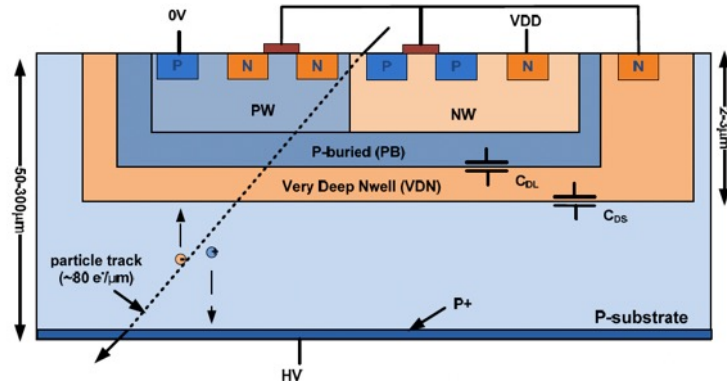


Figure 1-4 Cross section of a depleted MAPS detector with fully depleted bulk with backside contact where charge is collected by drift.

## Goals:

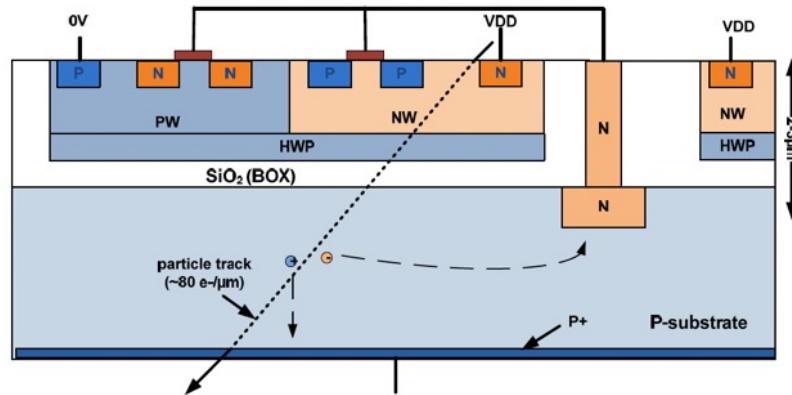
- large signals
- fast charge collection by drift in a 50 $\mu\text{m}$  – 200 $\mu\text{m}$  thick depleted layer
- the use of PMOS and NMOS transistors in the pixel cell (full CMOS),
- The entire CMOS pixel electronics is placed inside the deep n-well.
- This way, the pixel contains only one deep n-well without any inactive secondary wells that could attract the signal charge and cause detection inefficiency.
- it is reversely biased with respect to the substrate from the front side.
- By applying high voltage reverse bias (>60V) it is possible to create a depletion depth of a few to tens of microns
- implementation in a commercial technology





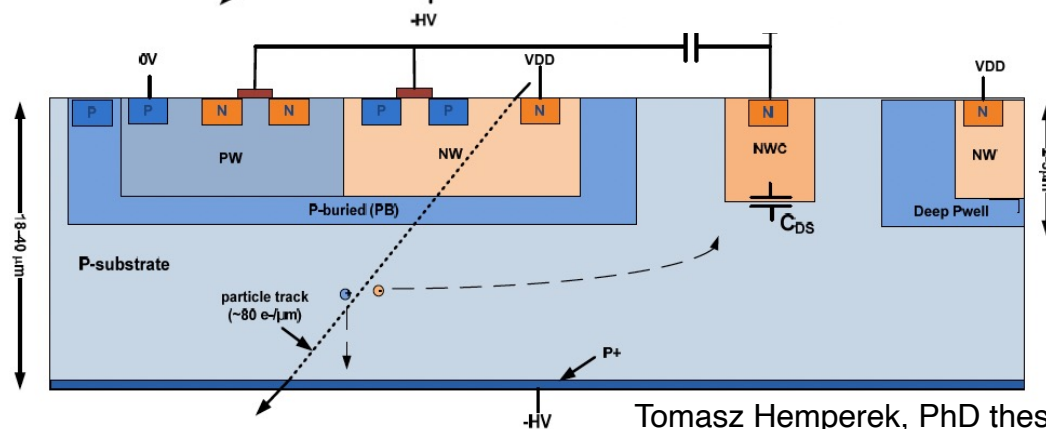
**Depleted MAPS**, logic inside collecting node

*Many different designs are being explored and tested*



**Depleted MAPS, HV-SOI**

(BOX = buried layer of silicon oxide)



**Depleted MAPS,**

Logic located outside collecting node

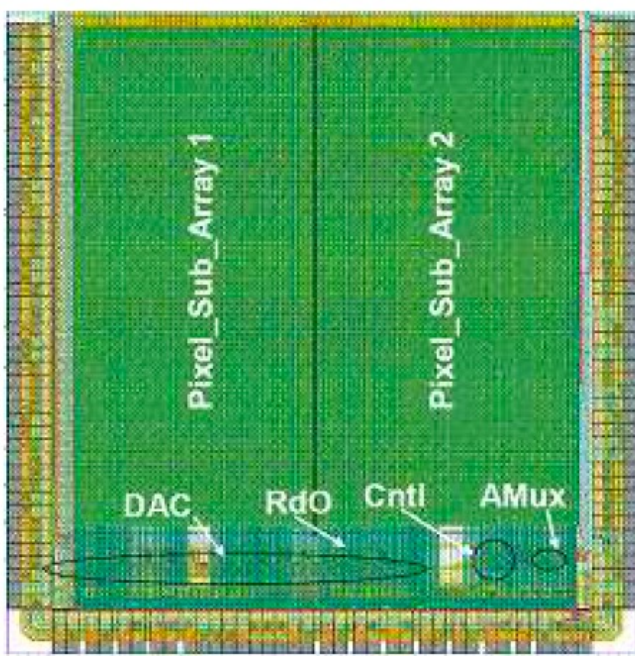
Tomasz Hemperek, PhD thesis

# Building Vertex detectors with MAPS

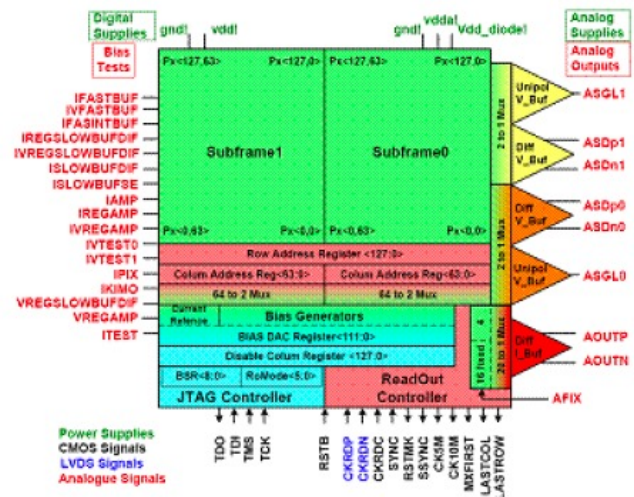
## STAR experiment at RHIC, BNL

First large scale application of MAPS in an experiment

- 2 layers of MAPS for pixel vertex detector



(a) chip layout



(b) functional diagram of the chip

M. A. Szelezniak PhD thesis 2008

Figure 6.3: MIMOSTAR chip - layout, (a), and a functional schematic diagram, (b).



# STAR experiment at RHIC, BNL

First large scale application of MAPS in an experiment

- 2 layers of MAPS for pixel vertex detector



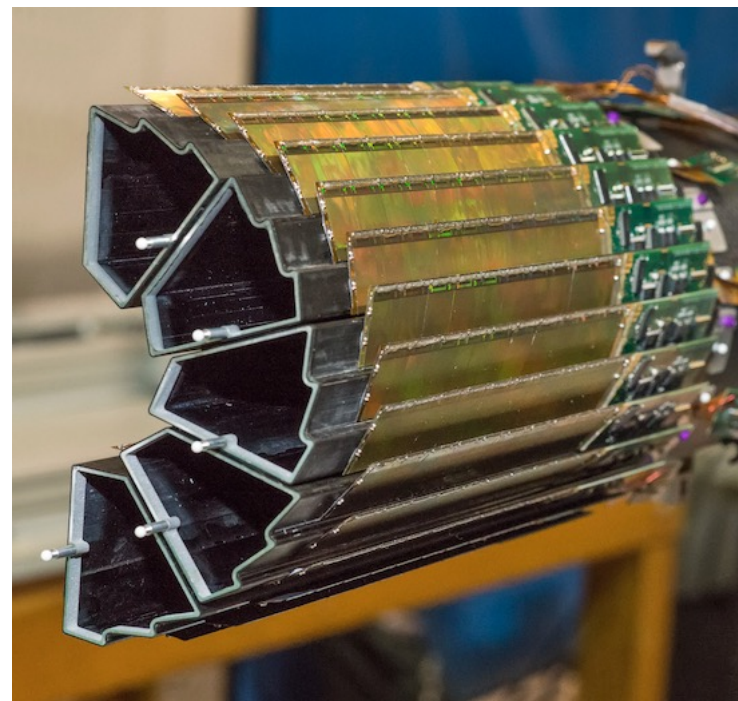
356 M pixels in 2 layers  $\sim 0.16 \text{ m}^2$

$R=28\text{mm}, 80\text{mm}$

Pixels size  $20.7 \times 20.7 \mu\text{m}^2$

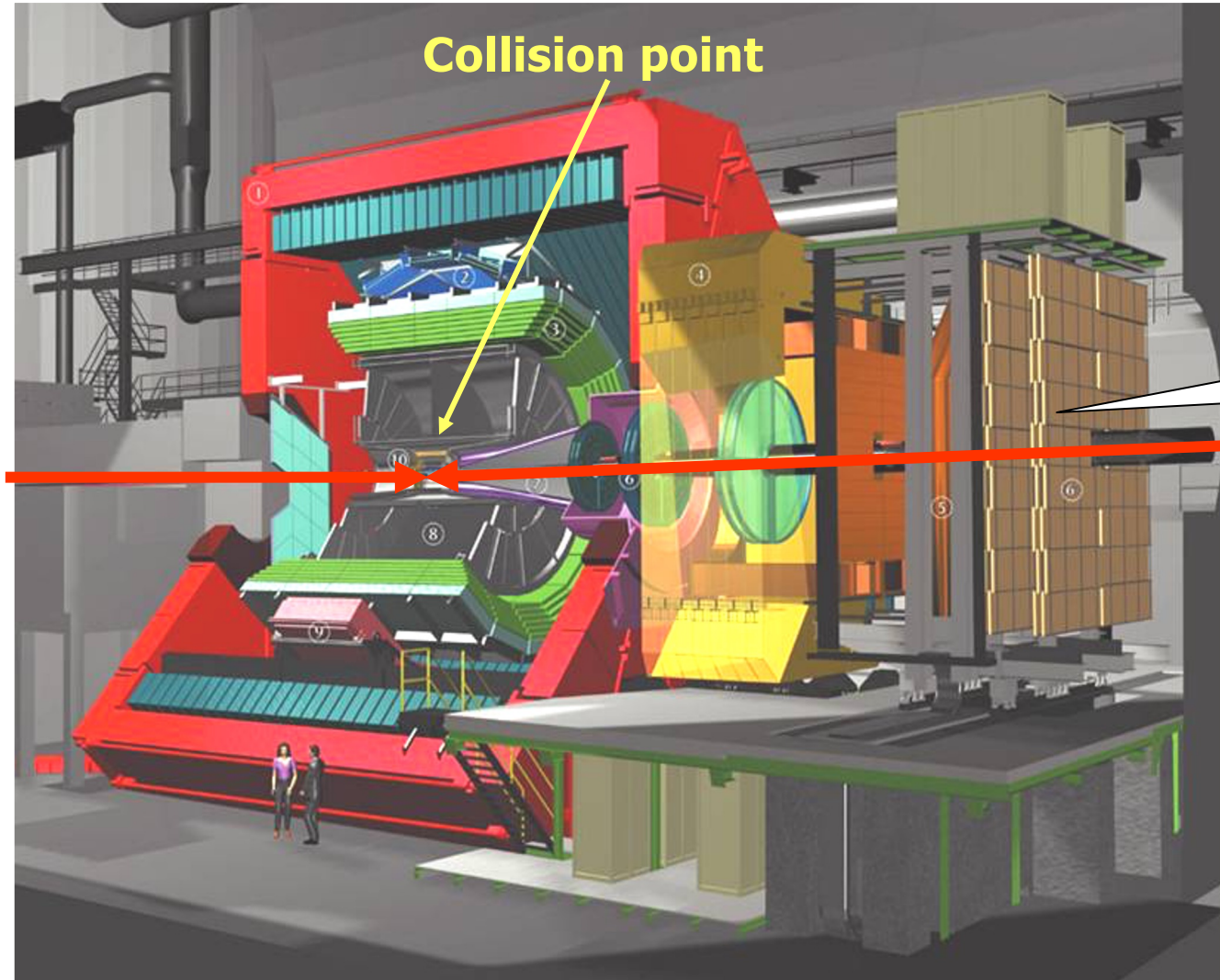
$X/X_0 = 0.39\%$  for layer 1

Integration time  $185.6 \mu\text{s}$



carbon fiber sector tubes ( $\sim 200 \mu\text{m}$  thick)

# ALICE



**Over 1000  
physicists**

**Muon  
spectrometer**

**Dimensions :**

**Length : 26m.**

**• Hight : 16m.**

**• Weight : 10000  
tonnes.**



# Building Vertex detectors with MAPS

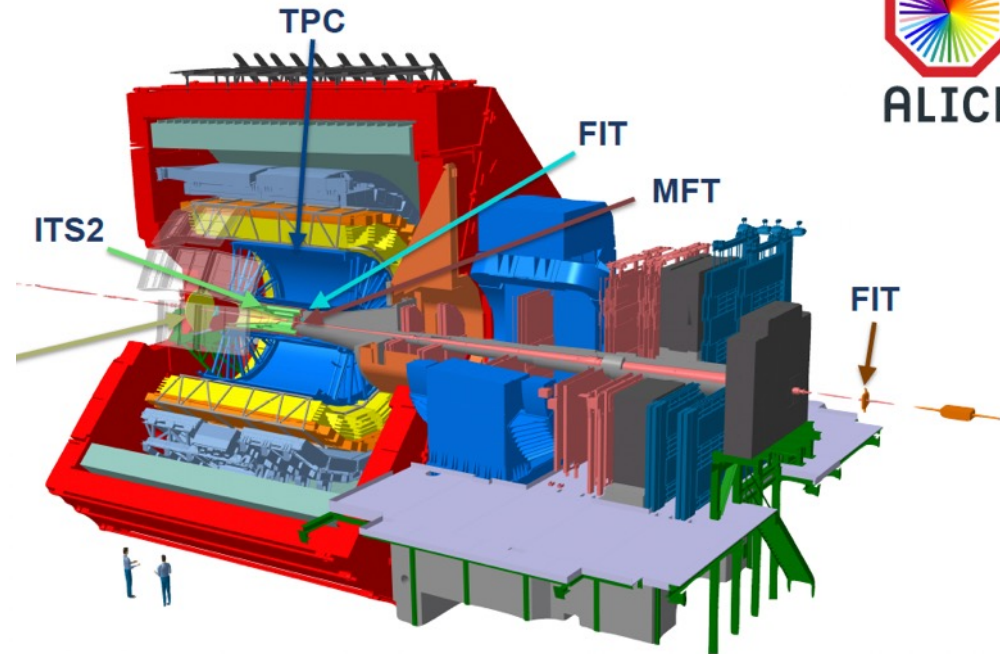
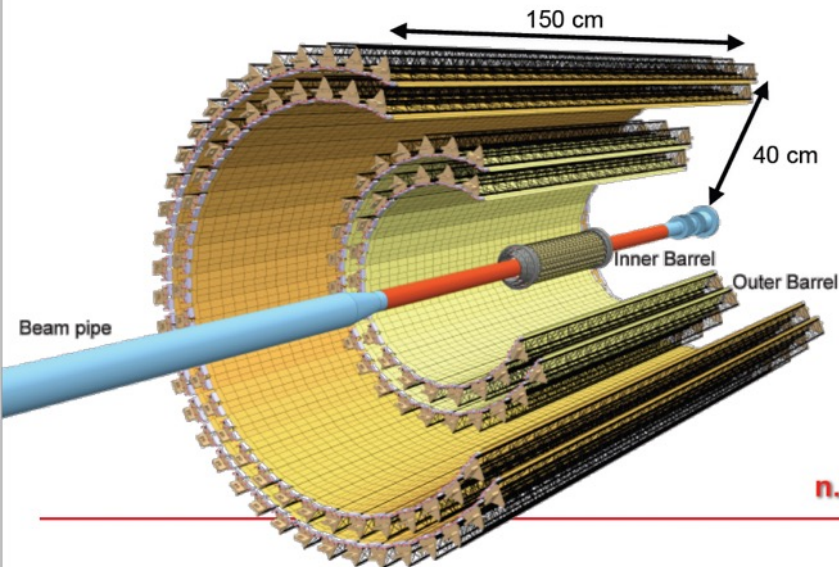
## ALICE (LHC-CERN)

A Large Ion Collider Experiment

### ITS2 layout

- 7 layers (inner/middle/outer): 3/2/2  
from  $R = 23 \text{ mm}$  to  $R = 400 \text{ mm}$
- 192 staves (IL/ML/OL): 48/54/90
- Ultra-lightweight support structure and cooling

**10 m<sup>2</sup> active silicon area, 12.5×10<sup>9</sup> pixels**



**CMOS MAPS:**

**Spatial resolution  $\approx 5 \mu\text{m}$**

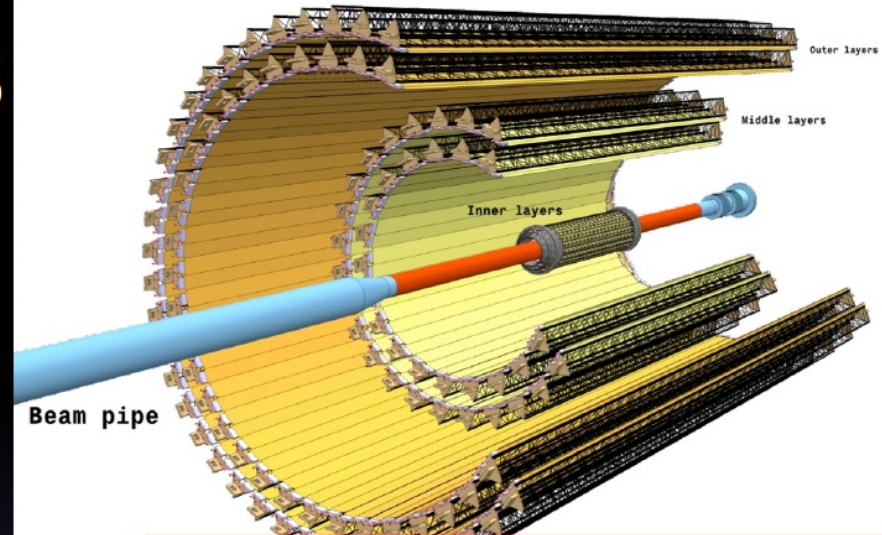
**Integration time  $< 10 \mu\text{s}$**

**high-resistivity silicon epitaxial layer**

UNIVERSITY OF  
OXFORD

# ALICE: MAPS

- Improve impact parameter resolution by a factor of  $\sim 3$  in  $(r-\phi)$  and  $\sim 5$  in  $(z)$ 
  - Closer to IP: 39 mm  $\rightarrow$  21 mm (layer 0)
  - Reduce beampipe radius: 29 mm  $\rightarrow$  18.2 mm
  - Reduce pixel size:  $(50 \mu\text{m} \times 425 \mu\text{m}) \rightarrow O(30 \mu\text{m} \times 30 \mu\text{m})$
  - Reduce material budget: 1.14 %  $X_0 \rightarrow$  0.3 %  $X_0$  (inner layers)



**$\sim 10 \text{ m}^2$  12.5 G pixel**



- High tracking efficiency and  $p_T$  resolution
  - Increase granularity and radial extension  $\rightarrow$  7 pixel layers
- Fast readout of Pb-Pb interactions at 50 kHz (now 1kHz) and 400 kHz in p-p interactions
- Rad hard to TID: 2.7 Mrad, NIEL:  $1.7 \times 10^{13} \text{ 1 MeV n}_{\text{eq}} \text{ cm}^{-2}$  (safety factor 10)
- Fast insertion/removal for maintenance



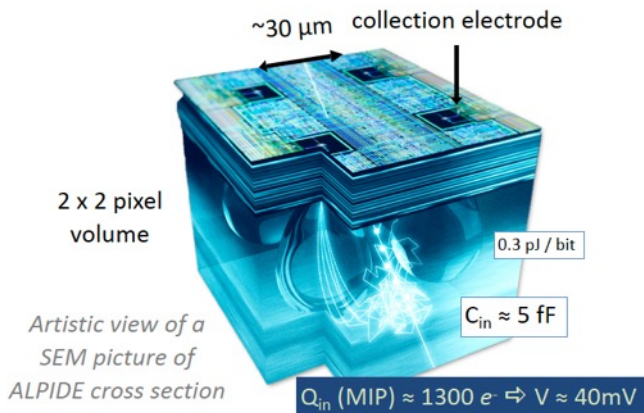
# Building Vertex detectors with MAPS

## ALICE (LHC-CERN)

A Large Ion Collider Experiment



### ALPIDE — the Monolithic Active Pixel Sensor (MAPS) for ITS2



- Developed within the ITS2 project

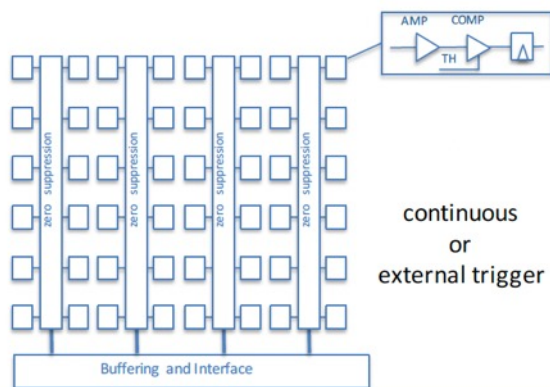
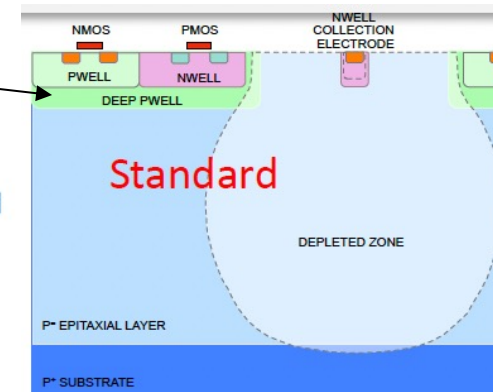
#### Technology

Technology now used in other applications

- TowerJazz 180 nm CMOS Imaging Process
- High-resistivity ( $> 1 \text{ k}\Omega \text{ cm}$ ) p-type epitaxial layer (25  $\mu\text{m}$ ) on p-type substrate
- Small n-well diode (2  $\mu\text{m}$  diameter),  $\sim 100$  times smaller than pixel ( $\sim 30 \mu\text{m}$ )  
→ low capacitance ( $\sim \text{fF}$ )
- Reverse bias voltage ( $-6 \text{ V} < V_{BB} < 0 \text{ V}$ ) to substrate to increase depletion zone around NWELL collection diode
- Deep PWELL shields NWELL of PMOS transistors  
→ full CMOS circuitry within active area

#### Key features

- In-pixel amplification and shaping, discrimination and Multiple-Event Buffers (MEB)
- In-matrix data sparsification
- On-chip high-speed link (1.2 Gbps)
- Low total power consumption  $< 40 \text{ mW/cm}^2$



# ALICE (LHC-CERN) ITS 2

A Large Ion Collider Experiment

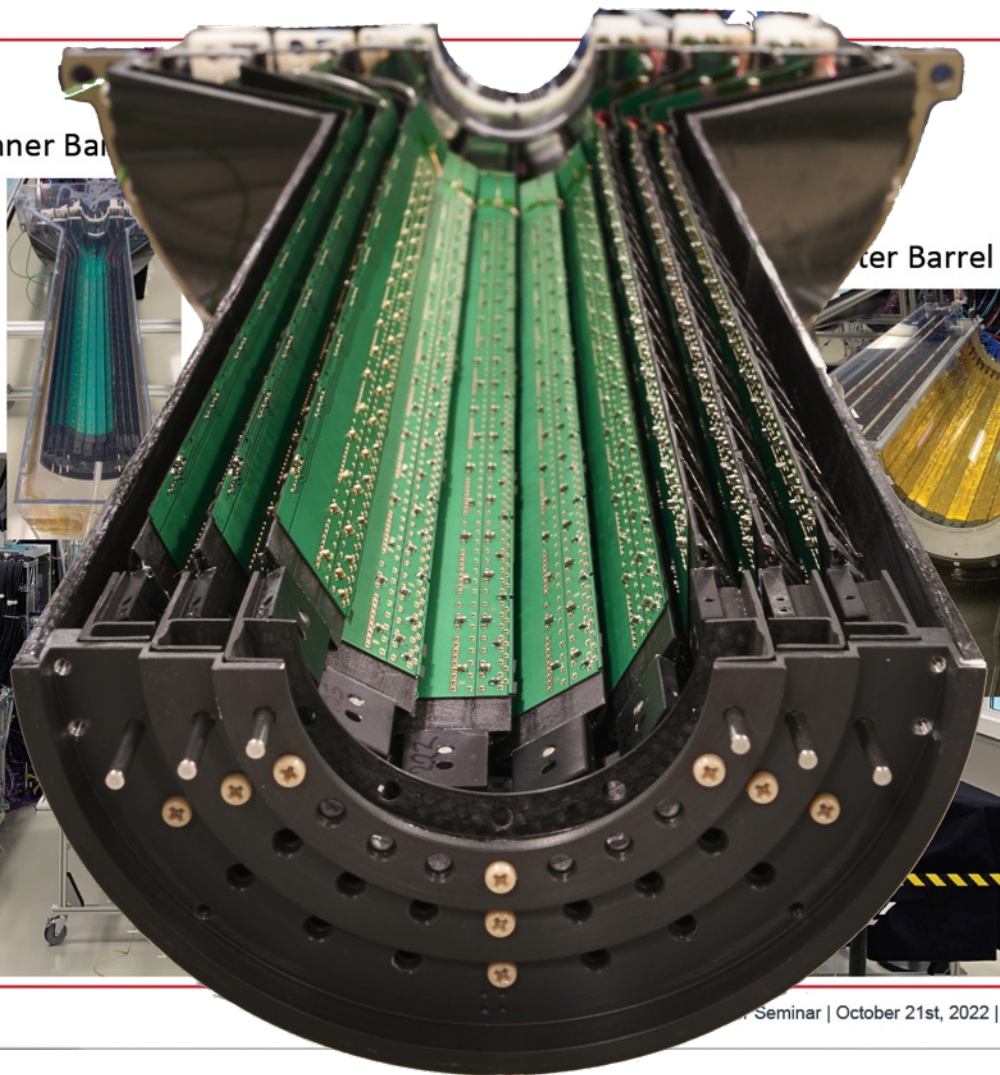
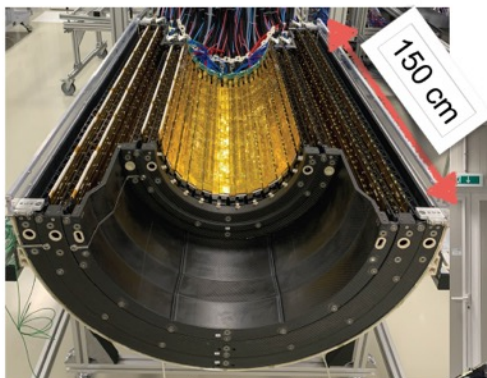


## On-surface commissioning

Inner Barrel

Outer Barrel Bottom

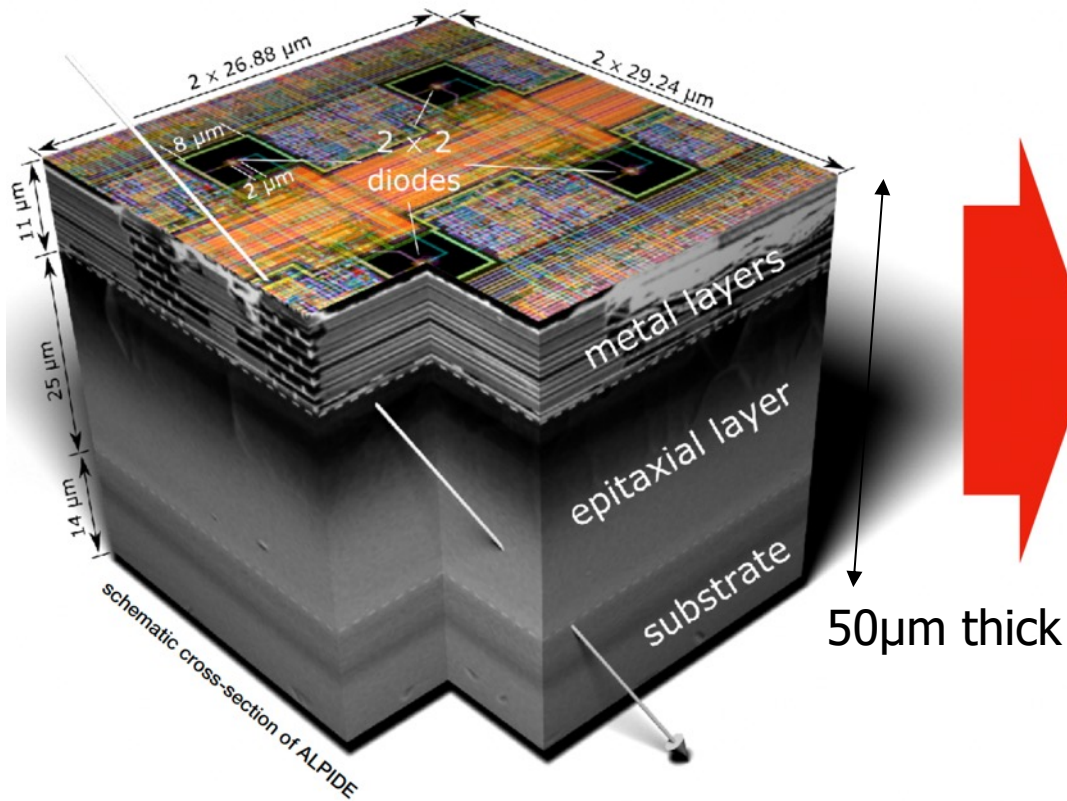
Outer Barrel Top



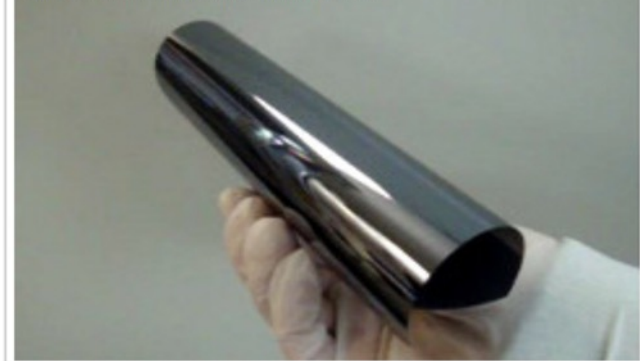


# ITS3

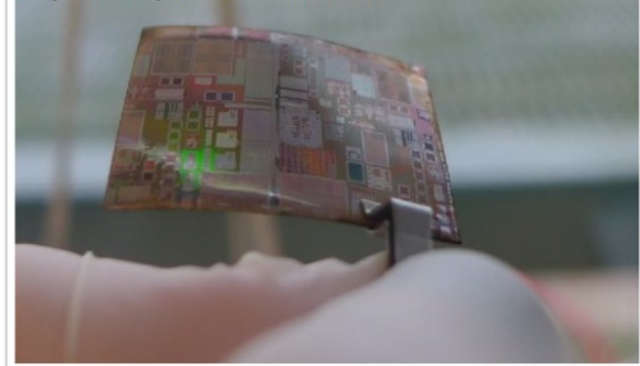
the idea (1): make use of the flexible nature of thin silicon



Silicon Genesis: 20 micron thick wafer



Chipworks: 30 $\mu\text{m}$ -thick RF-SOI CMOS



Magnus Mager (CERN) | ALICE ITS3 | CERN detector seminar | 24.09.2021 | 9

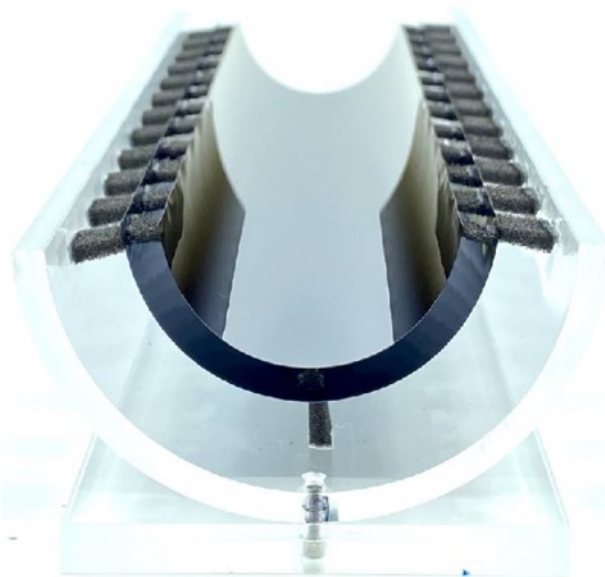
# Layer assembly



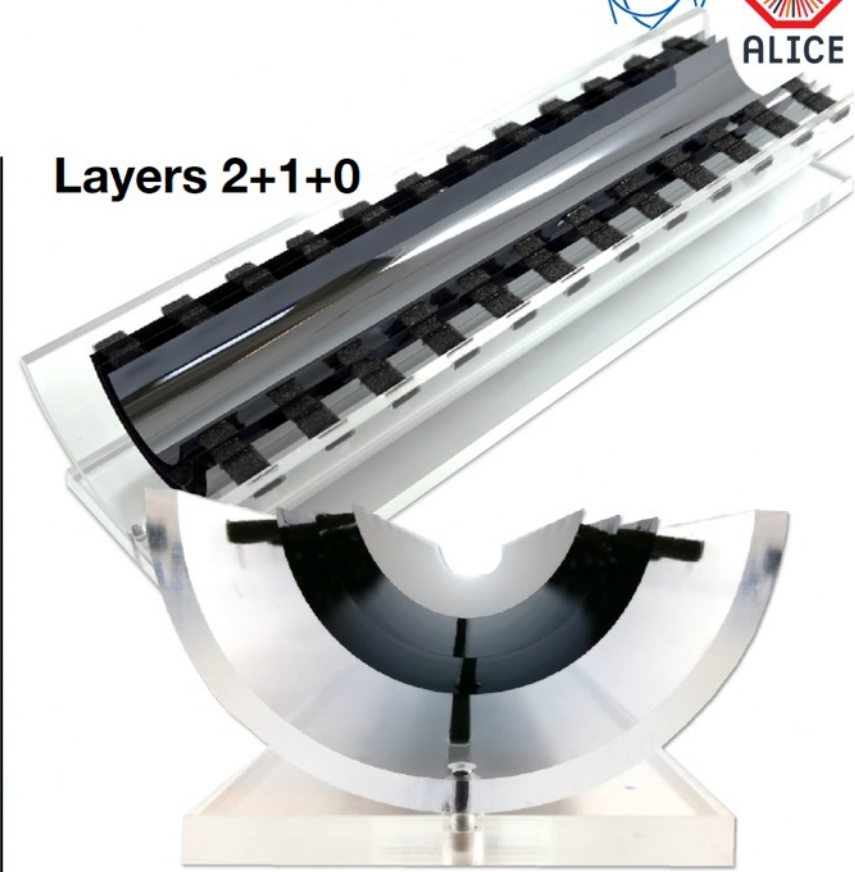
Layer 2



Layers 2+1



Layers 2+1+0



3-layer integration successful!

Magnus Mager (CERN) | ALICE ITS3 | CERN detector seminar | 24.09.2021 | 26

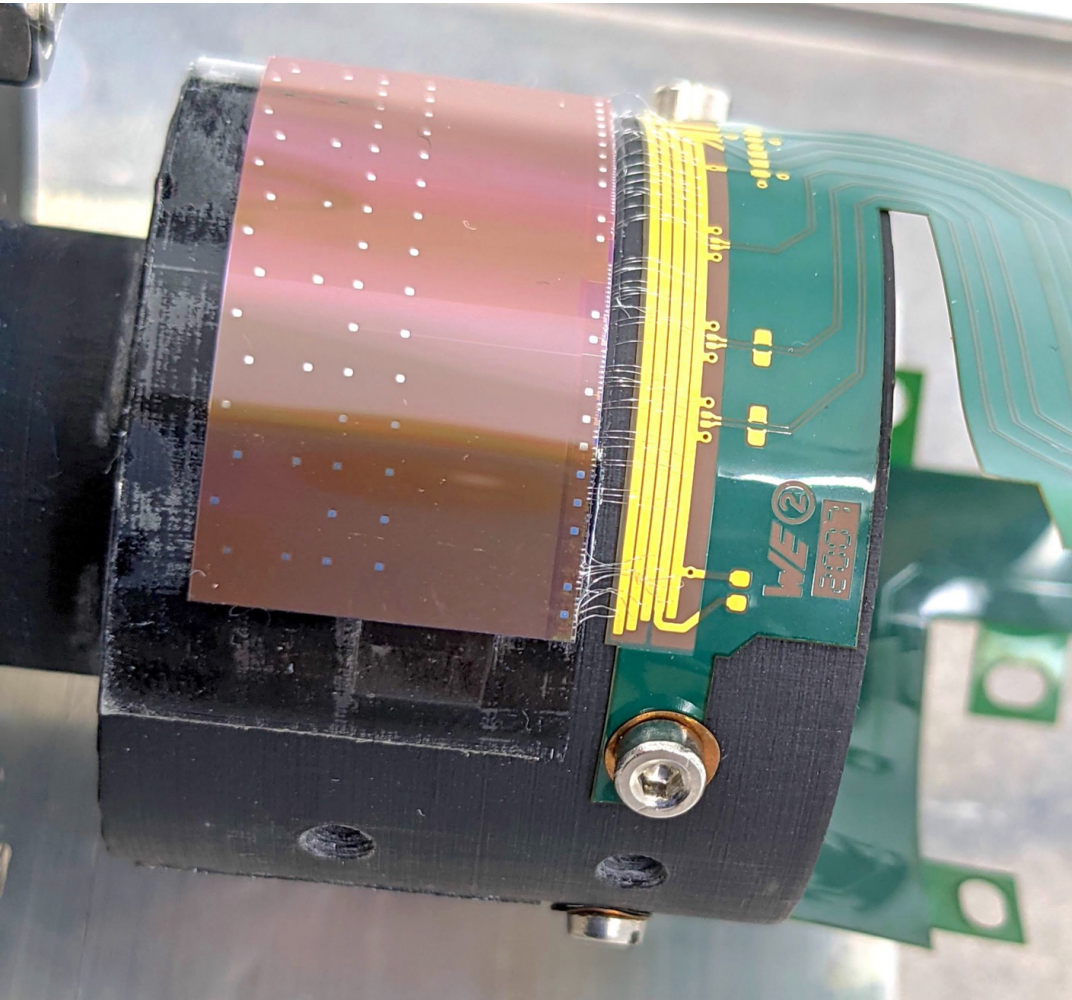


## Development of Interconnects

### Bonding on curved chips and circuits

Procedures, jigs, mandrels,  
integration

with bonding machine

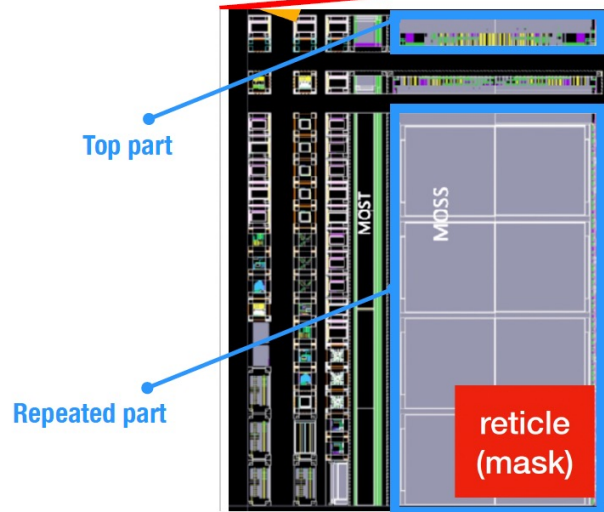


**ALICE**

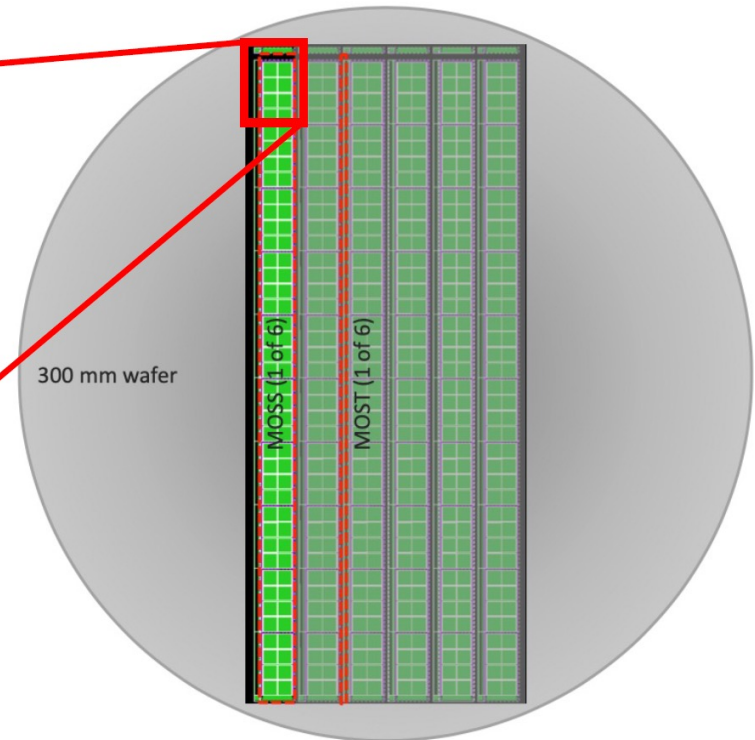
# Stitching – MOlonithic Stitched Sensor prototype

our target: ~280 x 94 mm → wafer scale sensor  
→ stitching needed: a true single piece of silicon

What we designed...



...what we want to fabricate

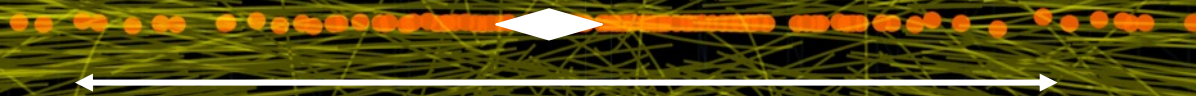


MOSS: 1.4 x 26 cm monolithic stitched sensor





CMS Experiment at the LHC, CERN  
Data recorded: 2016-Oct-14 09:56:16.733952 GMT  
Run / Event / LS: 283171 / 142530805 / 254



**First Tracker layer  $R \sim 3\text{cm}$   $\sim 0.7$   
hits/BX/mm<sup>2</sup> = 2.8 GHz/cm<sup>2</sup>**



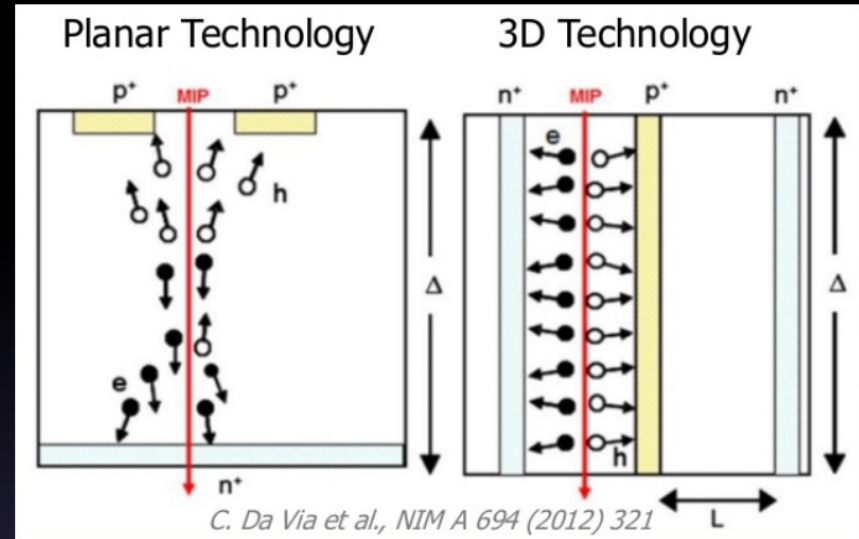
# 3D sensors

- Advantages

- Decouple thickness from electrode distance
- Lower depletion voltage, less power dissipation
- Smaller drift distance, less trapping

- Disadvantage

- More complex production process
- Lower yield, higher costs
- Higher capacitance (more noise)

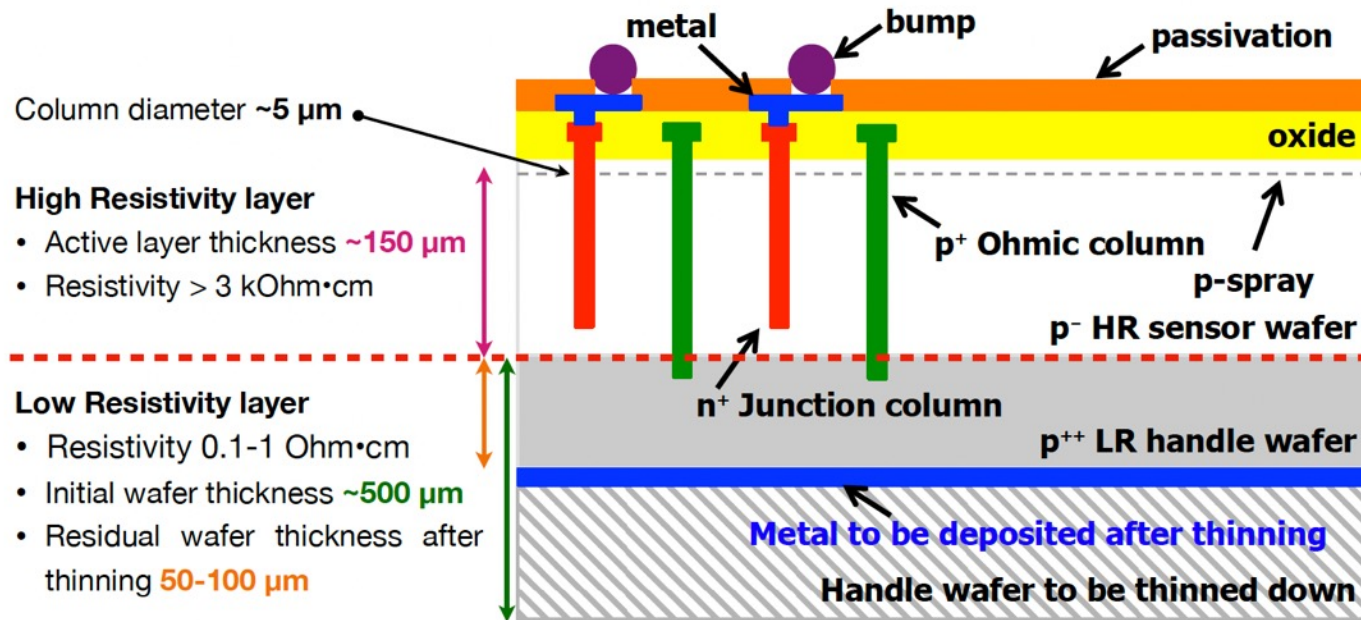


- 3D is the most radiation hard technology to-day
- Similar performance than planar sensors, but less demanding in terms of bias voltage and cooling.
- For the HL-LHC we need :
  - More radiation hard (innermost layer(s),  $1-2E16 n_{eq}/cm^2$ )
  - Smaller pixels (compatible with new readout chip,  $50 \mu m - 25 \mu m$ )
  - Thinner (reduce cluster size/merging,  $200 \mu m - 100 \mu m$ )



# 3D Silicon

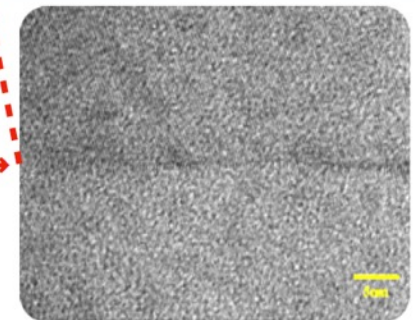
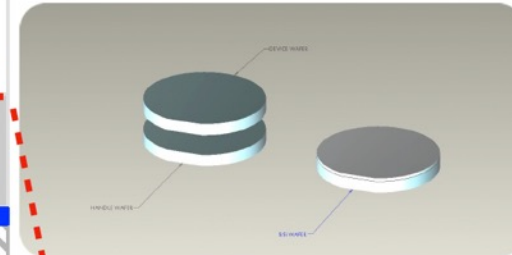
## Silicon pixels: 3D FBK – single-side



G.F. Dalla Betta et al., NIMA 824 (2016) 386

### Two wafers:

High-Resistivity and Low-Resistivity, bonded with Direct Wafer Bond - DWB technique by IceMos Technology, Belfast



High resolution TEM image of two bonded wafers cross section

### Columns produced by:

single-side **Deep Reactive Ion Etching - DRIE** process  
optimised by **FBK** (less expensive than double-side process)

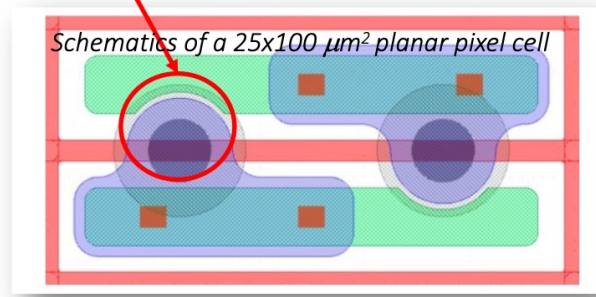
Divide between layers →

# CMS Pixel upgrade for HL-LHC

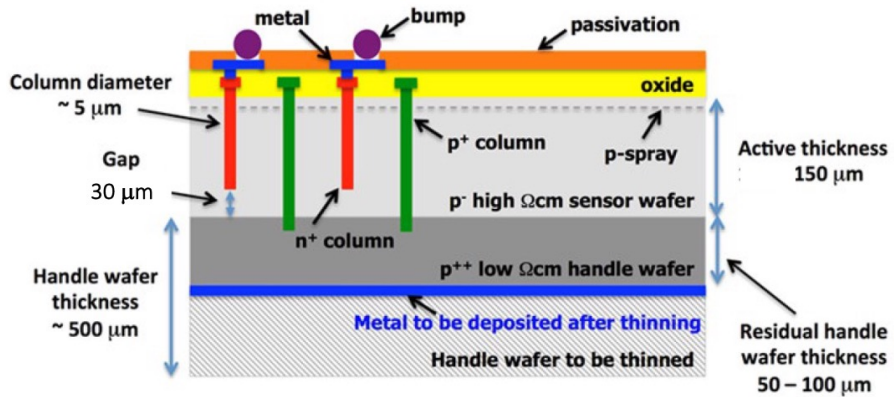
## Pixel sensors

- 150  $\mu\text{m}$  bulk thickness, 25x100  $\mu\text{m}^2$  pixels cells everywhere
- Planar n-in-p sensors:
  - Bias up to 600V and spark protection between ROC and sensors
  - Three vendors qualified in the Market Survey, Tender being closed in these days
- Bump bonding pattern is 50x50  $\mu\text{m}^2$ 
  - Cross-talk issues studied and minimized (i.e. bitten implant on planar)
  
- 3D sensors for barrel L1
  - Short drift distance  $\sim 50 \mu\text{m}$  (3D) vs 150  $\mu\text{m}$  (Planar)
  - Slim edges (150  $\mu\text{m}$ ) vs planar ( $\sim 450 \mu\text{m}$ )  $\rightarrow$  smaller dead zone
  - Sensors produced at FBK on 6" wafers and CNM on 4" wafers

No n<sup>+</sup> implant under metal to reduce x-talk



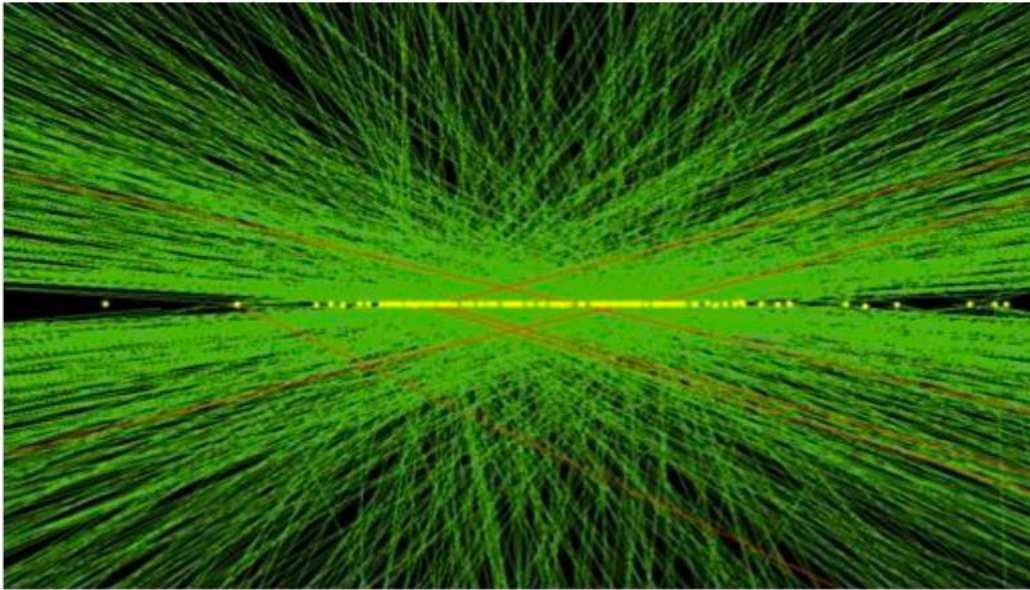
Structure of a 3D sensor – FBK process



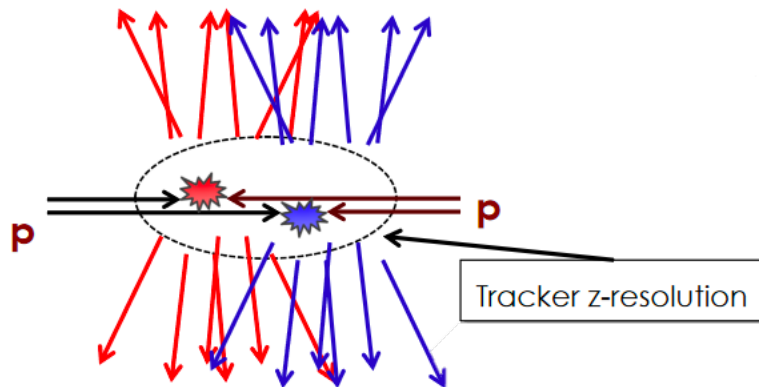
A. Macchiolo, The CMS Pixel Upgrade, Pixel 2022, 13 Dec 2022



# 4D Detectors (x,y,z and time)



Tracking z-resolution can be larger than vertex-separation: Ambiguous Track-to-vertex association



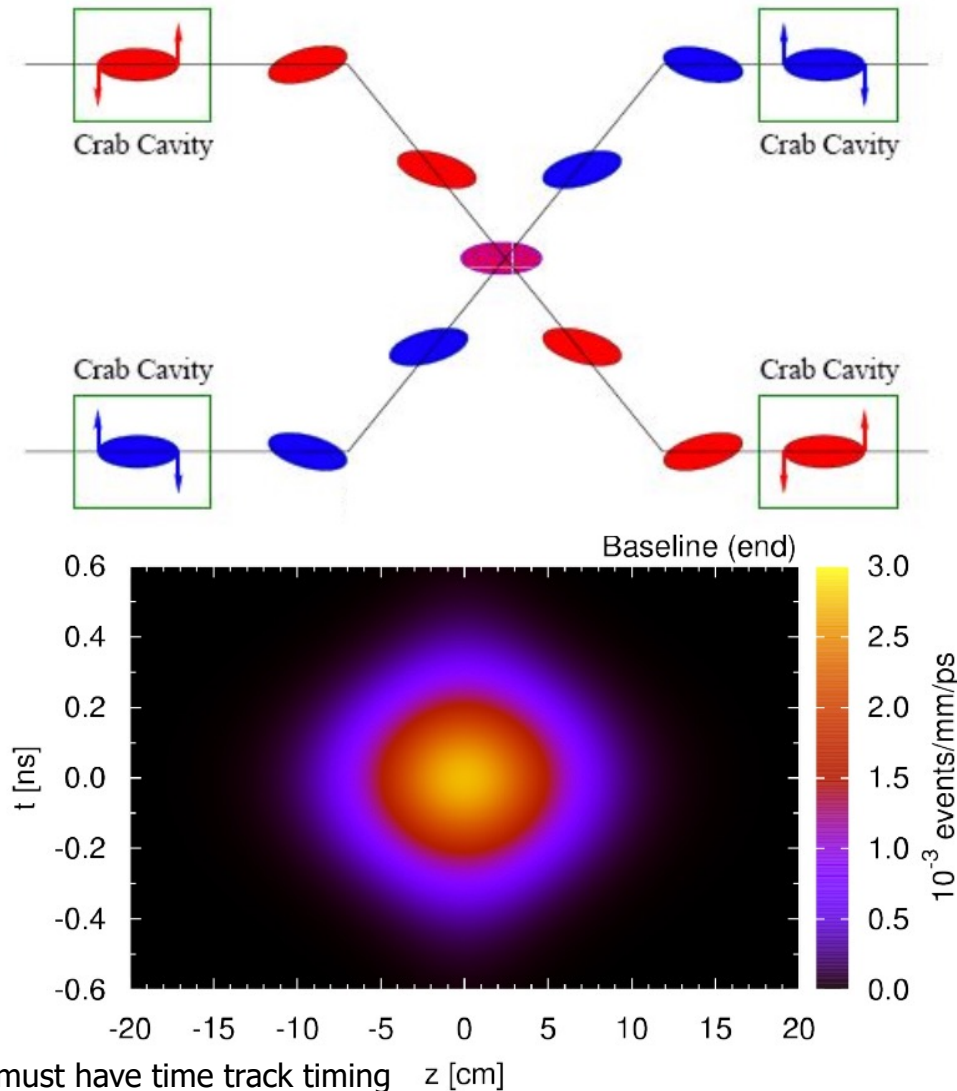
Timing at each point along the track:

- Massive simplification of pattern recognition
- Faster tracking algorithm
- Even in very dense environments by using only “time compatible points »

N. Cartiglia, INFN, Hiroshima Conference 2017

# The Time Structure of Crossing Bunches

- In addition to extent in  $z$ , there is an extent of the bunch crossing in time
- For nominal HL-LHC optics the core of the bunches pass through each other in  $\sim 300$  ps
- When bunches overlap entirely, achieve maximum spread in  $z$  and maximum pileup density
- Normally an experiment only sees the integral of this distribution over time



Need to discriminate vertices with time spread of  $\sim 180$  ps, must have time track timing resolution significantly smaller than beamspot spread so that tracks cluster in time.



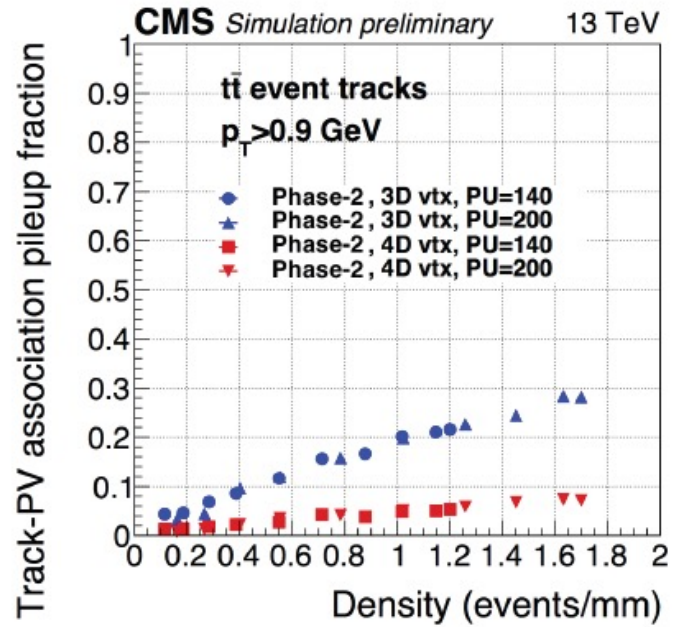
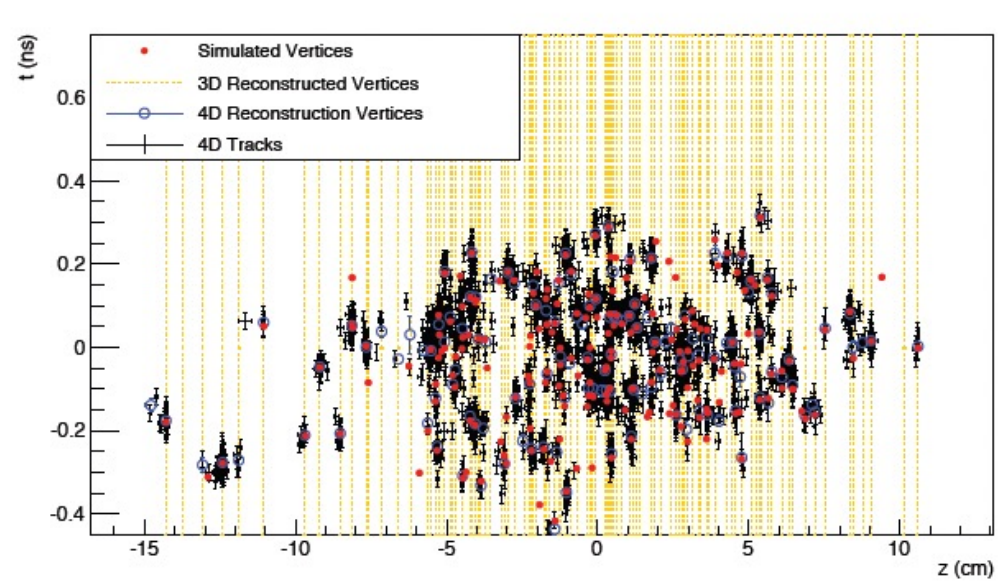
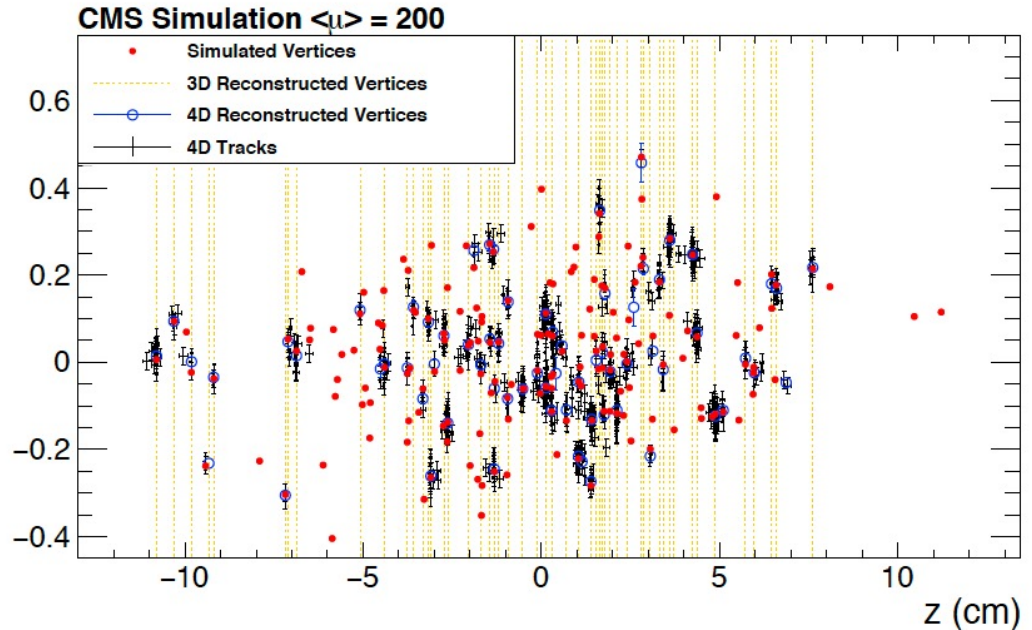


Figure 1.2: Left: Simulated and reconstructed vertices in a 200 pileup event assuming a MIP timing detector covering the barrel and endcaps. The vertical lines indicate 3D-reconstructed vertices, with instances of vertex merging visible throughout the event display. Right: Rate of tracks from pileup vertices incorrectly associated with the primary vertex of the hard interaction normalized to the total number of tracks in the vertex.

# Using the Time-at-vertex in Reconstruction

- With the track-time at distance of closest approach  $t$  (ns) it becomes possible to cluster tracks in 2D into vertices
- This significantly increases the distance between vertices and hence makes them harder to confuse
- Expect 5-10x improvement in vertex merging rate (achieved 9x)
- Expect 3-5x reduction in track-vertex association false positives (achieve  $\sim 3x$ )



CMS Simulation

$\langle \mu \rangle$	4D Merged Vertex Fraction	3D Merged Vertex Fraction	Ratio of 3D/4D
50	0.5%	3.3%	6.6
200	1.5%	13.4%	8.9



# Crystals

lutetium-yttrium orthosilicate crystals activated with cerium (LYSO:Ce) read out with SiPMs. The

The barrel timing layer will cover the pseudorapidity region up to  $|\eta| = 1.48$  with a total active surface of about 40 m<sup>2</sup>.

The fundamental detecting cell will consist of a thin LYSO:Ce crystal with about 12→12 mm<sup>2</sup> cross-section coupled to a 4x4 mm<sup>2</sup> SiPM.

The crystal thickness will vary between about 3.7 mm ( $|\eta| < 0.7$ ) and 2.4 mm ( $|\eta| > 1.1$ ),

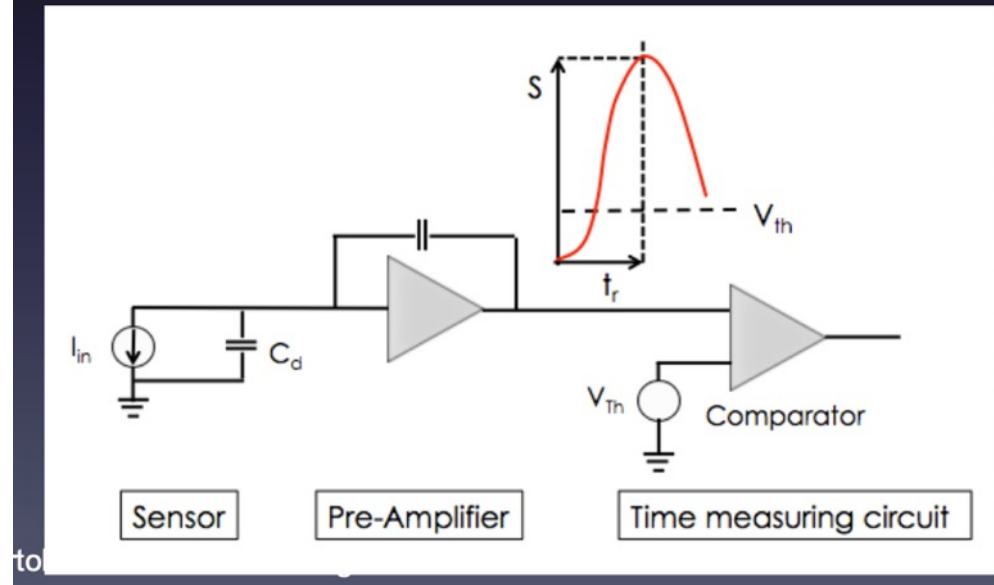
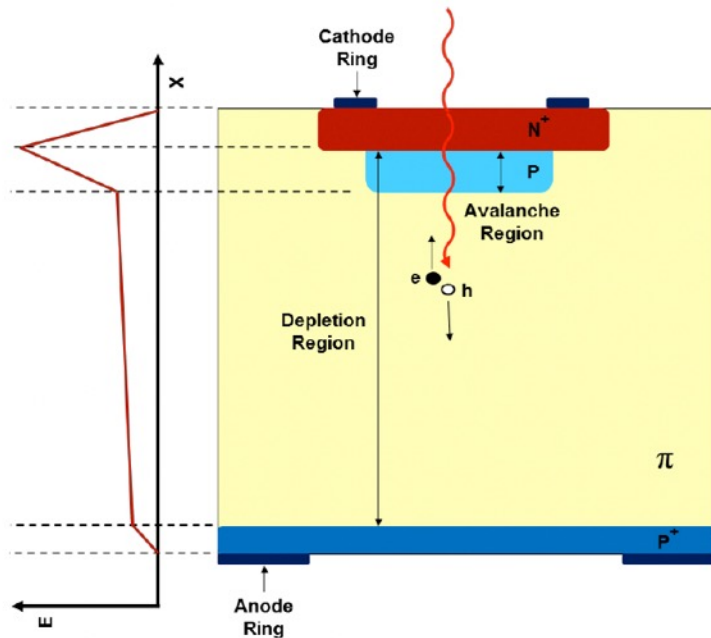


Figure 2.4: Top left: Set of  $11 \times 11 \times 3 \text{ mm}^3$  LYSO:Ce crystals with depolished lateral faces, before and after Teflon wrapping. Bottom left:  $6 \times 6 \text{ mm}^2$  HPK SiPMs glued on LYSO crystals. Right: Crystal+SiPM sensors plugged on the NINO board used for test beam studies.

# LGADs

Nicolo Cartiglia

- Achieve  $\approx 10$  ps timing resolution with Si detectors using charge amplification with Low-Gain Avalanche Detectors



**Lots of R&D, DC and AC coupled, chip design, test beams**

**Both ATLAS and CMS but also for Higgs factories etc**



# HL-LHC necessitates upgrades to the CMS detector

3

Experimental challenges	LHC	HL-LHC	General mitigation strategy
<ul style="list-style-type: none"> <li>• inst. luminosity</li> <li>• detector irradiation</li> <li>• pile-up interactions</li> </ul>	$2 \times 10^{34} \text{ s}^{-1} \text{ cm}^{-2}$ $O(10^{14} \text{ neq/cm}^2)$ $O(40)$	$\rightarrow$ up to $7.5 \times 10^{34} \text{ s}^{-1} \text{ cm}^{-2}$ $>O(10^{15} \text{ neq/cm}^2)$ 140-200	<ul style="list-style-type: none"> <li>• improved trigger &amp; computing</li> <li>• radiation-tolerant sensors &amp; electronics</li> <li>• timing and increased granularity</li> </ul>

## Compact Muon Solenoid (CMS) HL-LHC Upgrades

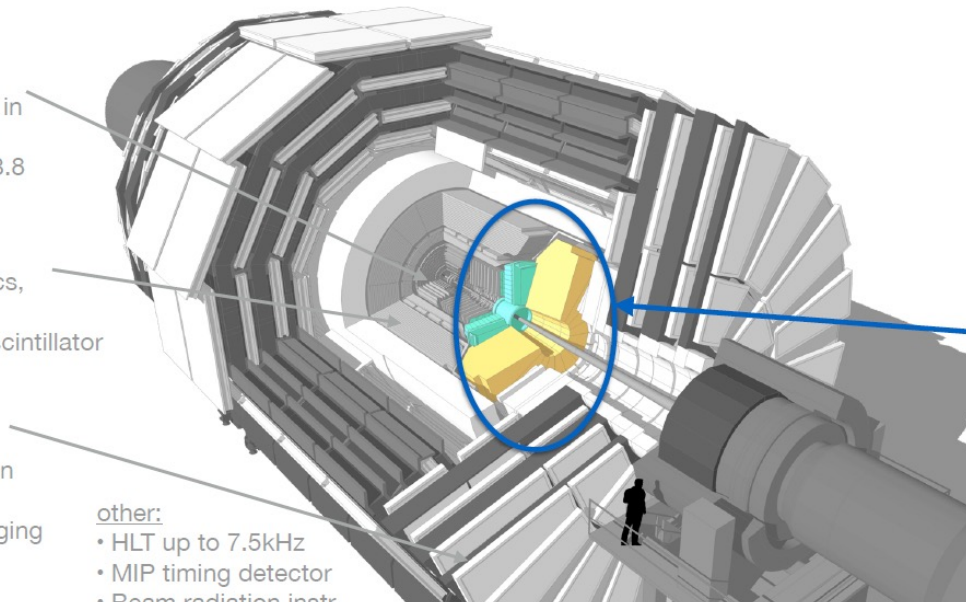
Tracker:  
Radiation tolerant,  
high granularity,  
less materials, tracks in  
hardware trigger (L1),  
coverage up to  $|\eta| = 3.8$

Barrel Calorimeter:  
New BE/FE electronics,  
ECAL: lower temp.,  
HCAL: partially new scintillator

Muon system:  
New electronics  
GEM/RPC coverage in  
 $1.5 < |\eta| < 2.8$ ,  
investigate muon tagging  
at  
higher  $\eta$

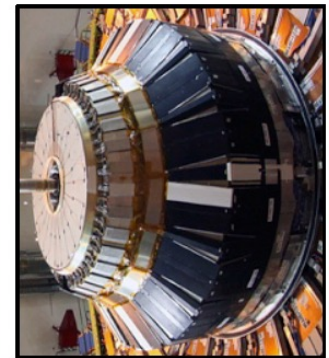
other:

- HLT up to 7.5kHz
- MIP timing detector
- Beam radiation instr.  
and luminosity



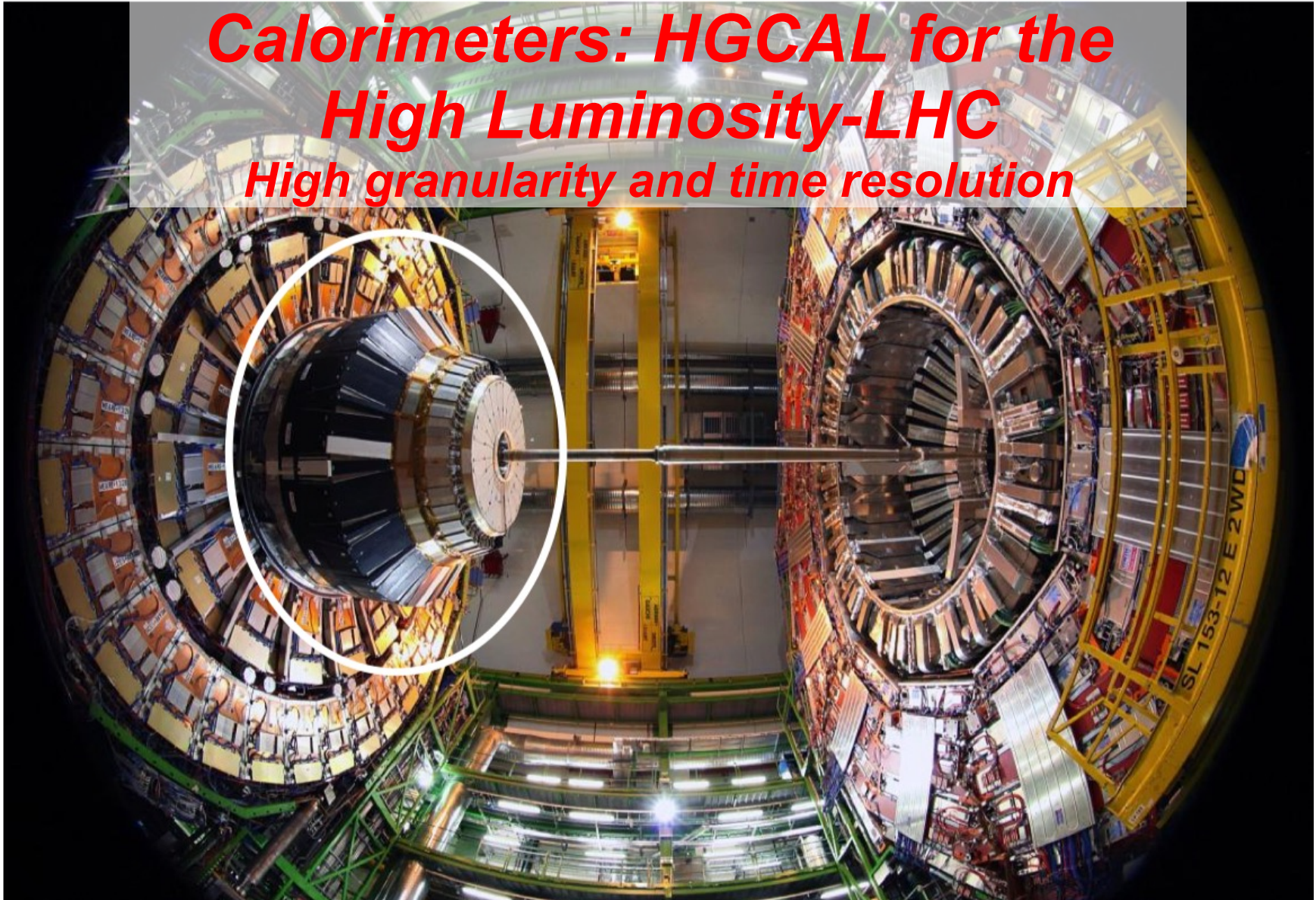
To be replaced  
for HL-LHC

**Endcap Calorimeters:**  
 $1.5 < |\eta| < 3.0$





# Calorimeters: HGCAL for the High Luminosity-LHC High granularity and time resolution

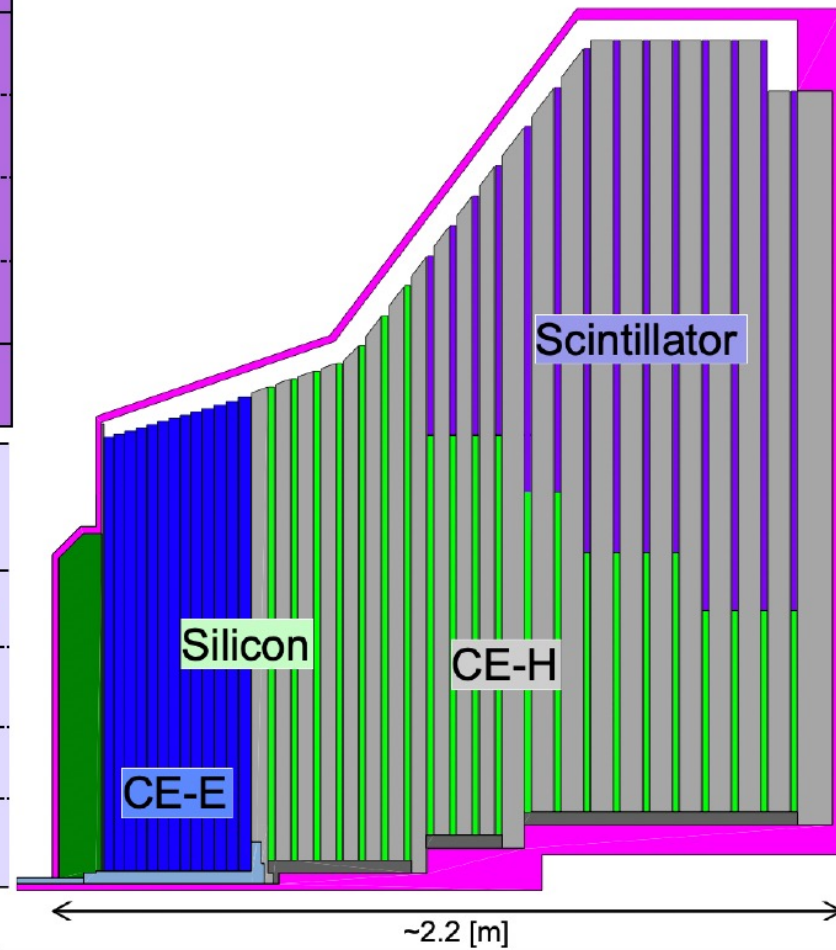




# Technology Choices

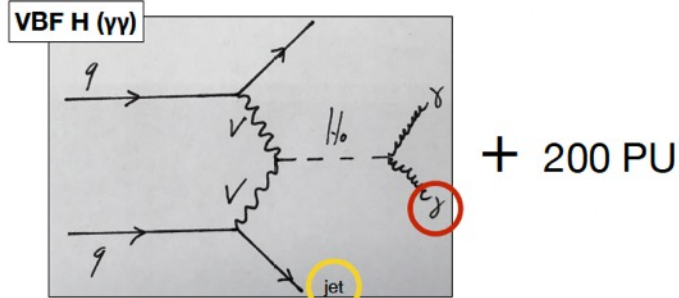
Both Endcaps	Silicon	Scintillator
Area	~620 m <sup>2</sup>	~370 m <sup>2</sup>
Channel Size	0.5 - 1.2 cm <sup>2</sup>	4 - 30 cm <sup>2</sup>
# Channels	~6 M	~240 k
# Modules	~27000	~4000
Op. Temp.	-30 C	-30 C

Per Endcap	CE-E	CE-H	
		Si	Si+Scint
Absorber	Pb, CuW, Cu	Stainless steel, Cu	
Depth	27.7 X <sub>0</sub>	10 λ	
Layers	26	7	14
Weight	23 t	205 t	

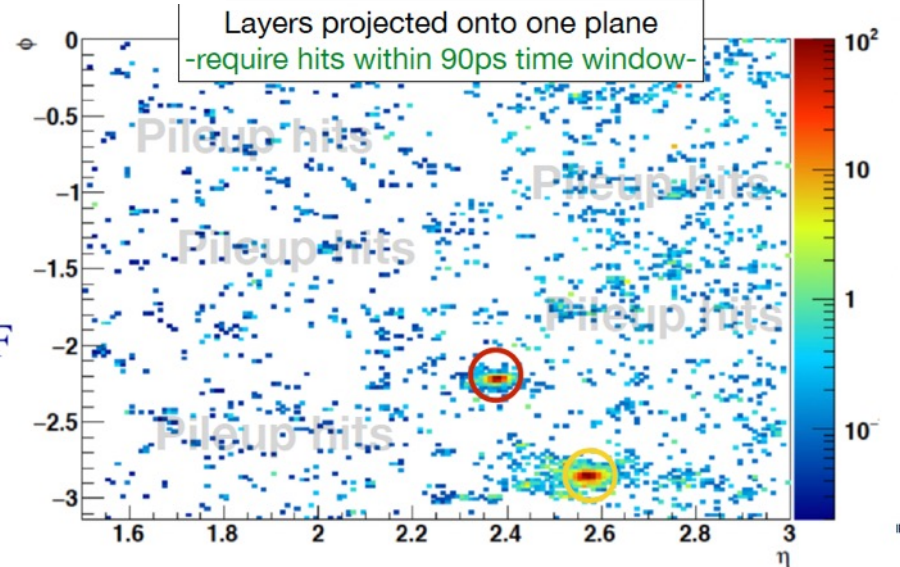
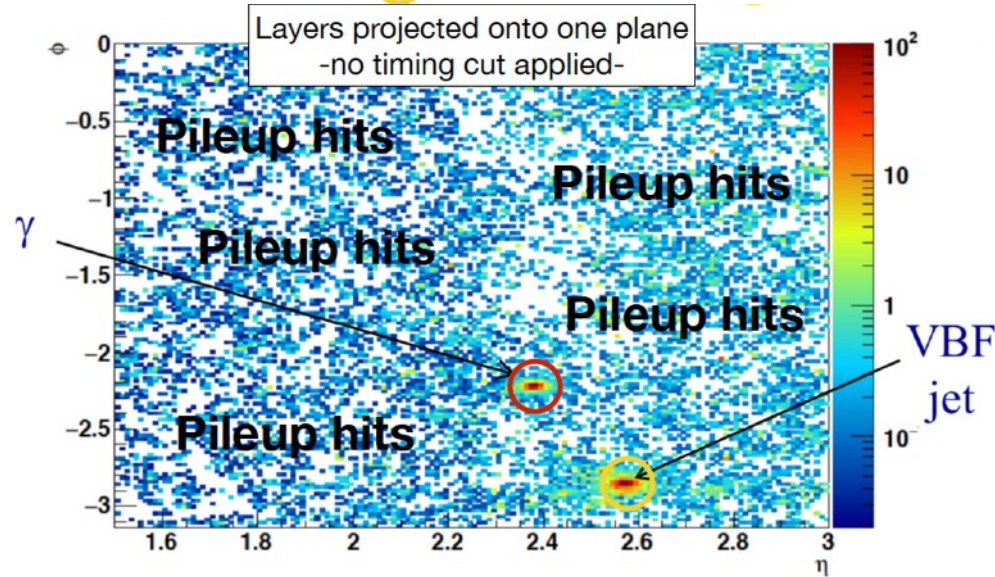


- Dissipated power ~250 kW
- Removed with two-phase CO<sub>2</sub> cooling operated at -35 C
- Geometry slightly adjusted since the TDR release

# Idea: HGCal will be 3D imaging calorimeter **with timing capabilities** 8



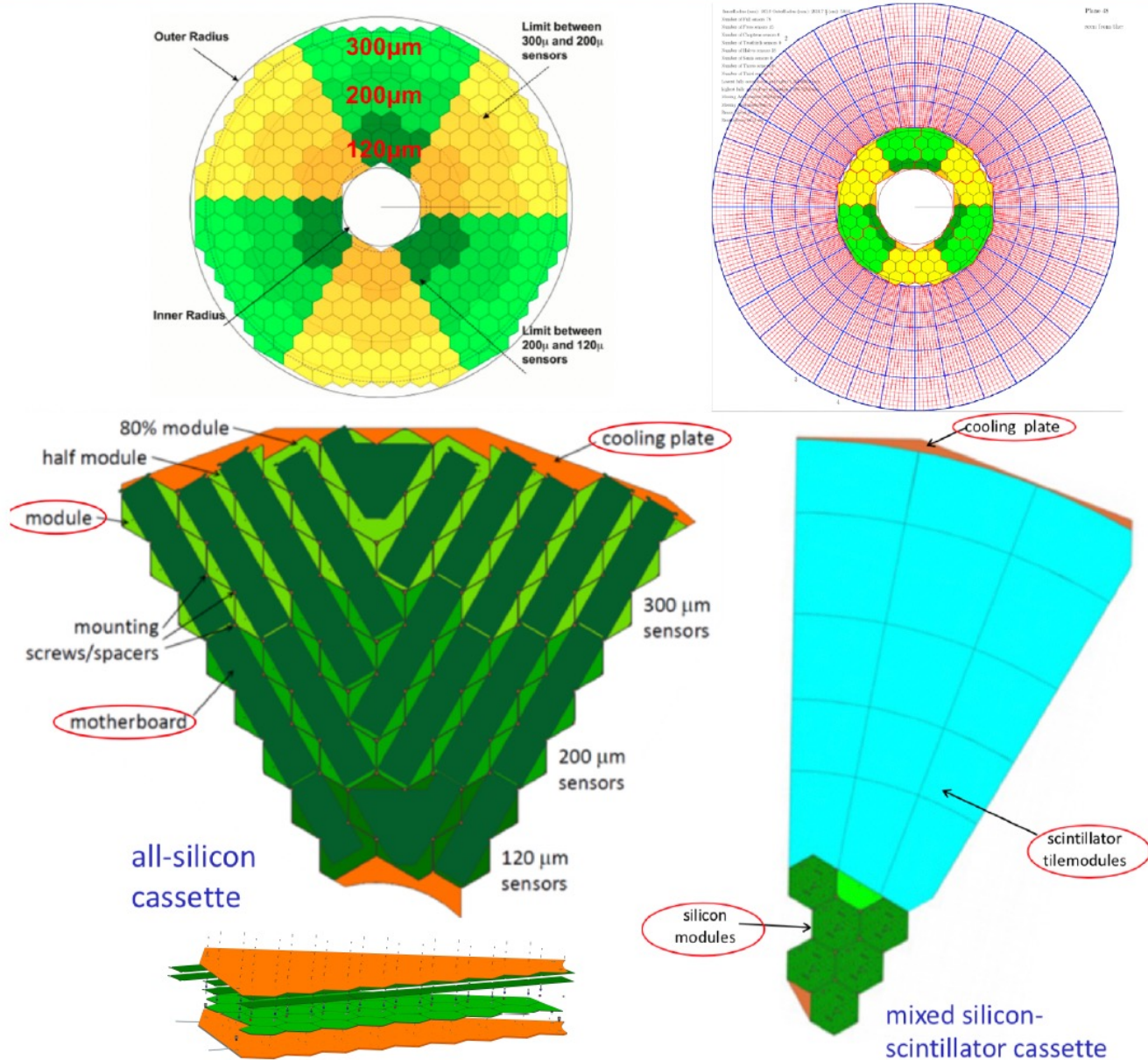
- Plots show cells with  $E > \sim 3.5$  MIPs, projected to the front face of the endcap calorimeter
- Concept: identify high-energy clusters, then make timing cut to retain hits of interest
- Design HGCal to obtain a  $\sim 30$ ps timing measurement for multi-MIP energy deposits





# Lateral Structure, Cassettes

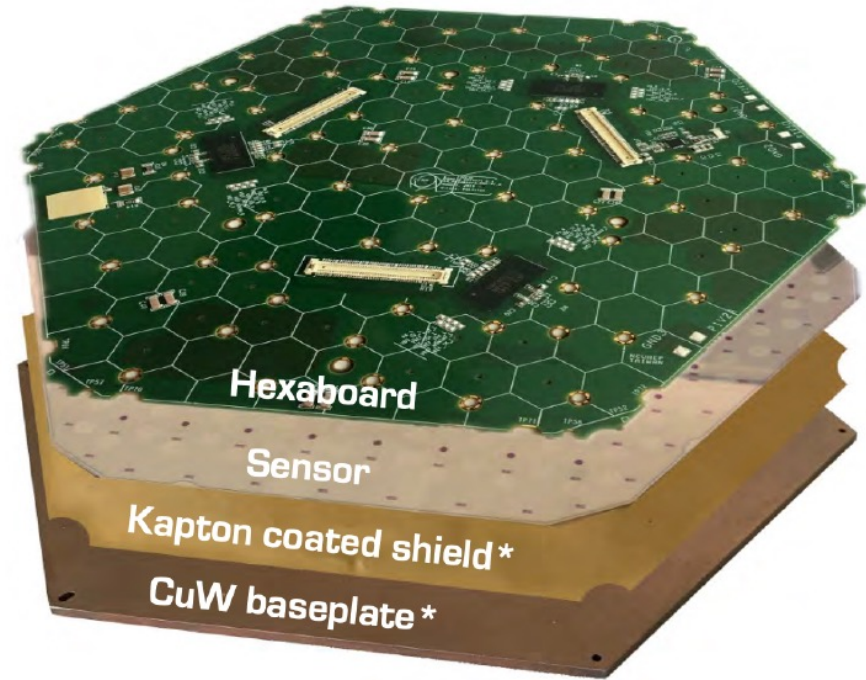
- Silicon and scintillator modules assembled into cassettes
- Supported and cooled by copper cooling plate
- Data from modules collected by motherboards
- Cassettes house all services and DC2DC converters





# Silicon Modules

- **Glued stack of baseplate, sensor and readout hexaboard**
- **baseplates are made of CuW in CE-E, PCB in CE-H**
- **Relative alignment within ~50um achieved with gantry based automated assembly**
- **Electrical connections are done with wire-bonds**

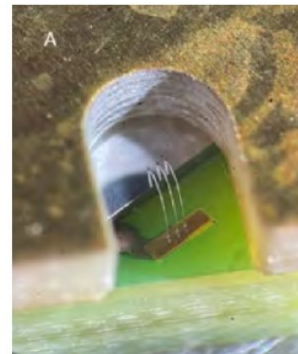
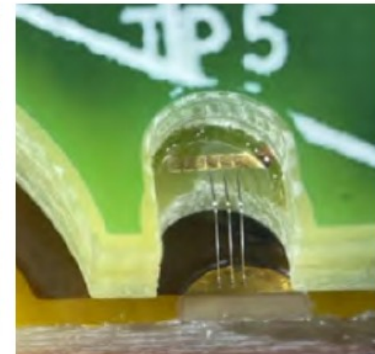
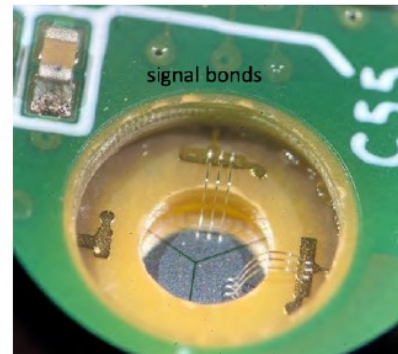
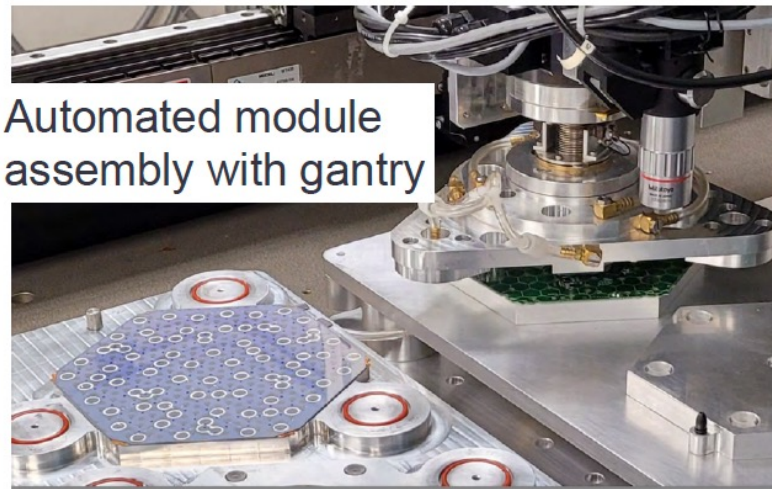


\* In CE-H, PCB baseplate with laminated Kapton™

signal bonds

shield bonds

backside HV bonds





# ***HGCAL for the High Luminosity-LHC is a very complex instrument***

# ***High purity segmented Ge-detectors for Nuclear physics***



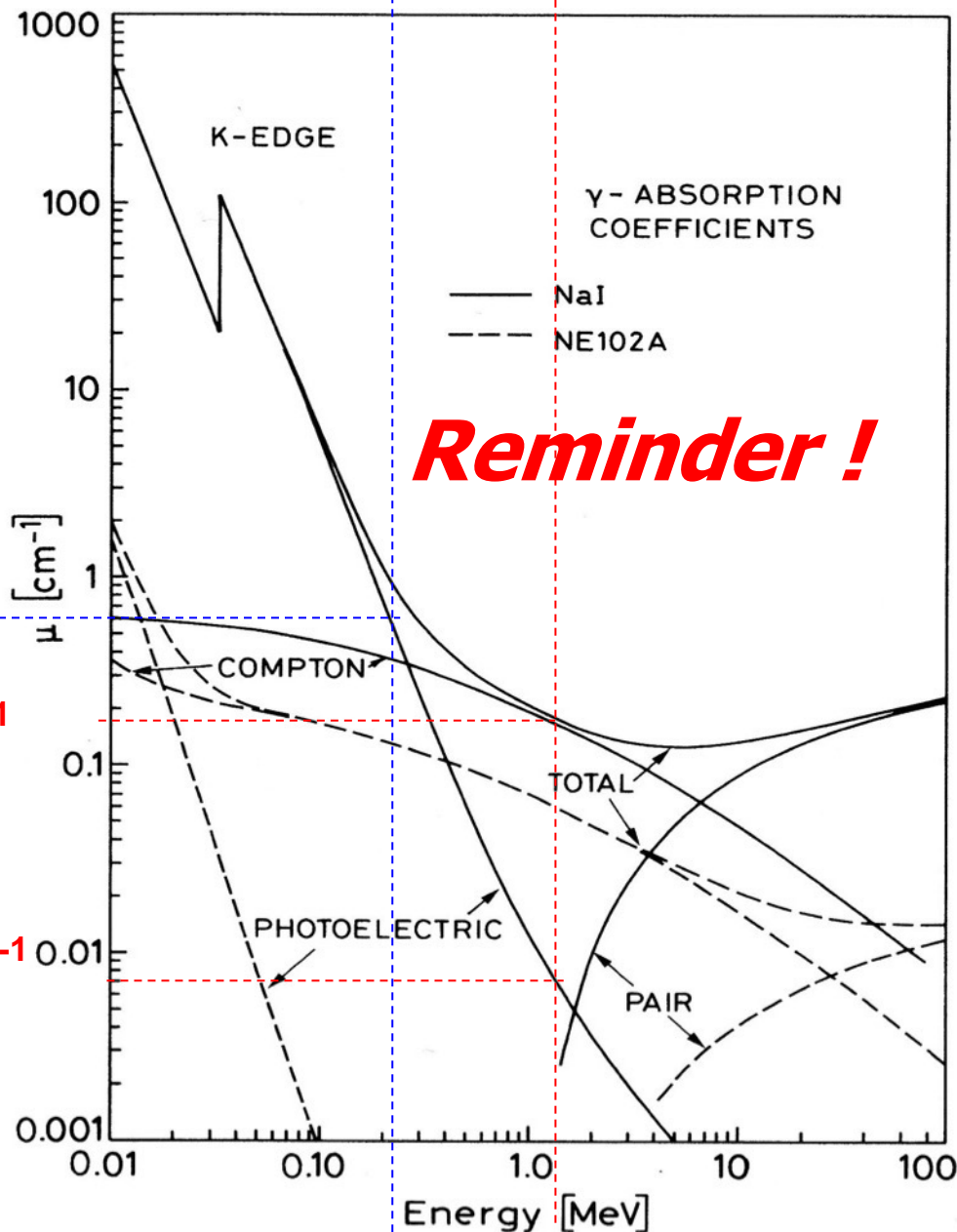


**Photo-electric effect**

**Absorption of  $\gamma$**

**Compton scattering**

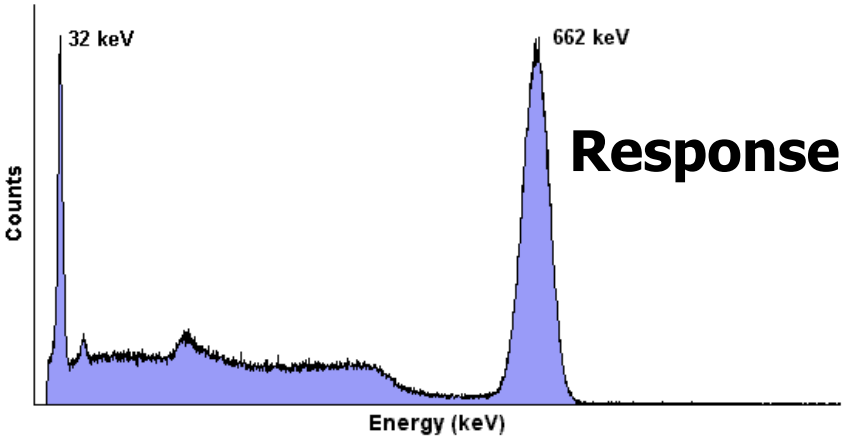
**scattering  $\gamma \rightarrow \gamma'$**

**Creation of  $(e^+e^-)$**

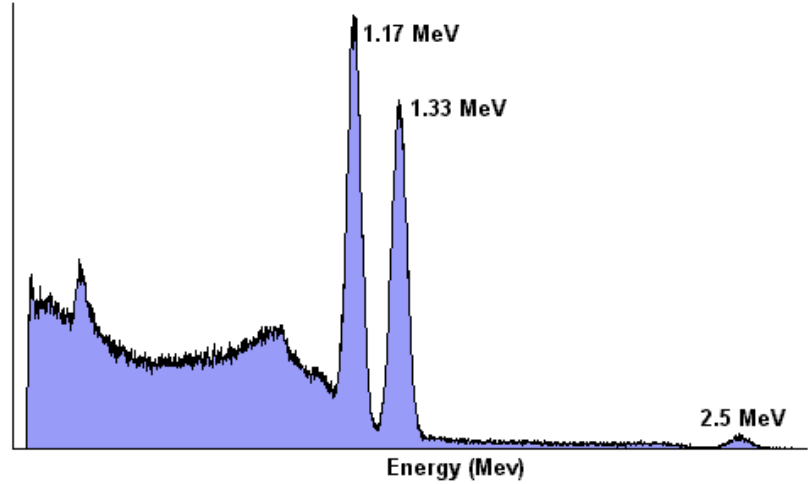
**pairs**

**Absorption of  $\gamma$**

76B76 NaI Detector:  $^{137}\text{Cs}$  Spectrum

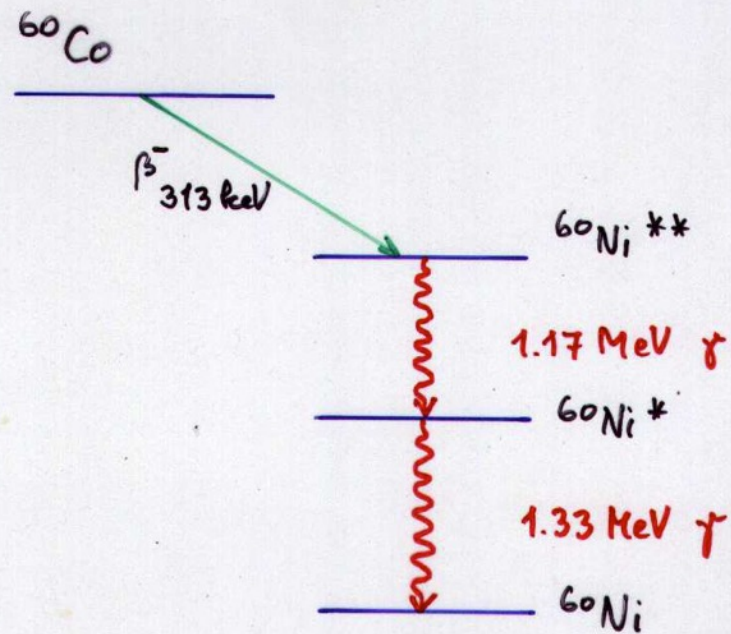
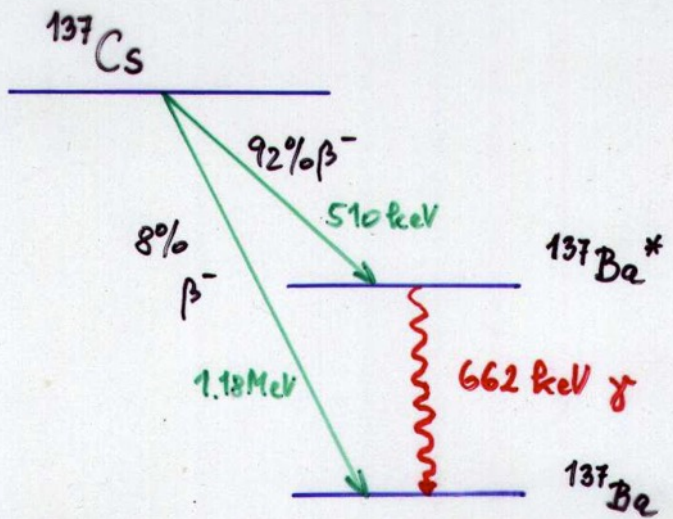


76B76 NaI Detector:  $^{60}\text{Co}$  Spectrum



# Response of NaI

Univ. of Tennessee, Dept. of Physics & Astronomy





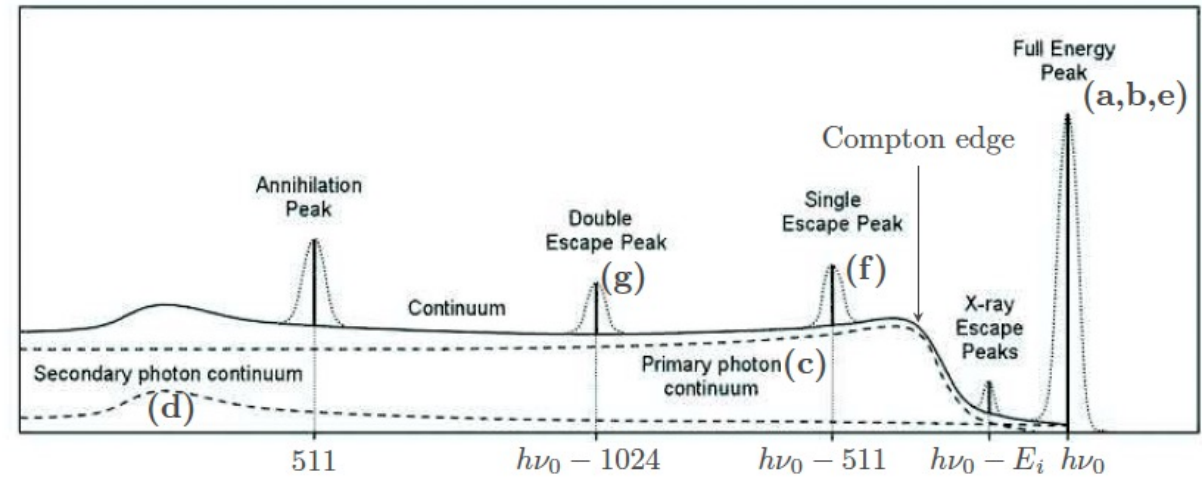


PHOTO-ELECTRIC EFFECT

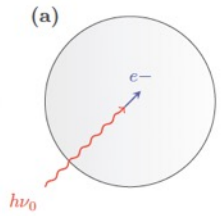
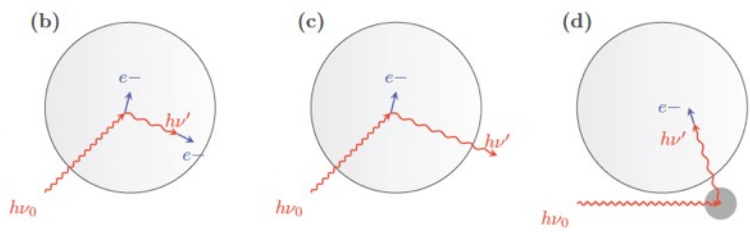
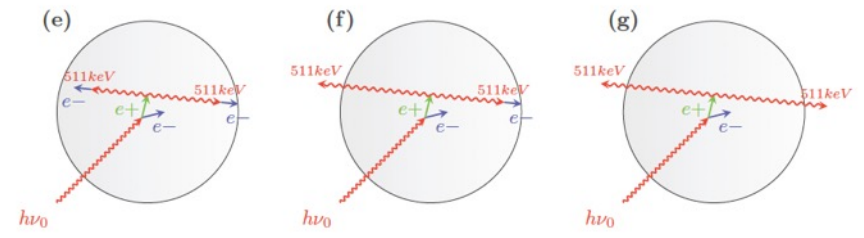


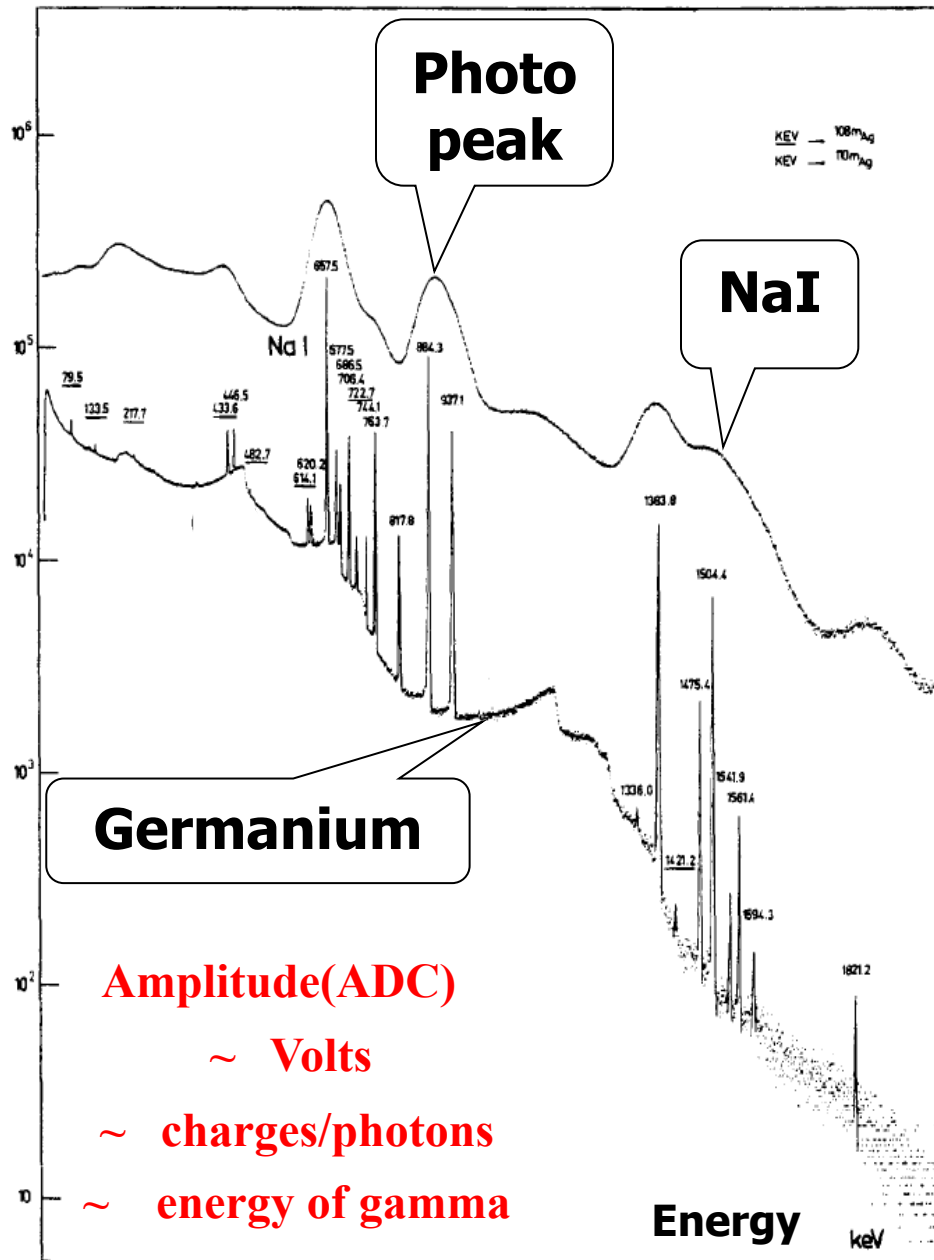
Figure 1.3: Effect of interaction processes on the predicted detector response peak function for mono-energetic  $\gamma$ -rays with  $h\nu_0 \gg 1.022\text{MeV}$ .

COMPTON SCATTERING



PAIR CREATION





**Large volume semi-conductor detector**



# Semi-conductor detectors

Material	$E_g$ [eV]	$w$ [eV]	Mobility (velocity/E)		$\tau_e$ [s]	$\tau_h$ [s]	density g/cm <sup>3</sup>	Z [a.m.u]
			$\mu_e$ [cm <sup>2</sup> /Vs]	$\mu_h$ [cm <sup>2</sup> /Vs]				
<b>C</b> (diamond)	5.5	13	1800	1200	$2 \cdot 10^{-9}$	$2 \cdot 10^{-9}$	3.515	6
<b>Si</b>	1.12	3.61	1350	480	$5 \cdot 10^{-3}$	$5 \cdot 10^{-3}$	2.33	14
<b>Ge</b>	0.67	2.98	3900	1900	$2 \cdot 10^{-5}$	$2 \cdot 10^{-5}$	5.32	32
<b>GaAs</b>	1.42	4.70	8500	450	$5 \cdot 10^{-8}$	$5 \cdot 10^{-8}$	5.32	31,33
<b>CdTe</b>	1.56	4.43	1050	100	$1 \cdot 10^{-6}$	$1 \cdot 10^{-6}$		48,52
<b>HgI<sub>2</sub></b>	2.13	4.20	100	–	$1 \cdot 10^{-6}$	$2 \cdot 10^{-6}$		53,80

$$\frac{dN}{N} = \frac{1}{\sqrt{N}} ; E \sim N ; N = \text{numb. of (e,h)}$$

Parameters Values for Materials Used in Fabricating Semiconductor Radiation Sensors

[3]

# Inverse Polarisation

Holes move to « - »

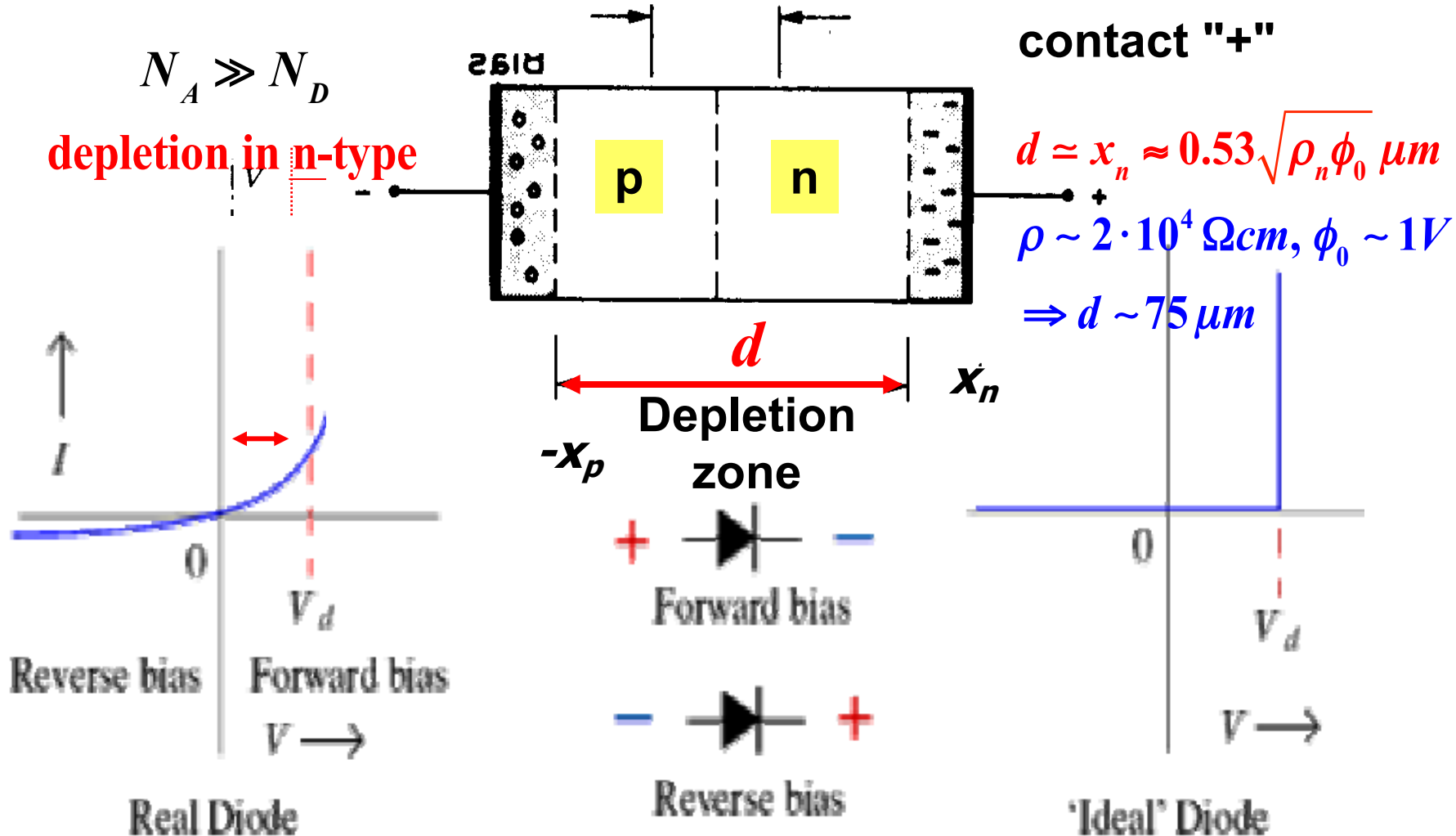
$$d|_{V_{bias}} = x_n + x_p = \sqrt{\frac{2\epsilon(\phi_0 + V_{bias})}{e} \frac{(N_A + N_D)}{N_A N_D}}$$

electrons move to contact "+"

$$N_A \gg N_D$$

depletion in n-type

I  
c





# Large volume detectors

## Depletion zone :

$$d|_{V_{bias}} = x_n + x_p = \sqrt{\frac{2\varepsilon(\phi_0 + V_{bias})(N_A + N_D)}{e N_A N_D}}$$

$$N = N_A \ll N_D; \phi_0 \ll V_{bias}$$

$$d|_{V_{bias}} = \sqrt{\frac{2\varepsilon V_{bias}}{eN}}; N = N_A \text{ ou } N_D = \text{net impurity of material}$$

$$N = 10^{+13} \text{ atoms / cm}^3; V_{bias} = 3000 \text{ Volt};$$

$$d|_{V_{bias}=3000 \text{ Volt}} = 2.2 \text{ mm}$$

## High purity :

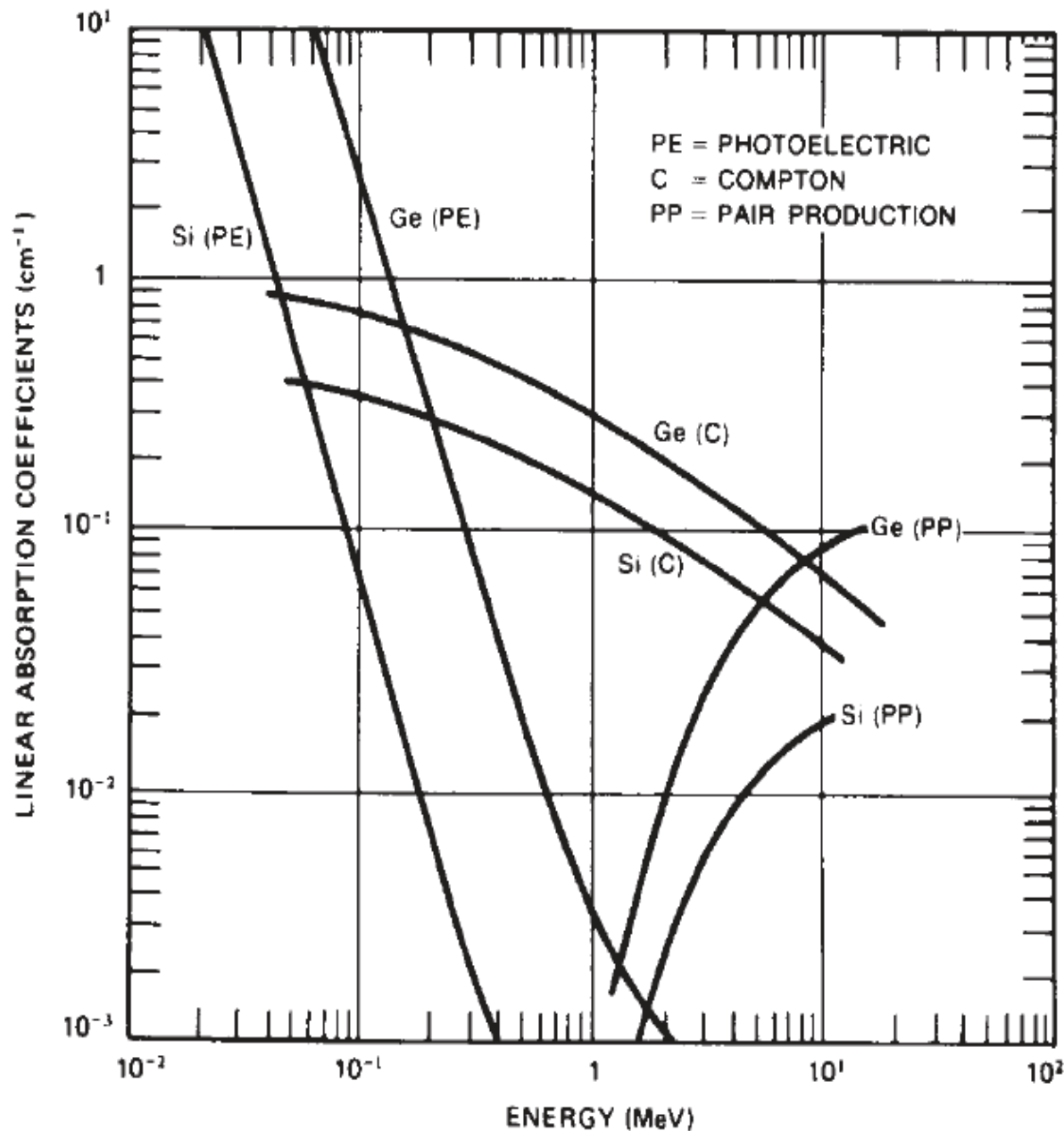
$$N_A \text{ ou } N_D = 10^{+10} \text{ atoms / cm}^3; V_{bias} = 1000 \text{ Volt}; \varepsilon = 16 \cdot \varepsilon_0;$$

$$\varepsilon_0 = 8.85 \cdot 10^{-12} \text{ F / m}; F = \text{Coulomb / Volt}; e = 1.6 \cdot 10^{-19} \text{ Coulomb}$$

$$d|_{V_{bias}=1000 \text{ Volt}} = 1.8 \text{ cm}$$

$$d|_{V_{bias}=2000 \text{ Volt}} = 2.5 \text{ cm}$$

$$d|_{V_{bias}=3000 \text{ Volt}} = 3.1 \text{ cm}$$



## High Purity Germanium

### Energy measurement of gammas

( $|N_A - N_D| \cong 10^{10} \text{ cm}^{-3}$ ):

- $E_{\text{gap}} = 0.74 \text{ eV} \Rightarrow$   
operation temperature  
:  $T = 77\text{K}$
- $w_{\text{eh}} = 2.98 \text{ eV}$   
 $\Rightarrow$  excellent resolution
  - $E_\gamma = 1 \text{ MeV}, dE \cong 1 \text{ keV}$
  - “High” photo peak efficiency

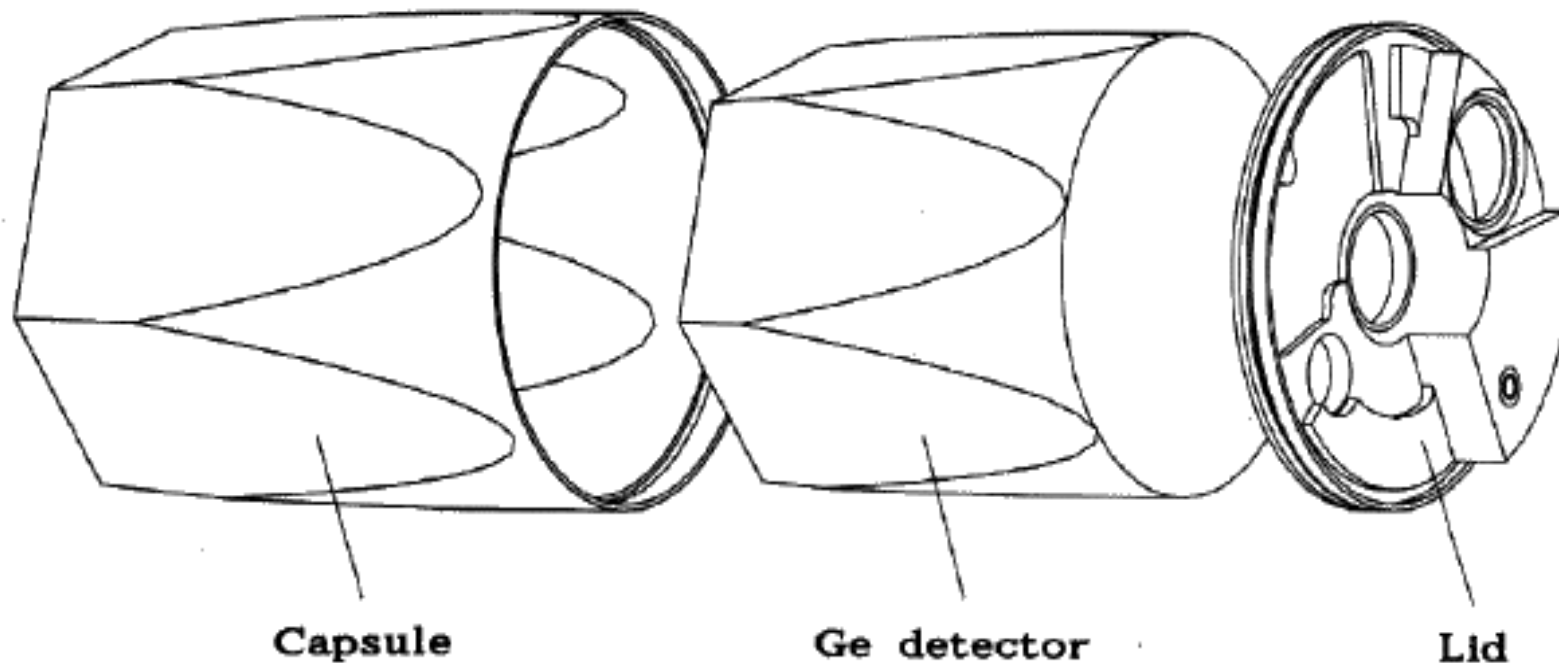


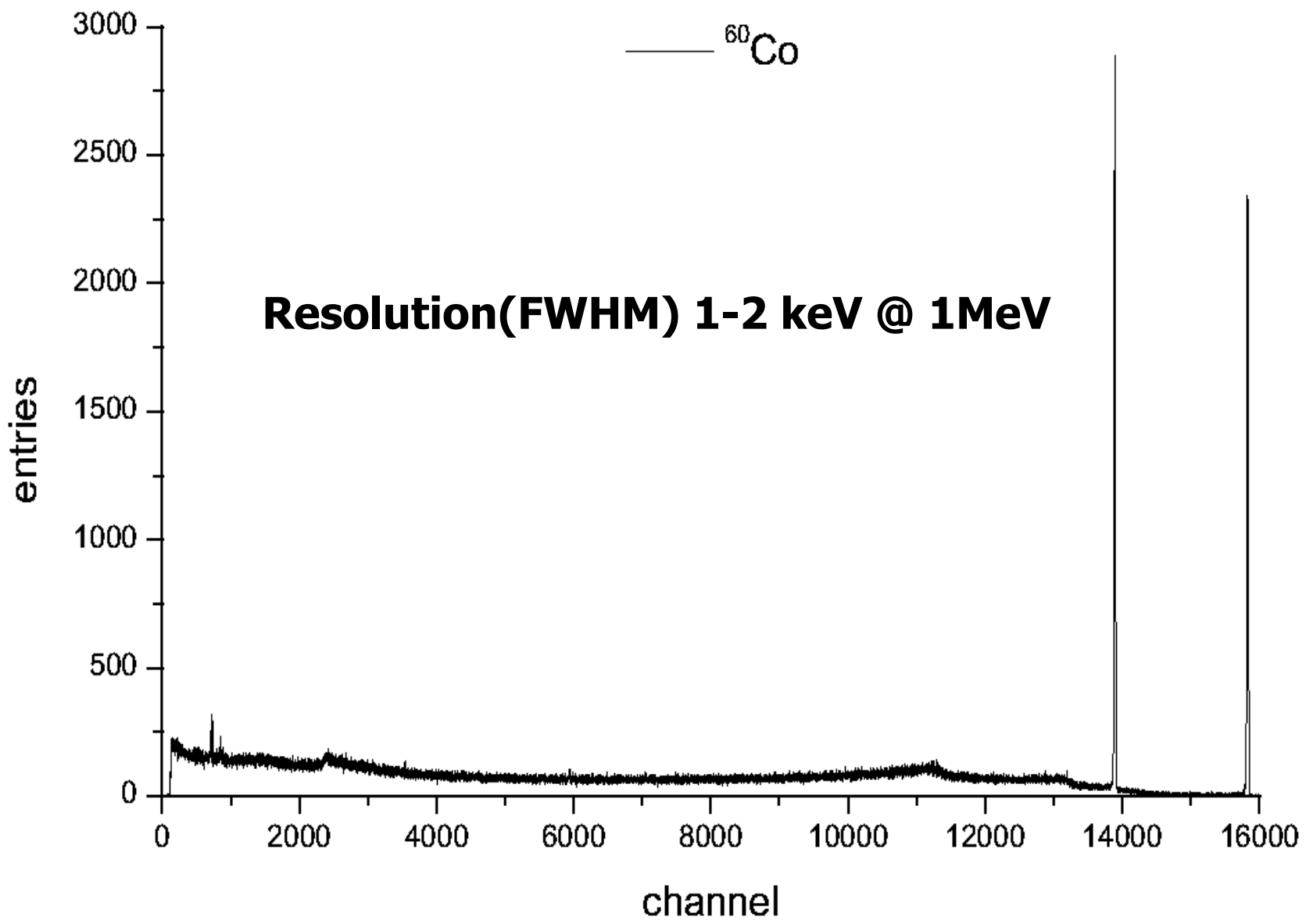
# Germanium detectors

Operation temperature:  $T = 77\text{K}$  (Liquid Nitrogen)

Configuration : co-axial

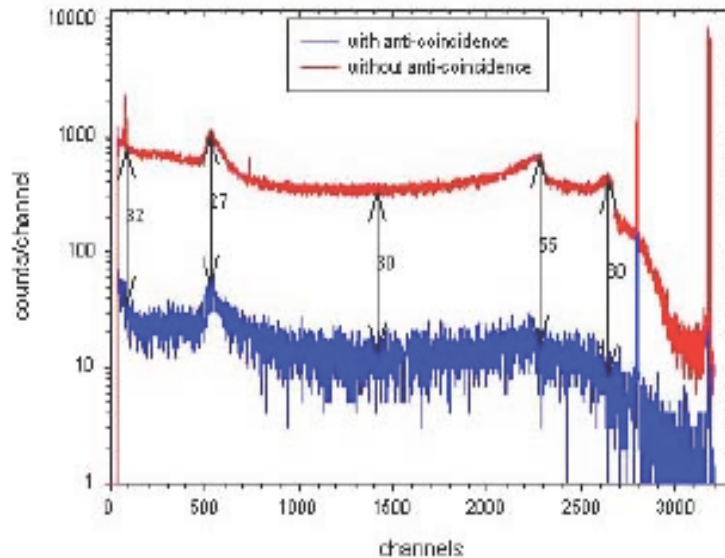
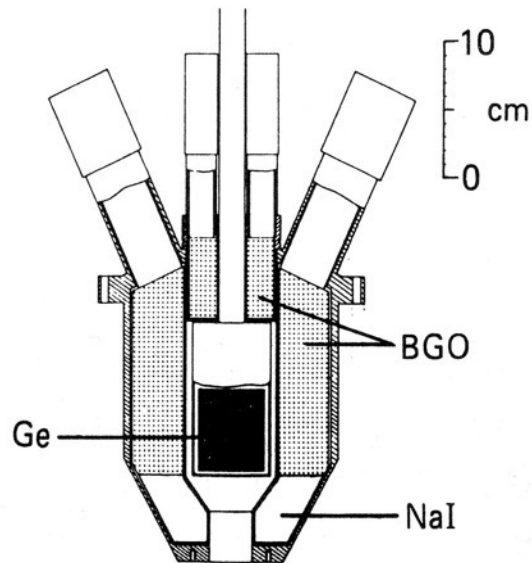
Electronics is mounted very close to the Crystal



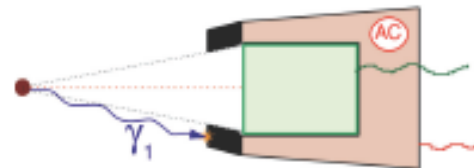




## incidence : système anti-Compton

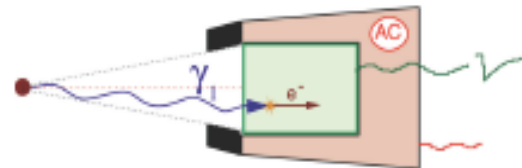


### Événement Collimaté



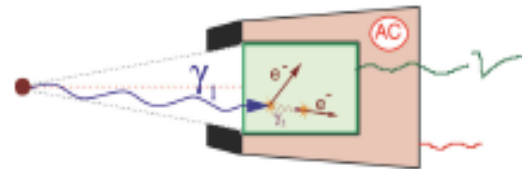
Pas de mesure

### Effet photoélectrique



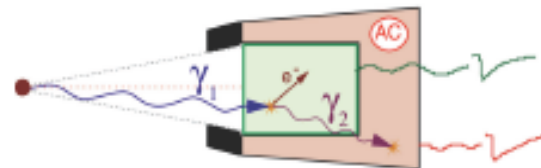
Validé

### Compton interne



Validé

### Echappement Compton



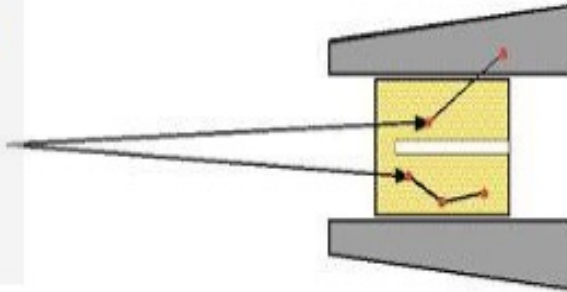
Rejeté

# The idea of $\gamma$ -ray tracking

## Compton Shielded Ge

$\epsilon_{\text{ph}} \sim 10\%$   
 $N_{\text{det}} \sim 100$

$\Omega \sim 40\%$   
 $\theta \sim 8^\circ$



large opening angle  
means poor energy  
resolution at high  
recoil velocity.

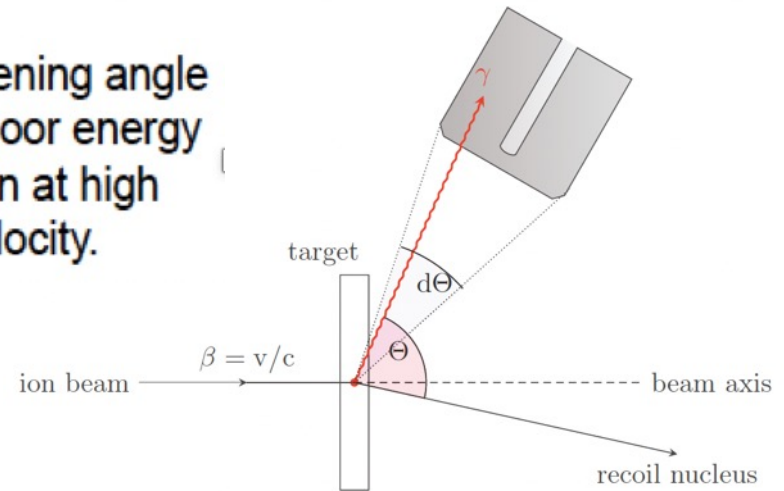


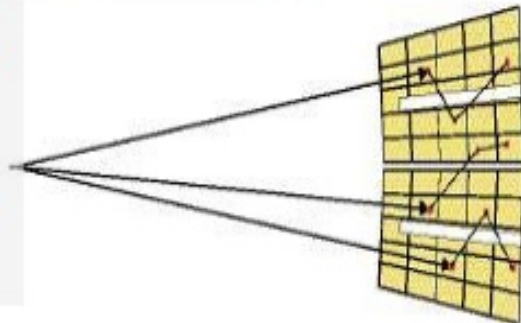
Figure 1.12: Doppler broadening

Previously scattered gammas were wasted.  
Technology is available now to track them.

## Ge Tracking Array

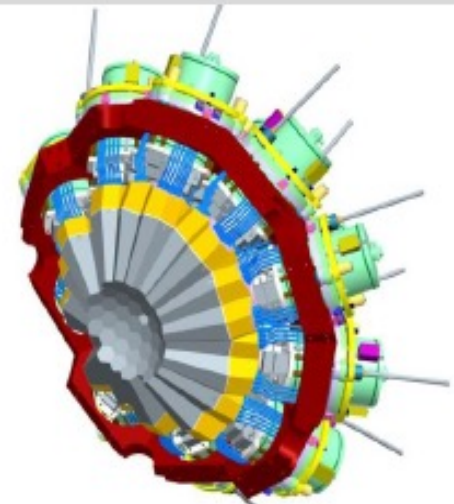
$\epsilon_{\text{ph}} \sim 50\%$   
 $N_{\text{det}} \sim 100$

$\Omega \sim 80\%$   
 $\theta \sim 1^\circ$



Combination of:

- segmented detectors
- digital electronics
- pulse processing
- tracking the  $\gamma$ -rays

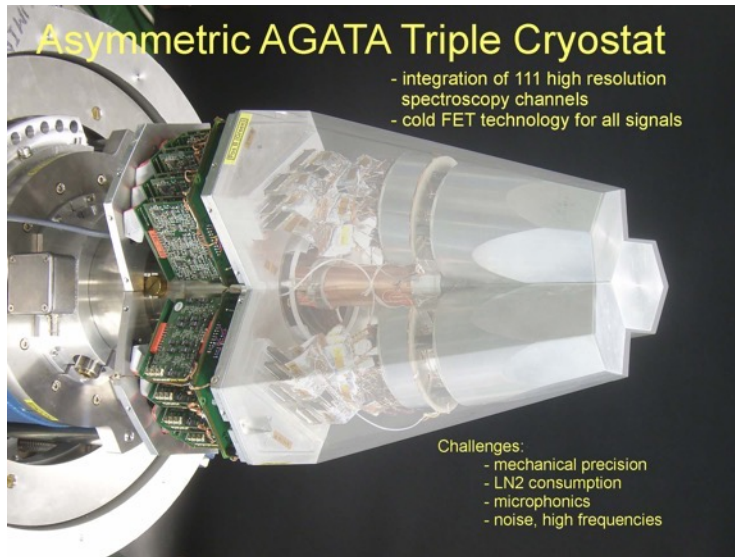




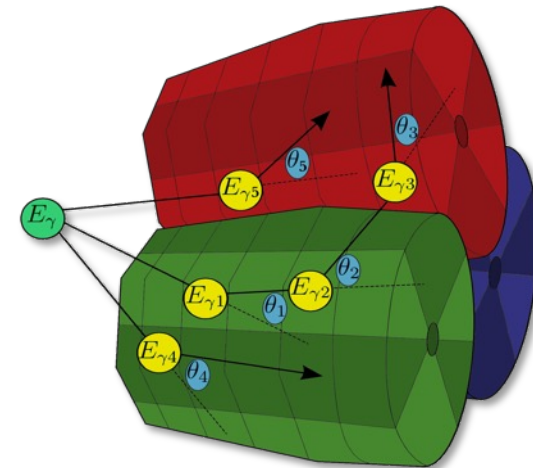
# What is AGATA?



13 Countries, > 40 Institutions



- **Solid Sphere of Ge material: Solid angle coverage  $\sim 82\%$**
- **36-fold segmentation of crystal**
- **Track each gamma interaction through the crystal**
- **Reconstruct and disentangle gammas**



Rates	3 MHz ( $M_\gamma = 1$ )	300 kHz ( $M_\gamma = 30$ )
Efficiency	43% ( $M_\gamma = 1$ )	28% ( $M_\gamma = 30$ )
Peak/Total	58% ( $M_\gamma = 1$ )	49% ( $M_\gamma = 30$ )
Angular Resolution	$\sim 1^\circ$	
FWHM (1MeV), $v/c = 50\%$	$\sim 6\text{keV}$	

180 hexagonal crystals: 3 shapes

3 fold clusters (cold FET): 60 all equal

Inner radius (Ge): 23.5 cm

Amount of germanium: 362 kg

36-fold segmentation

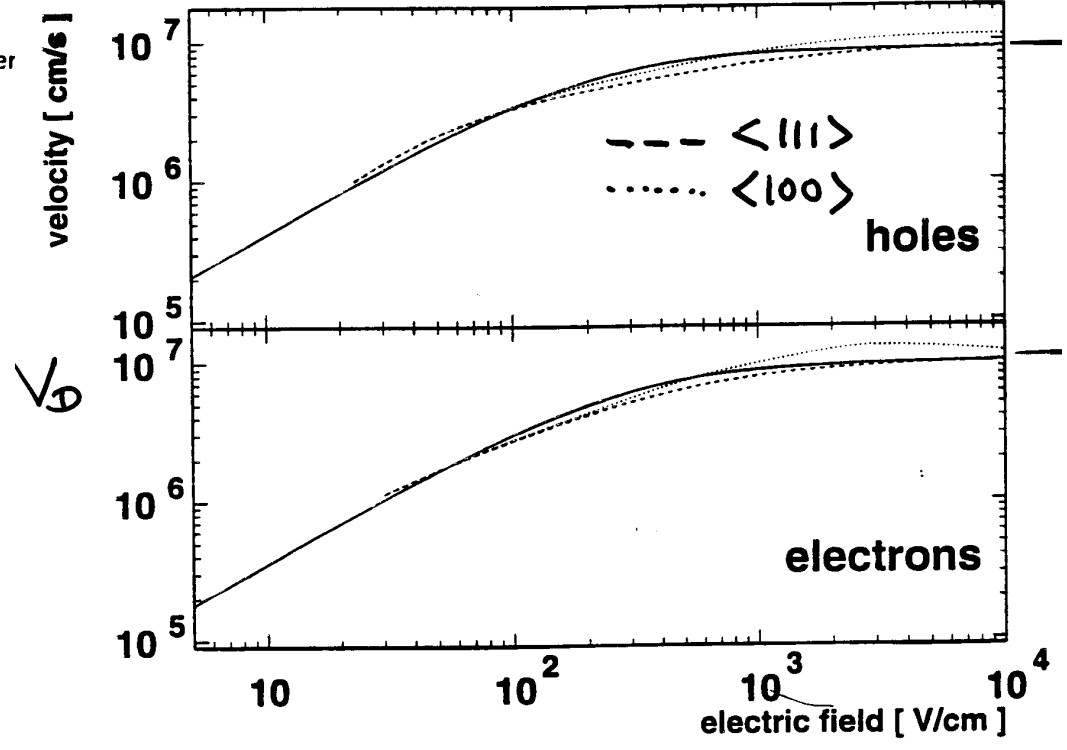
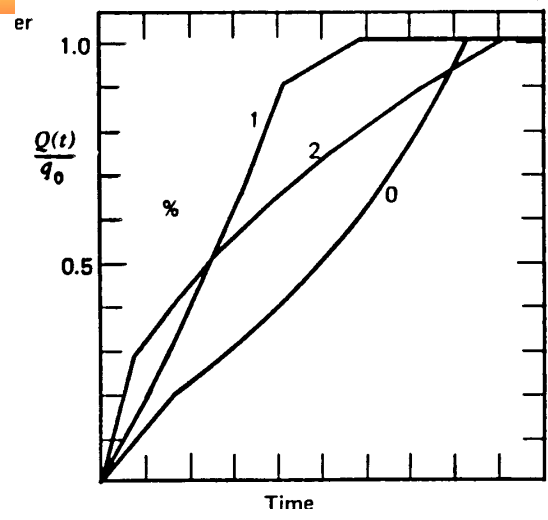
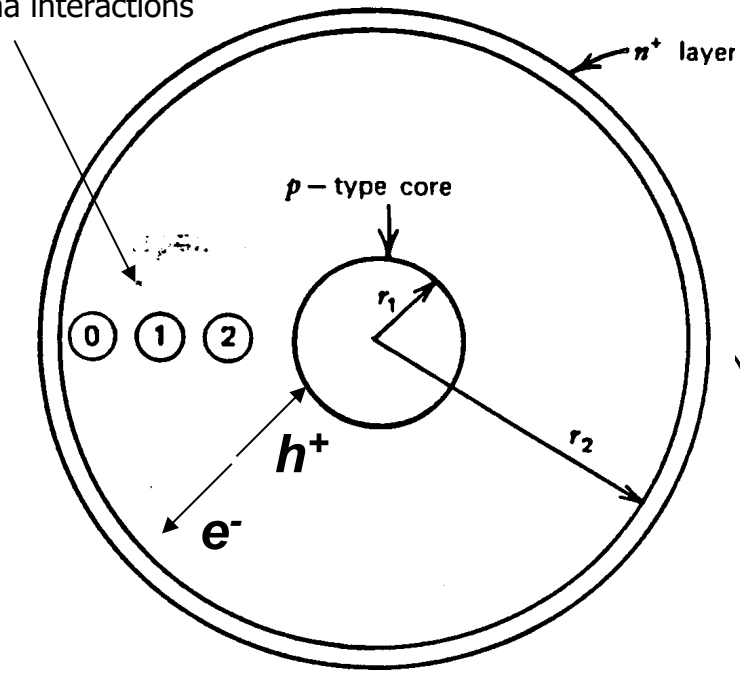
6480 segments



# signal formation in Ge-HP

## Cylindrical geometry

Gamma interactions





# Segmentation of High Purity Ge crystal

Divide the electrodes on the surface of the detector

Weighting field shows how the segmentation works

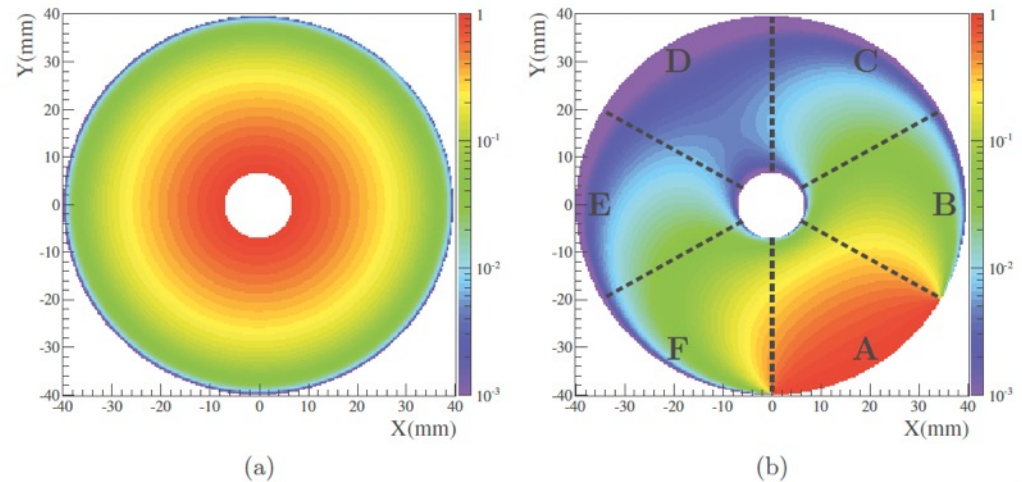
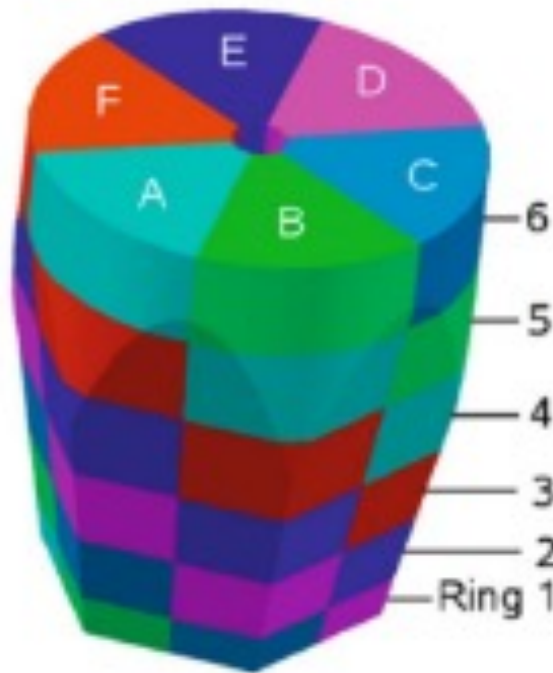


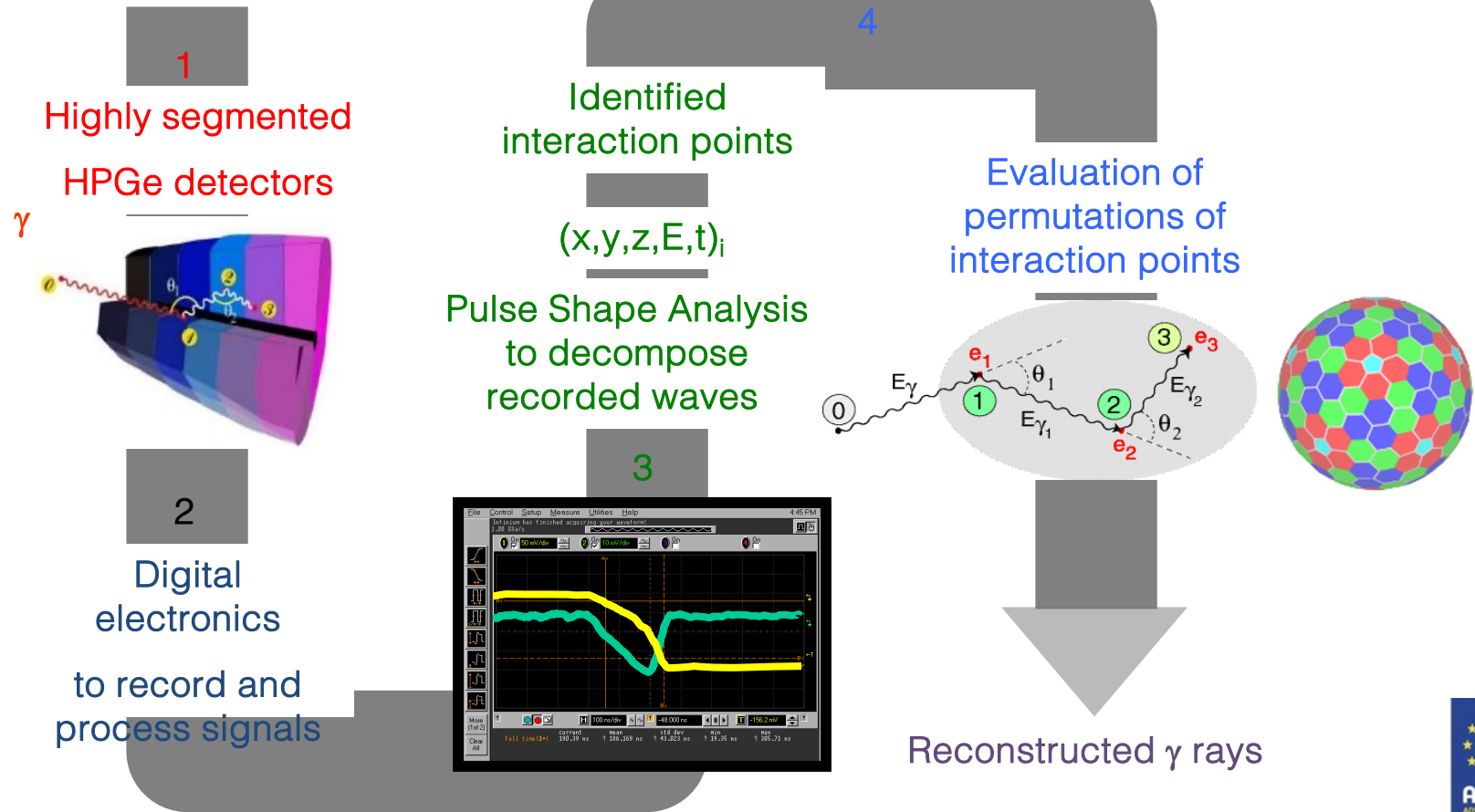
Figure 2.2: Weighting-potential distributions of the Core (a) and of segment A (b). Calculation conditions are the following: readout electrode at unit potential, all other electrode at zero potential, no space charge inside the material.

$$Q(t) = -q \cdot [\phi_w(x_h(t)) - \phi_w(x_e(t))]$$

$$i(t) = q \cdot [E_w(x_h(t)) \cdot v_h(t) - E_w(x_e(t)) \cdot v_e(t)]$$

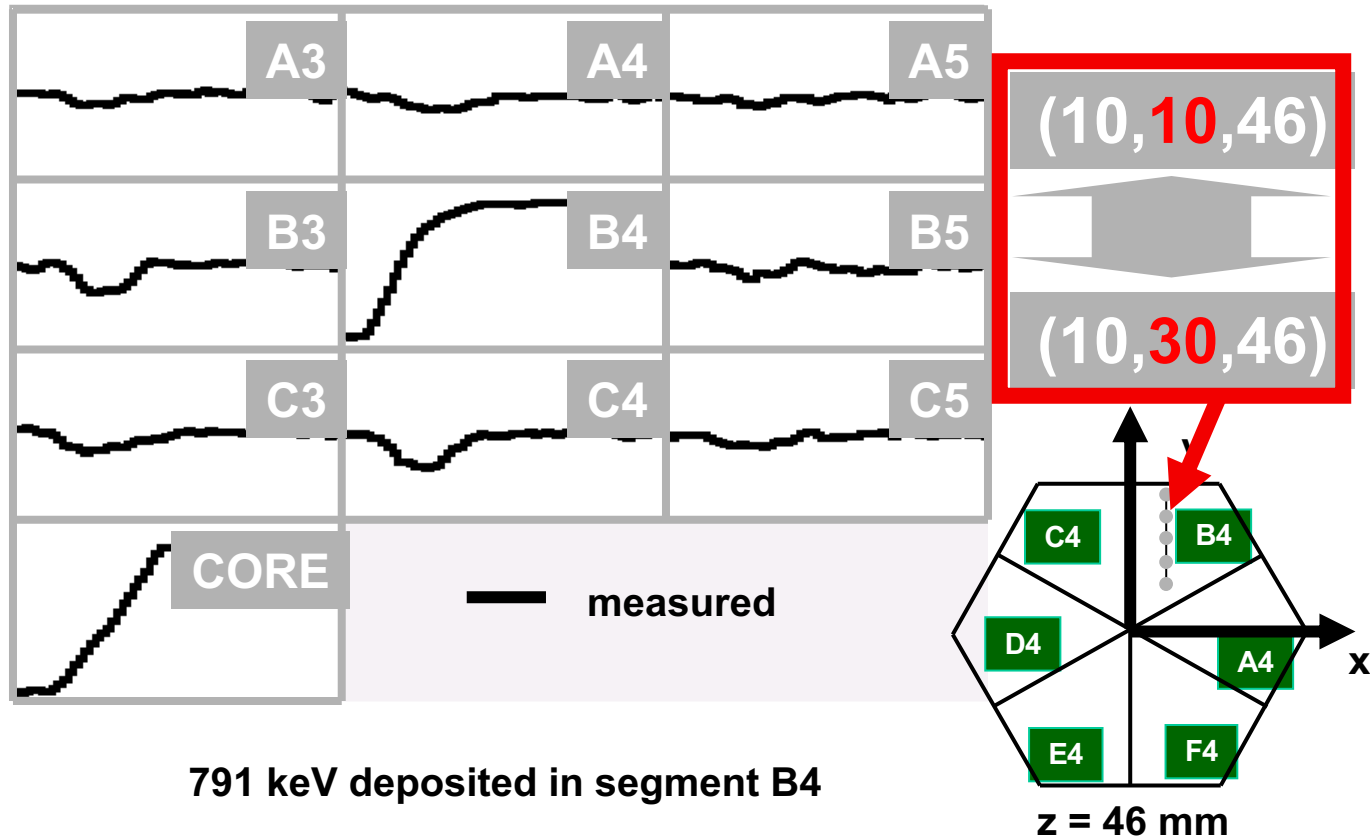
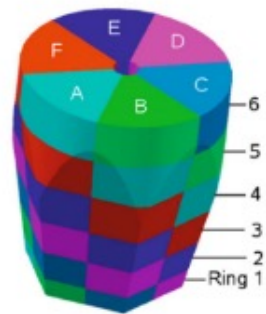
$\phi_w$  and  $E_w$  are the weighting potential and the weighting field.

# AGATA Tracking Concept

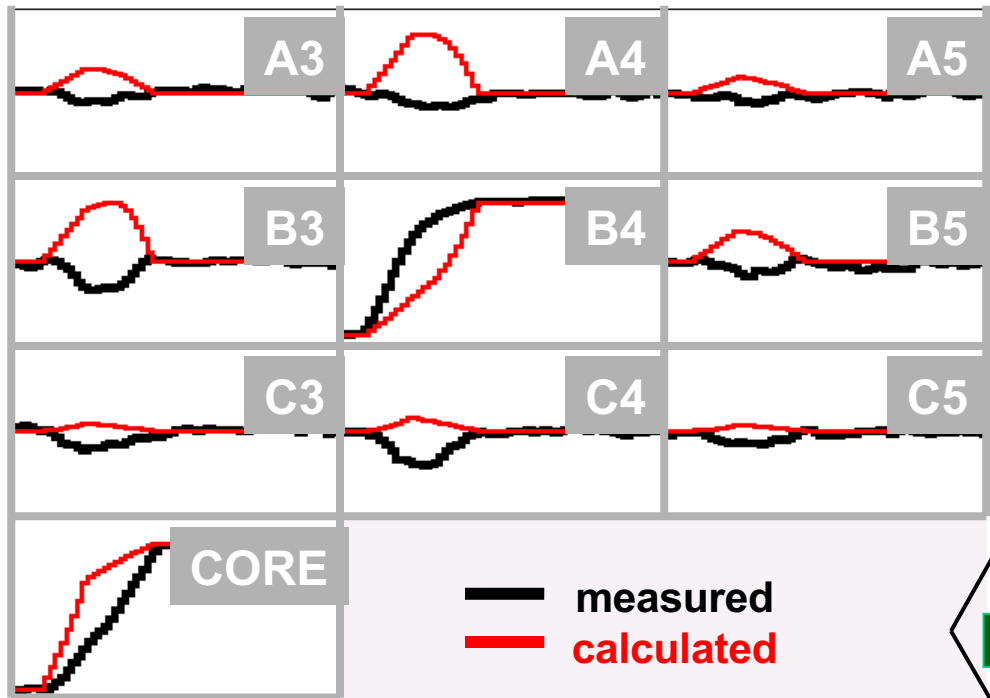




# Pulse Shape Analysis Concept

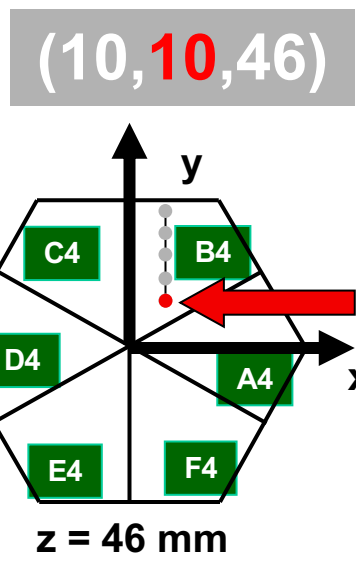


# Pulse Shape Analysis Concept

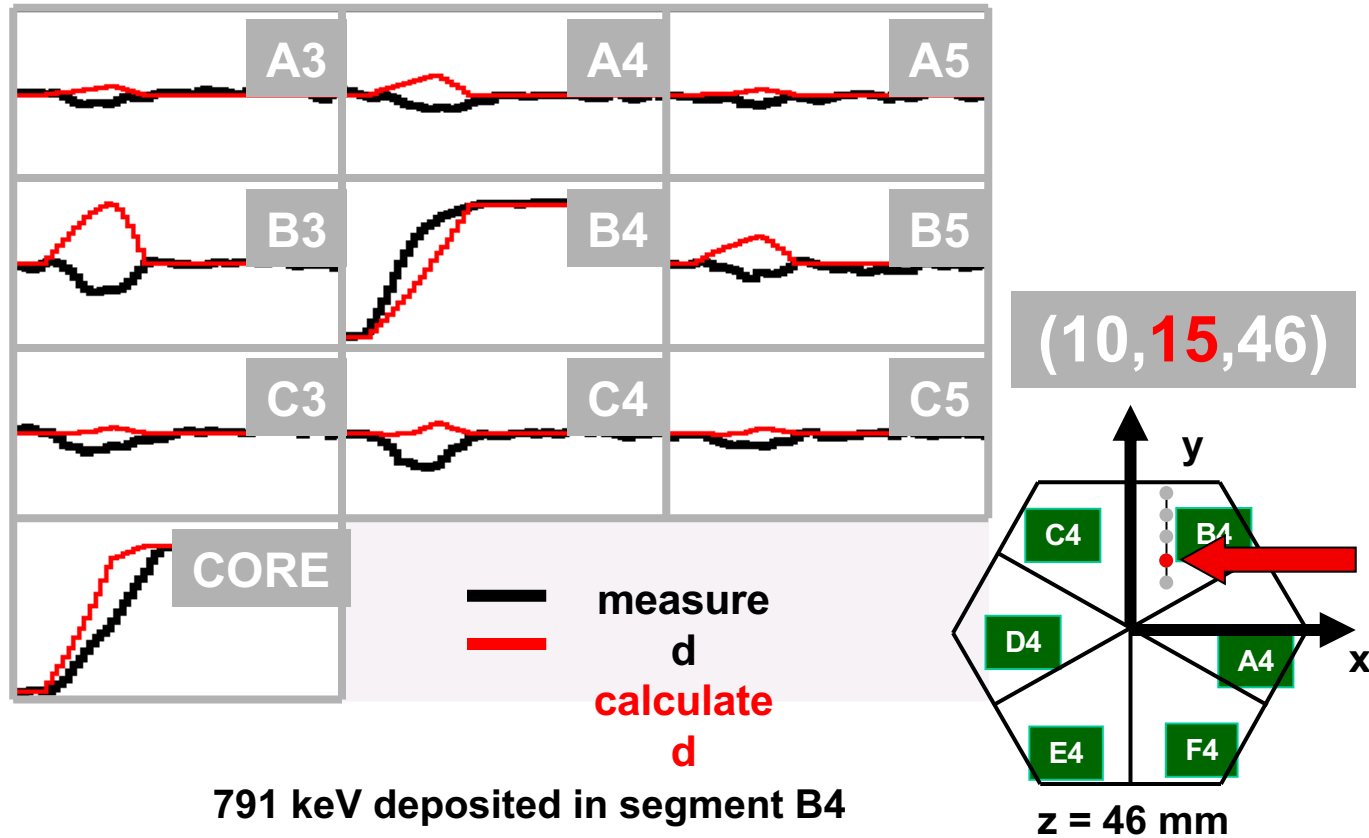


791 keV deposited in segment B4

Calculated from Electric field simulation

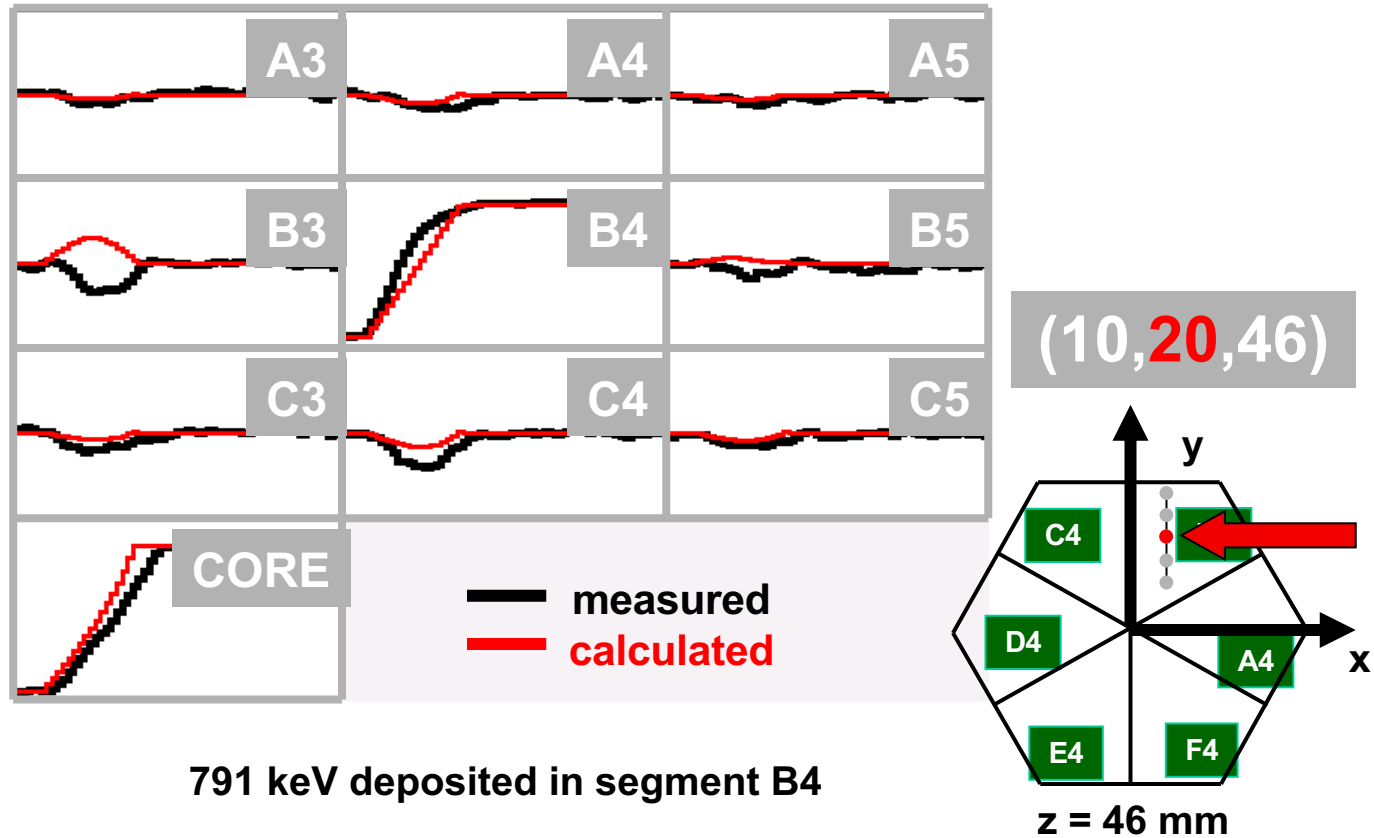


# Pulse Shape Analysis Concept

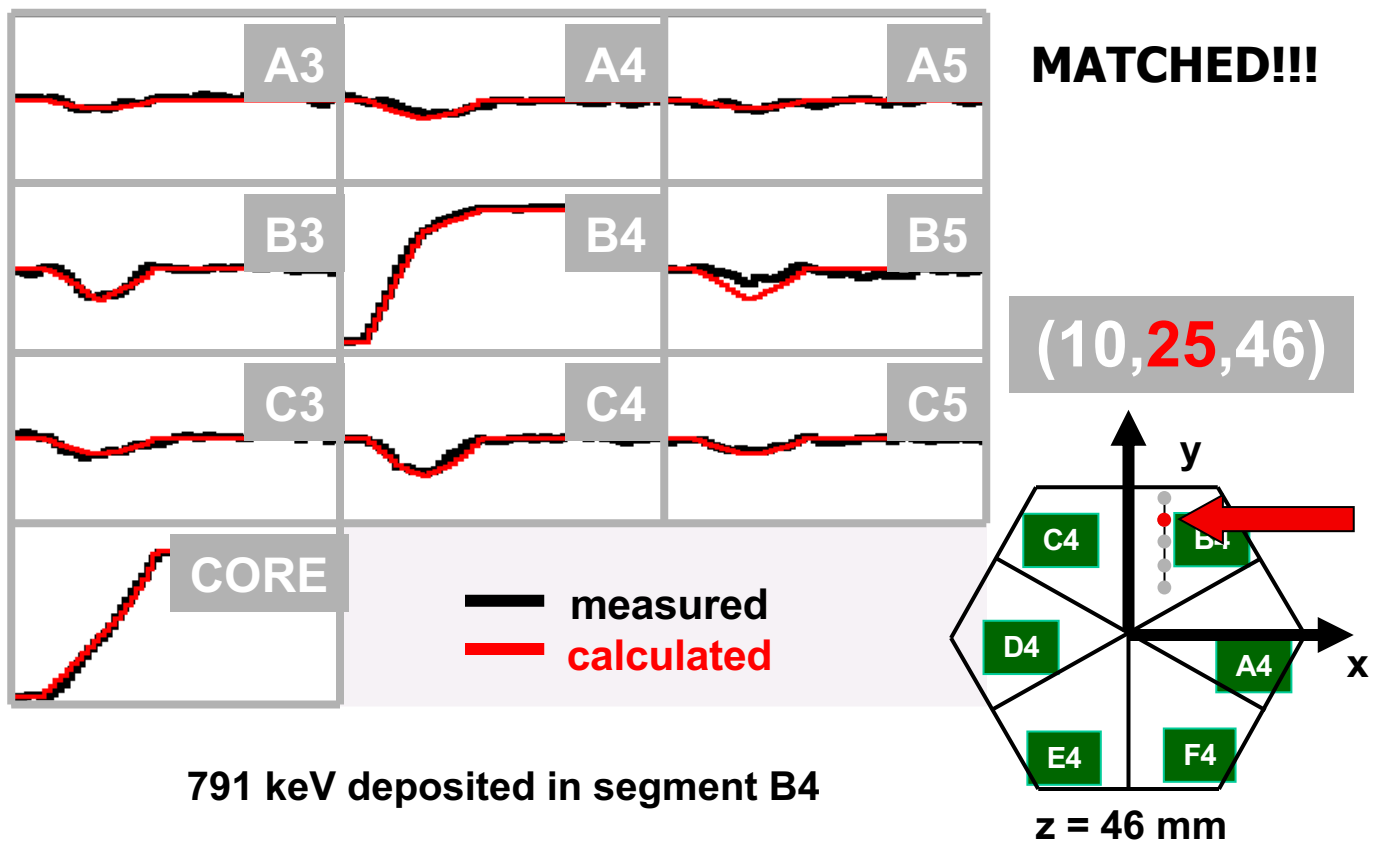




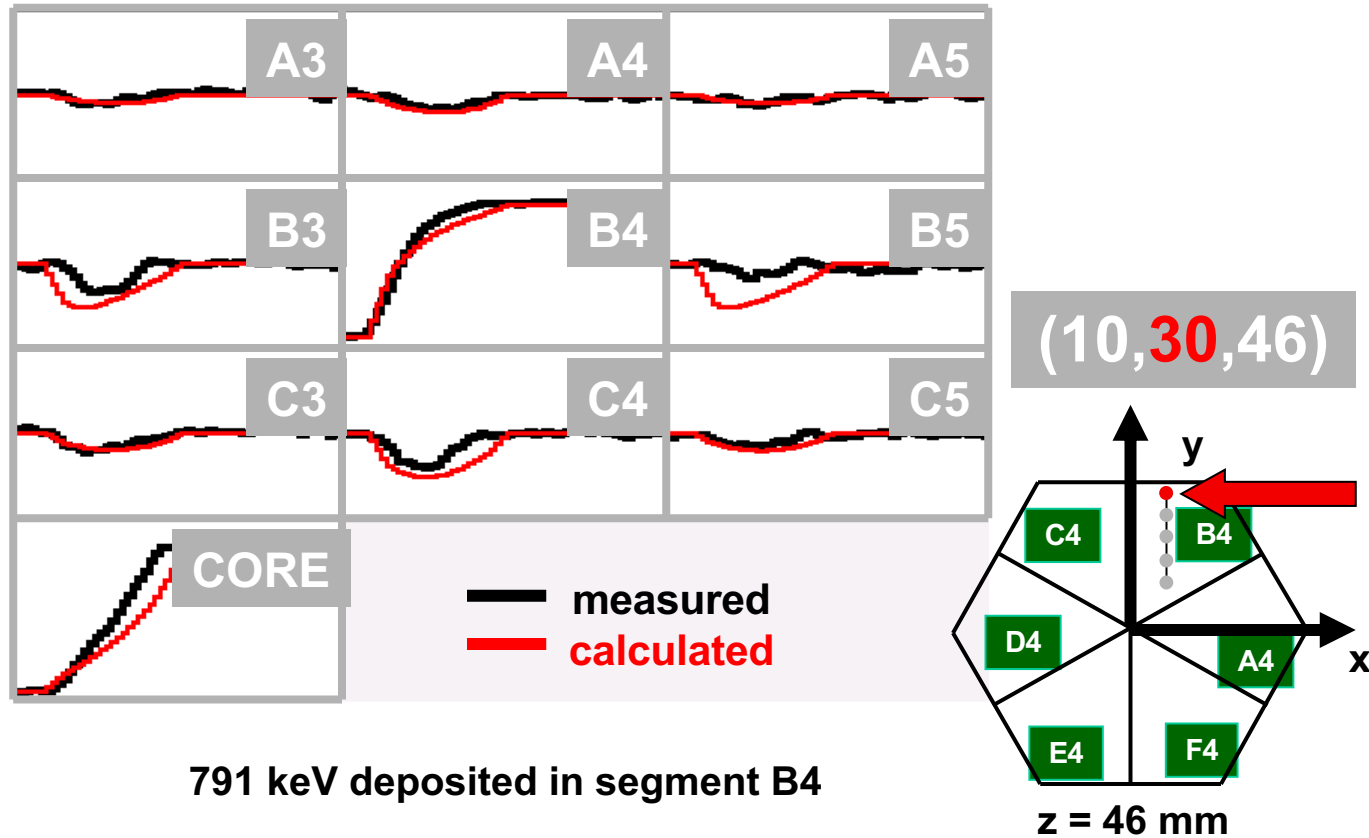
# Pulse Shape Analysis Concept



# Pulse Shape Analysis Concept



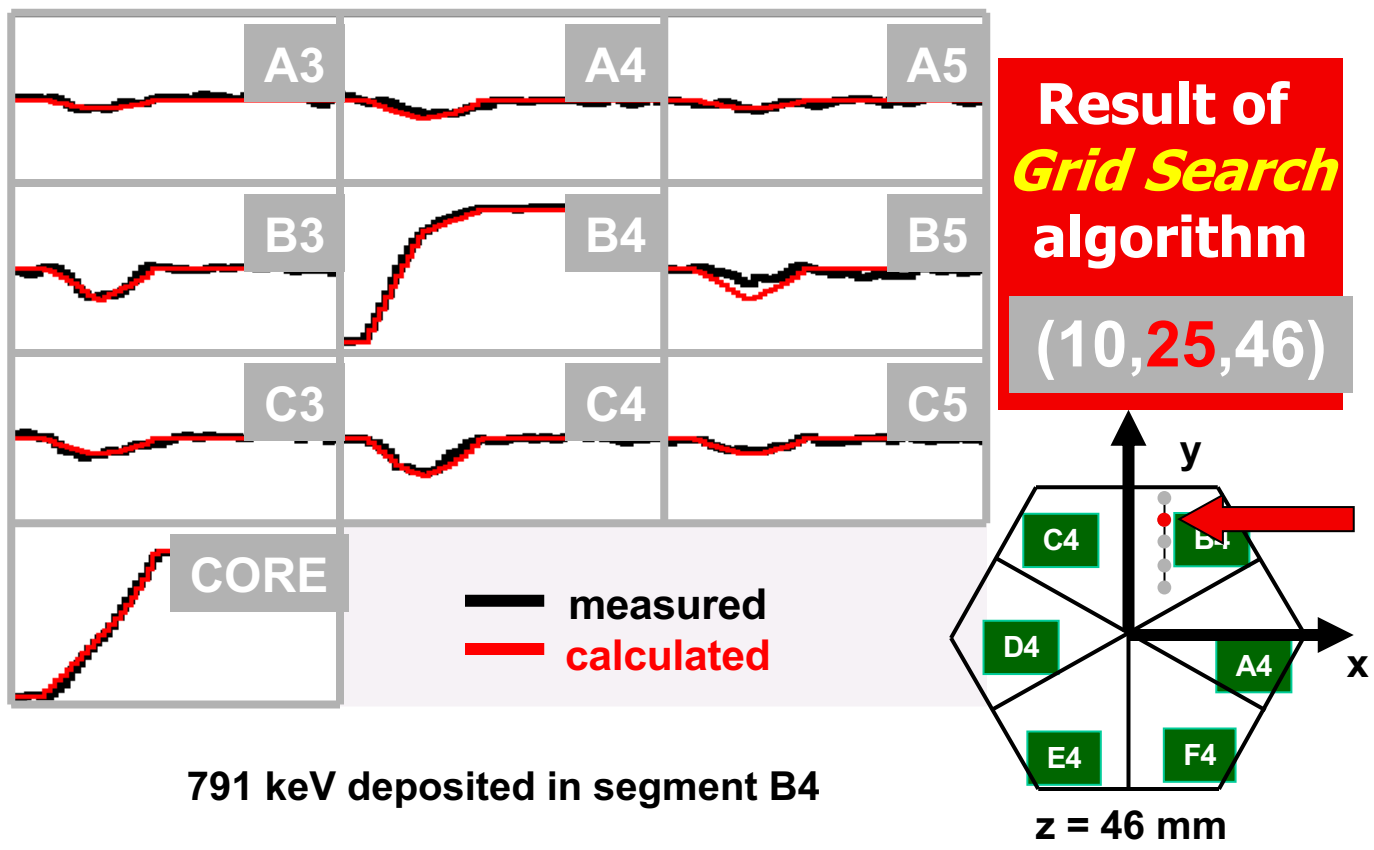
# Pulse Shape Analysis Concept



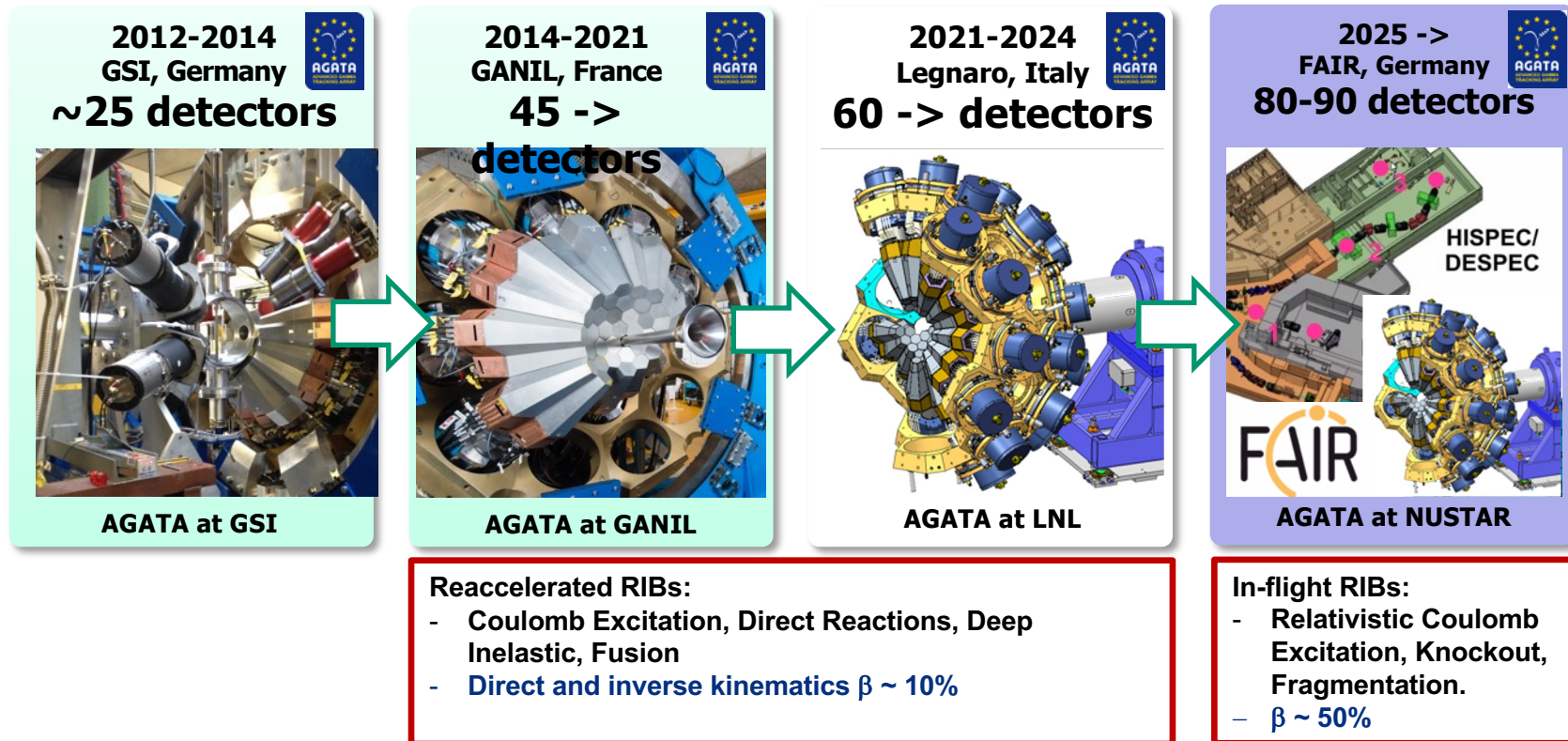
791 keV deposited in segment B4



# Pulse Shape Analysis Concept

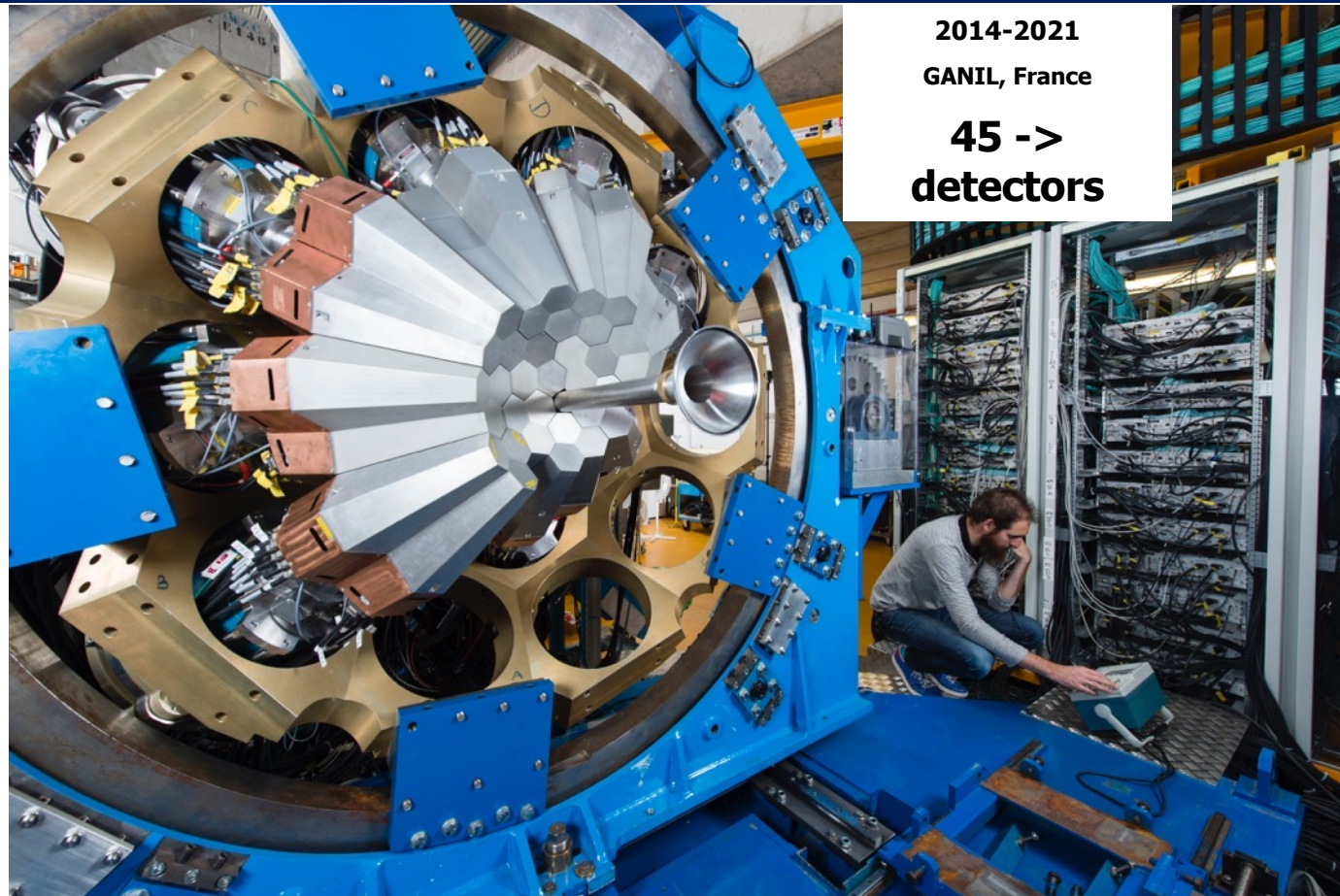


# Evolution of AGATA




They had about 60 detectors for AGATA by end 2023

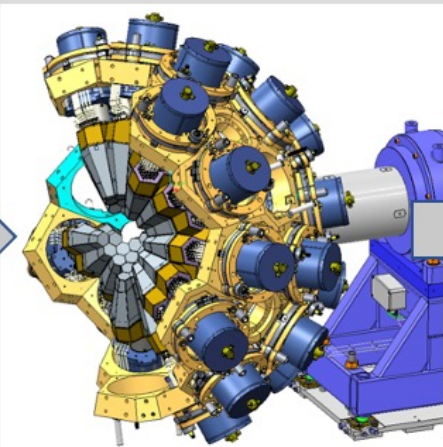
# Evolution of AGATA



2014-2021  
GANIL, France  
45 ->  
detectors



2021-2024  
Legnaro, Italy  
60 -> detectors



AGATA at LNL

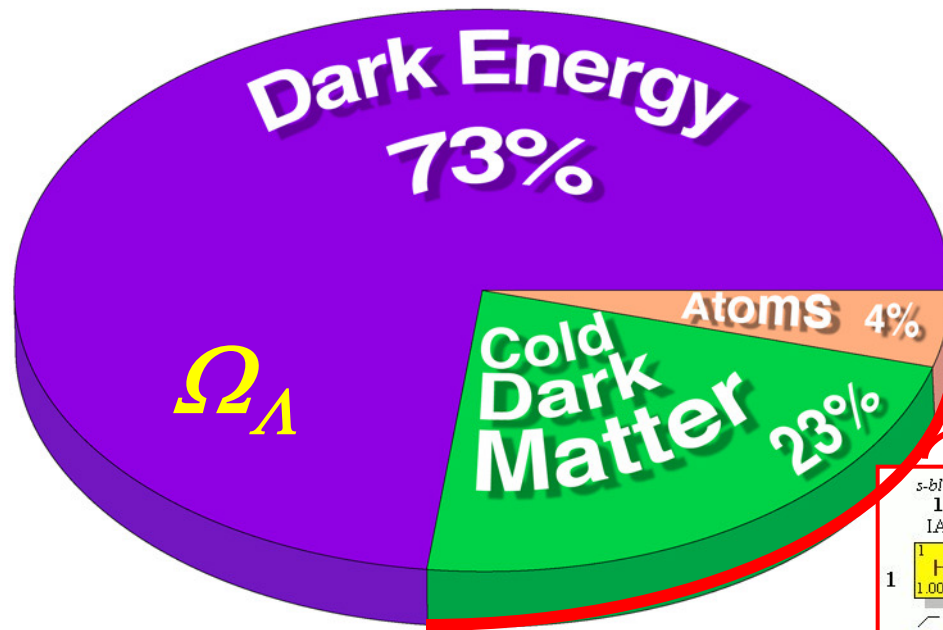


# **Conclusions**

## **(nuclear detectors)**

- **High Z Scintillators are used for gamma spectroscopy, particular for anti Compton spectrometers**
- **Low Z (organic)-Scintillators used for particle detection/stopping**
- **Semiconductors: Si used for charged particle spectroscopy (alpha, protons, ... Fission fragments)**
- **Semiconductors: HP-Ge for high resolution and high efficient Gamma spectroscopy**

We (and all of chemistry) are a small minority in the Universe.



$\Omega_M$

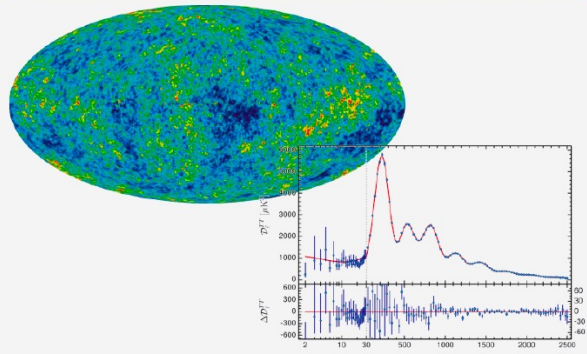
s-block		Transition Metals										Non-Metals						s-block	
1	2											13	14	15	16	17	18		
IA	IIA											IIIA	IVA	VA	VIA	VIIA	VIIIA		
1	2											3	4	5	6	7	8	9	10
s-block		d-block										p-block						s-block	
		Transition Metals																	
3	4	5	6	7	8	9	10	11	12	13	14	15	16	17	18				
Li	Be	Sc	Ti	V	Cr	Mn	Fe	Co	Ni	Cu	Zn	Al	Si	P	S	Cl	Ar		
6.941	9.0122		47.88	50.942	51.996	54.938	55.847	58.933	58.69	63.546	65.39	26.982	28.086	30.974	32.06	35.453	39.948		
11	12											13	14	15	16	17	18		
Na	Mg											Al	Si	P	S	Cl	Ar		
22.990	24.305											26.982	28.086	30.974	32.06	35.453	39.948		
19	20	21	22	23	24	25	26	27	28	29	30	31	32	33	34	35	36		
K	Ca	Sc	Ti	V	Cr	Mn	Fe	Co	Ni	Cu	Zn	Ga	Ge	As	Se	Br	Kr		
39.098	40.08	44.956	47.88	50.942	51.996	54.938	55.847	58.933	58.69	63.546	65.39	69.72	72.59	74.922	78.96	79.904	83.80		
37	38	39	40	41	42	43	44	45	46	47	48	49	50	51	52	53	54		
Rb	Sr	Y	Zr	Nb	Mo	Tc	Ru	Rh	Pd	Ag	Cd	In	Sn	Sb	Te	I	Xe		
85.468	87.62	88.906	91.224	92.906	95.94	(98)	101.07	102.91	106.42	107.87	112.41	114.82	118.71	121.75	127.60	126.91	131.29		
55	56	57	72	73	74	75	76	77	78	79	80	81	82	83	84	85	86		
Cs	Ba	to 71	Hf	Ta	W	Re	Os	Ir	Pt	Au	Hg	Tl	Pb	Bi	Po	At	Rn		
132.91	137.33		178.49	180.95	183.85	186.21	190.2	192.22	195.08	196.97	200.59	204.38	207.2	208.98	(209)	(210)	(222)		
87	88	89	104	105	106	107	108	109	110										
Fr	Ra	to 103	Unq	Unp	Unh	Uns	Uno	Une	Uun										
(223)	226.03		(261)	(262)	(263)	(262)	(265)	(266)	(267)										
Metals																Phases			
																Solid			
																Liquid			
																Gas			
Rare Earth Elements		d-block										f-block							
Lanthanide Series		57	58	59	60	61	62	63	64	65	66	67	68	69	70	71			
		La	Ce	Pr	Nd	Pm	Sm	Eu	Gd	Tb	Dy	Ho	Er	Tm	Yb	Lu			
		138.91	140.12	140.91	144.24	(145)	150.36	151.96	157.25	158.93	162.50	164.93	167.26	168.93	173.04	174.97			
Actinide Series		89	90	91	92	93	94	95	96	97	98	99	100	101	102	103			
		Ac	Th	Pa	U	Np	Pu	Am	Cm	Bk	Cf	Es	Fm	Md	No	Lr			
		227.03	232.04	231.04	238.03	237.05	(244)	(243)	(247)	(247)	(251)	(252)	(257)	(258)	(259)	(260)			

(Mass Numbers in Parentheses are from the most stable of common isotopes.)

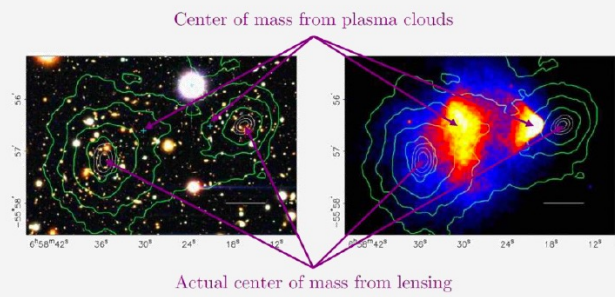
# Dark Matter ?

## Dark Matter Evidence

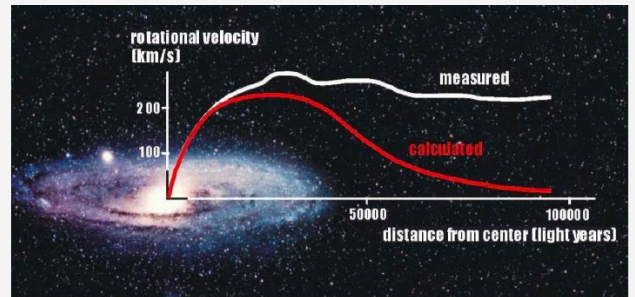
### Cosmic Microwave Background



### Bullet Cluster



### Rotation curves

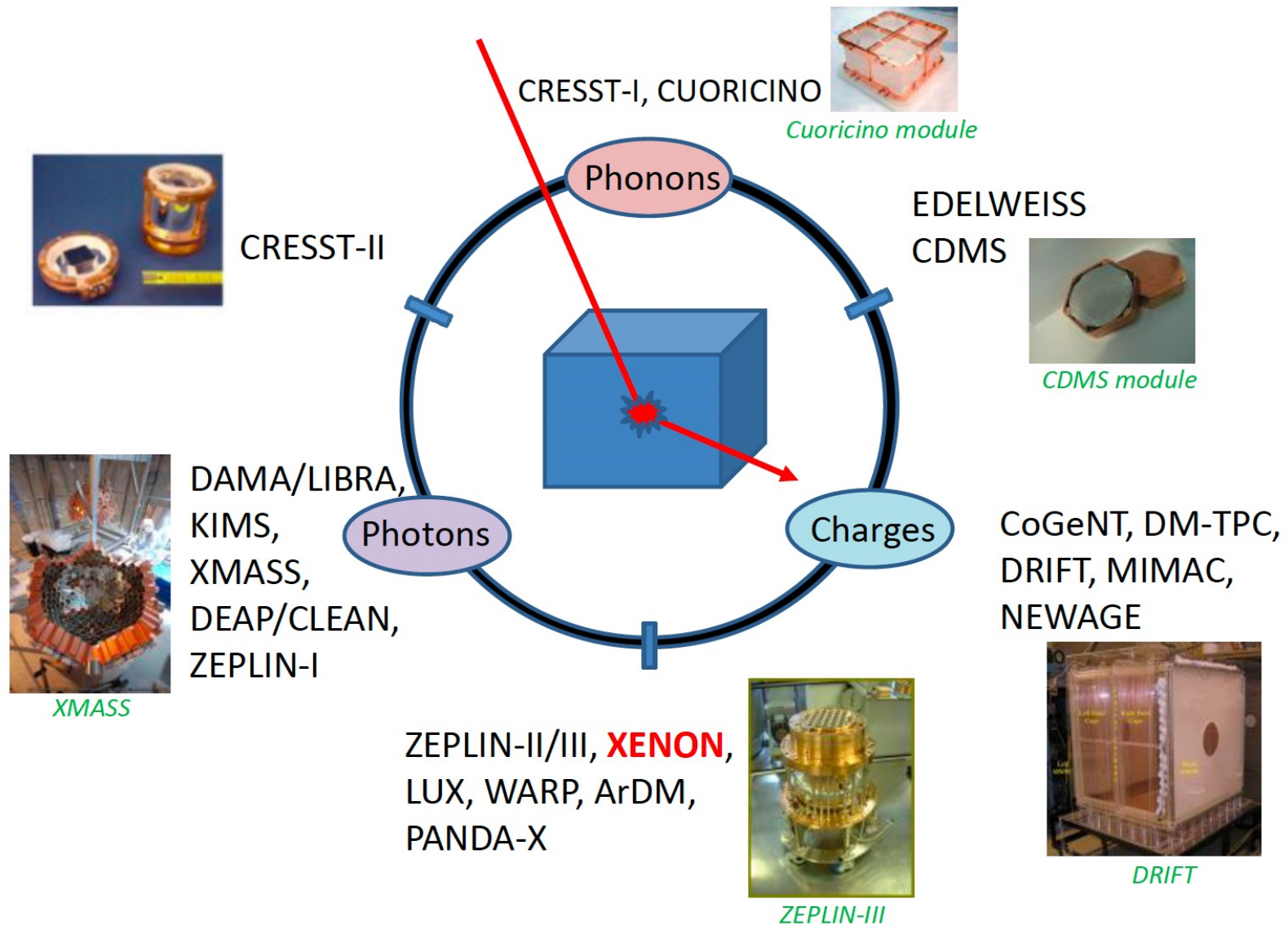


... non-atomic (if not PBH) – non-luminous – stable – neutral – massive – non-relativistic ...





# Direct Dark Matter Search Modalities



# A double phase liquid xenon TPC

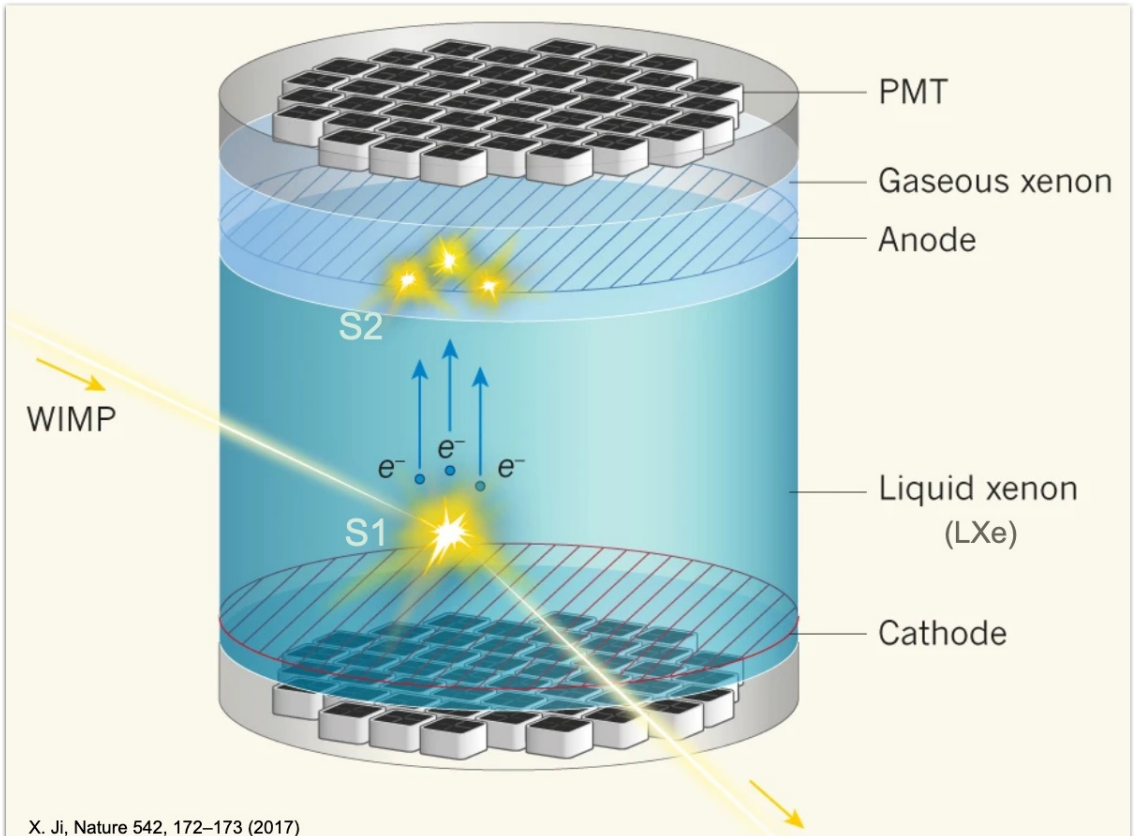
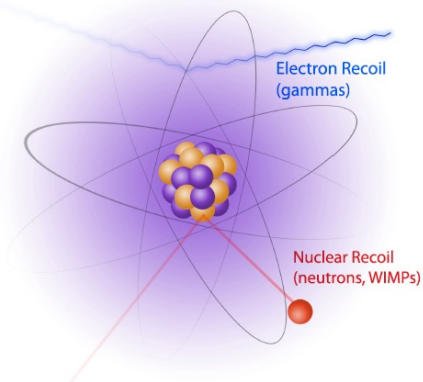
Dark Matter and Axion Searches - Belina von Krosigk

## Most recent results >1 GeV: LZ, XENONnT



**LZ:**  
5.5 t fiducial mass, LXe

**XENONnT:**  
4.2 t fiducial mass, LXe

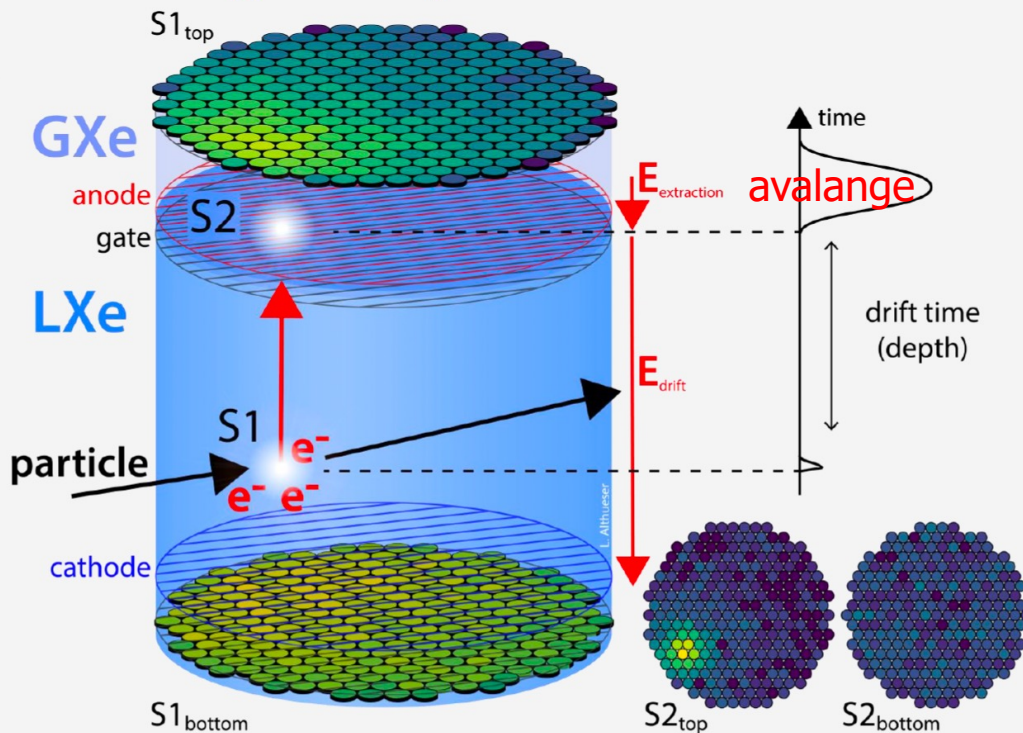


X. Ji, Nature 542, 172-173 (2017)

# A double phase liquid xenon TPC

Latest results from XENONnT

## Working Principle



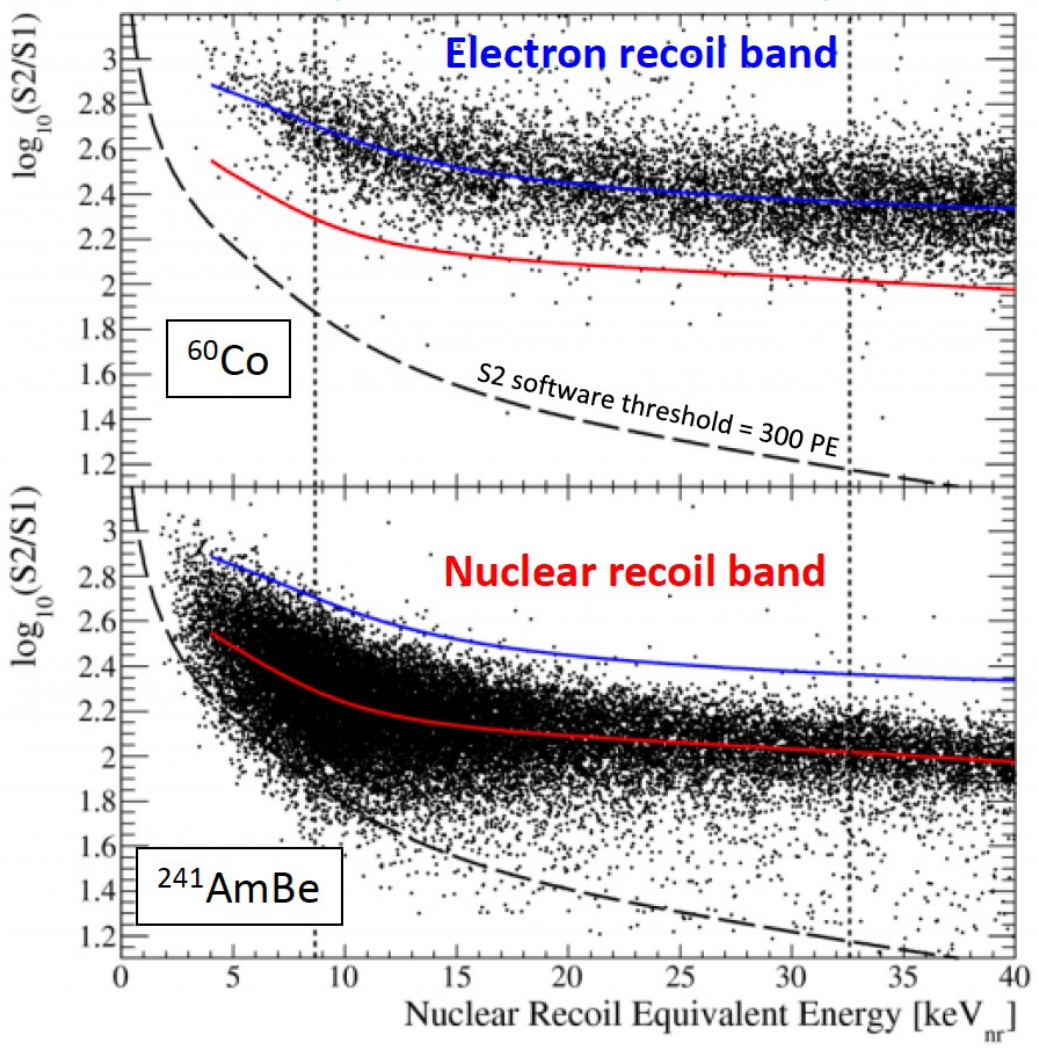
## Working principle of dual-phase liquid noble gas time projection chambers (TPCs)

- Prompt light signal (S1)
- Secondary light in GXe from drifted charges (S2)
- Energy reconstruction using the combined S1 and S2 signal
- Position reconstruction
  - $z$  from S1-S2-delay time
  - $x$ - $y$  from S2 hit pattern



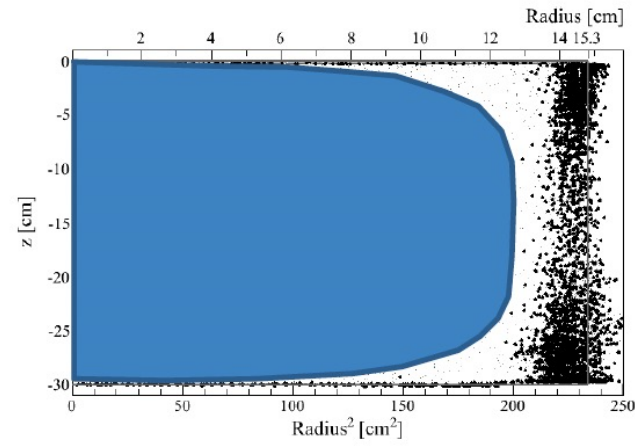
# Background discrimination

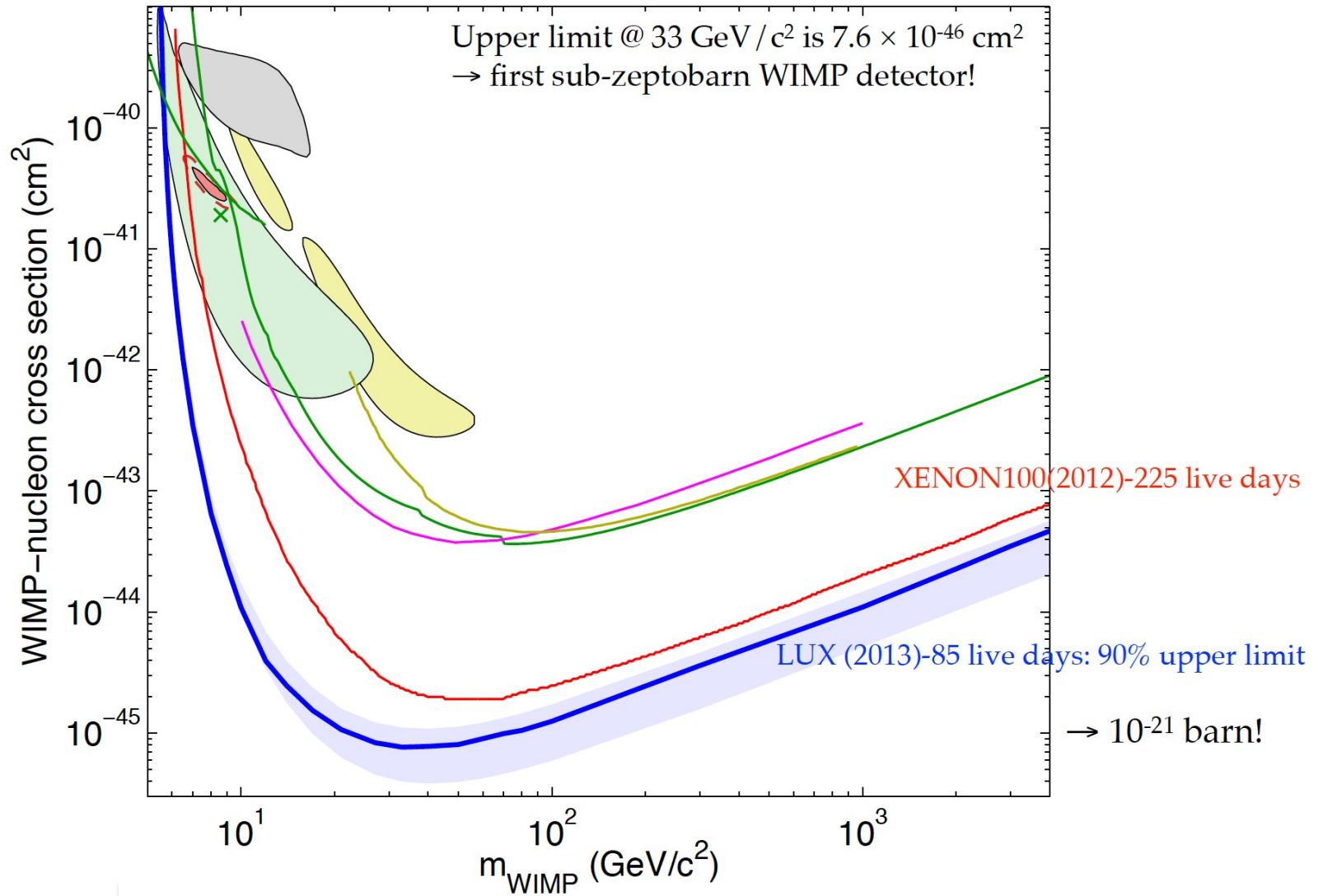
← WIMP search region →

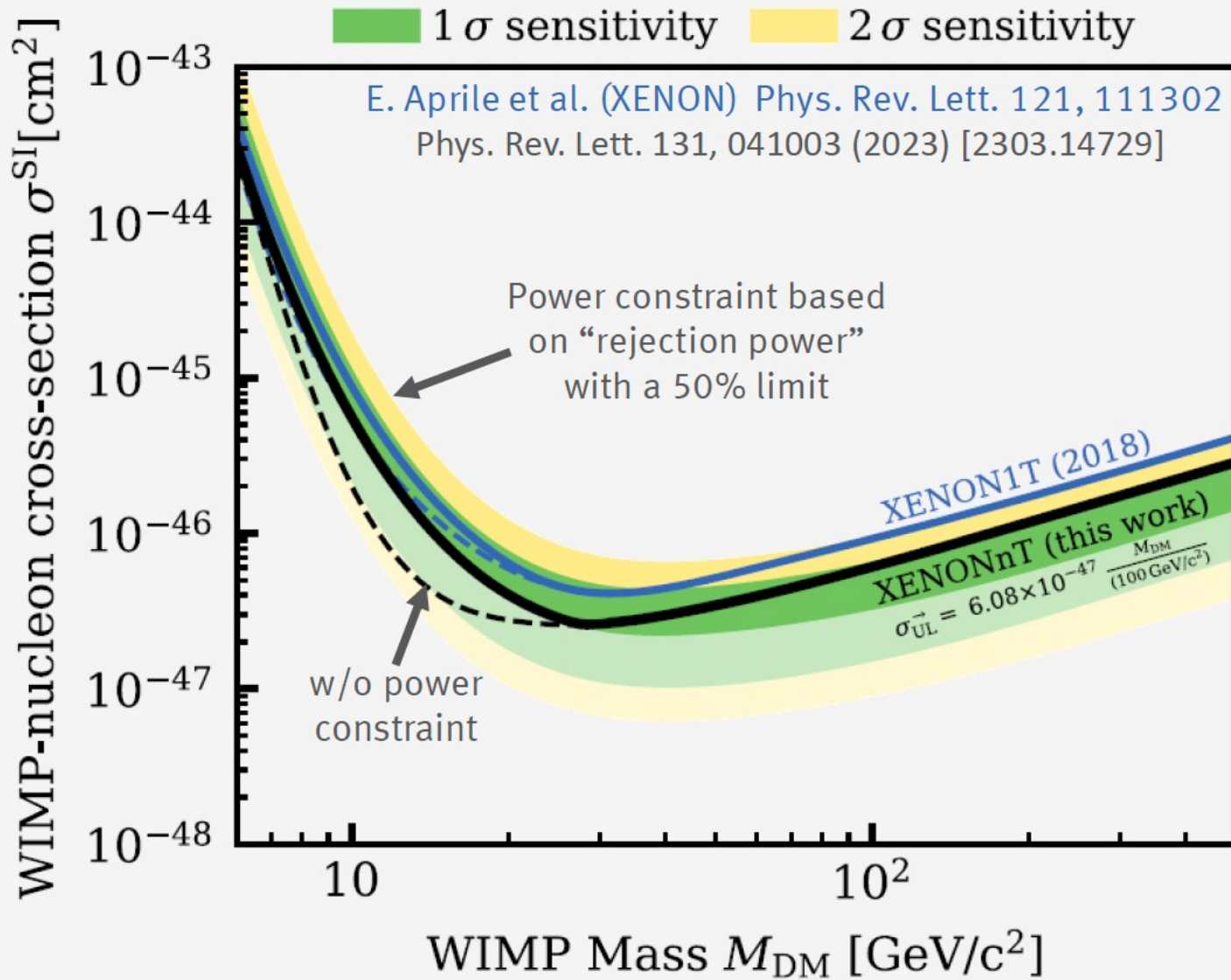


**Identification of recoil species by S2/S1 ratio**

- from  $^{60}\text{Co}$   $\gamma$ -ray source and  $^{241}\text{AmBe}$  neutron source
- selecting single scattered events



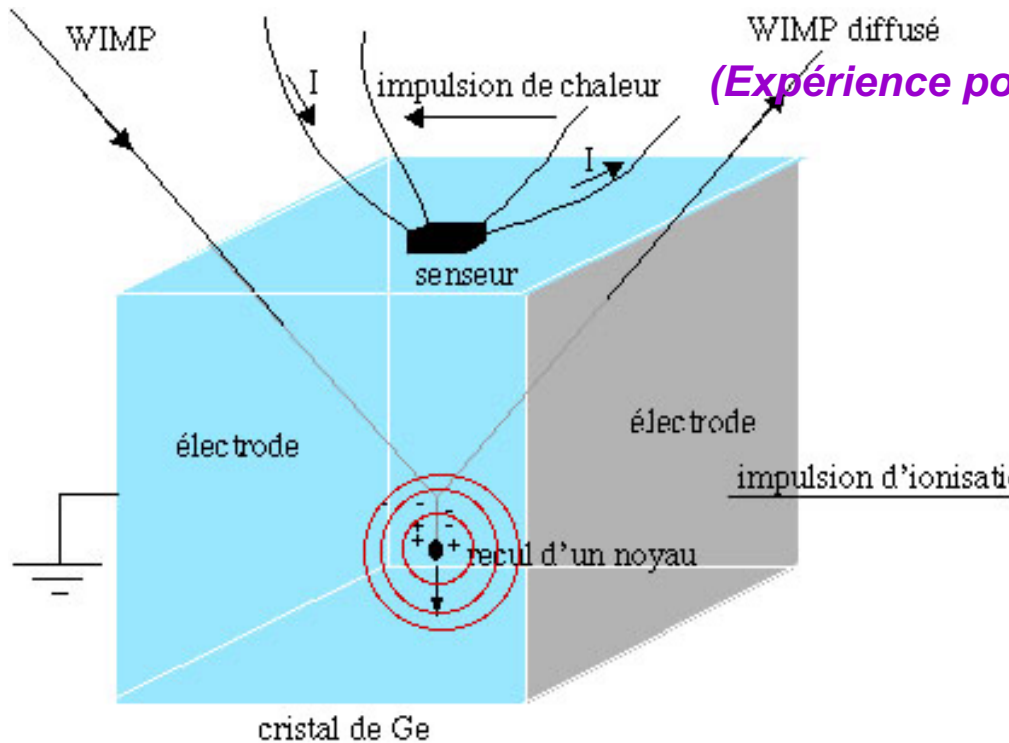




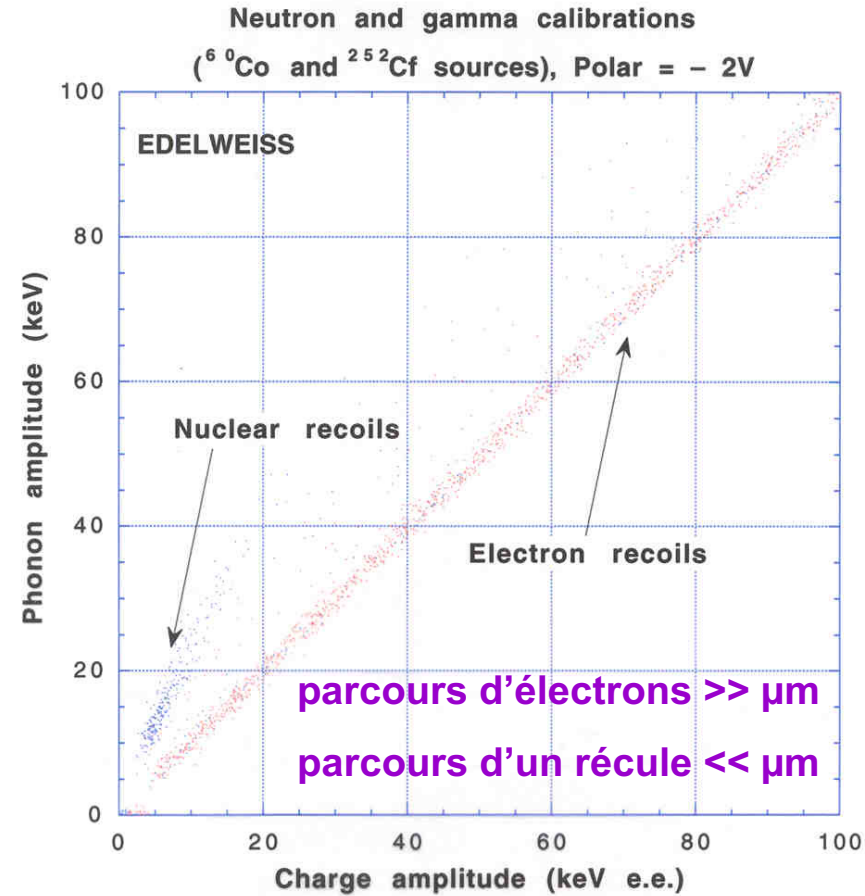


# EDELWEISS

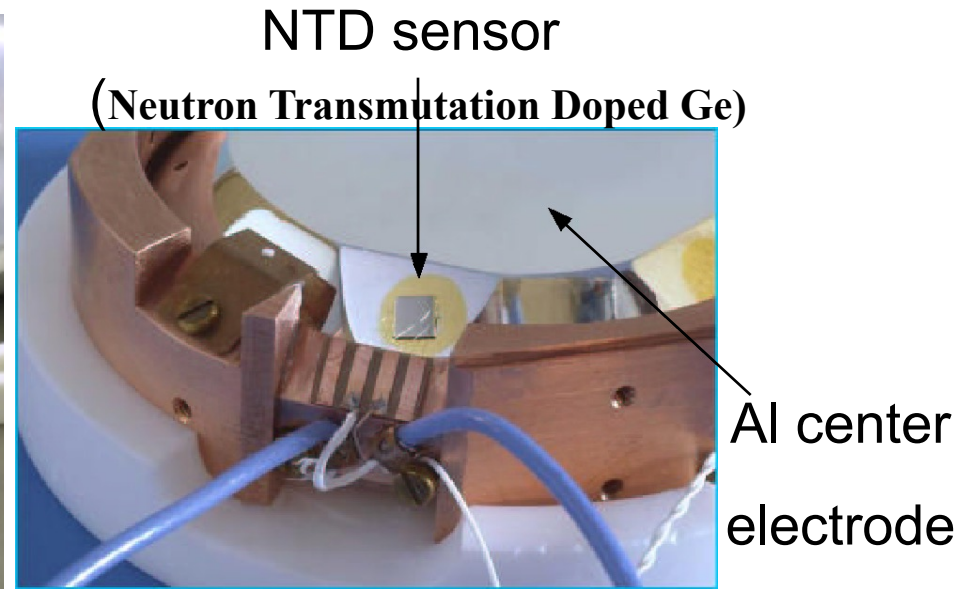
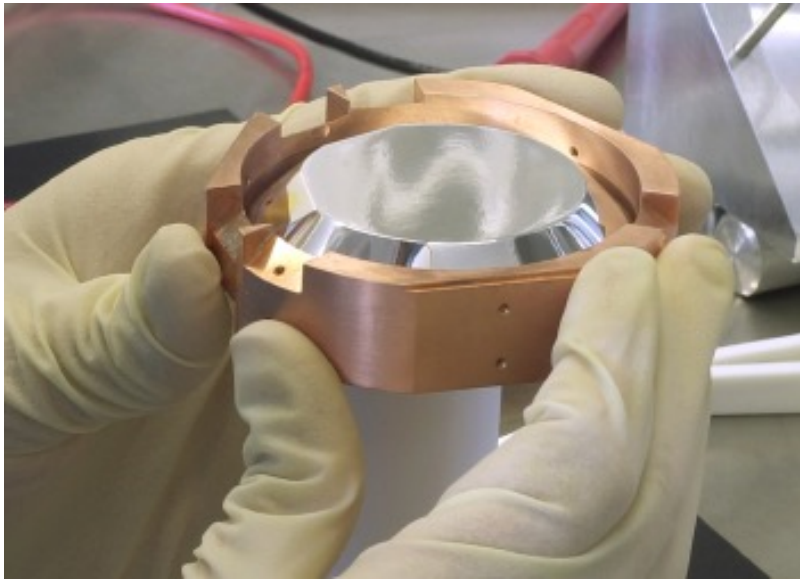
(Expérience pour Détecter Les Wimps en Site Souterrain)



- Ge crystals of up to 1Kg
- Very rare events about  
1 event/Kg/year
- Recoil of some keV
- Heat changes of
  - $\Delta T \approx \text{few mK} \Rightarrow \text{cryostat}({}^3\text{He}-{}^4\text{He})$
  - Operation temperatur of 10 milli-Kelvin



# Ge ionization – phonon detectors I



➤ bolometer mass: 320 g

➤ 100nm sputtered Al layer as electrode (center + guard ring)

➤ 60nm Ge(Si) amorphous layer below electrode

➤ NTD temperature sensor glued on sputtered gold pad on guard ring electrode

➤ electrical contacts/heat links via gold wire bonding ( $\varnothing=25\mu\text{m}$ )

➤ **operating temperature  $T=17.00\pm 0.01\text{mK}$**

# Ionisation&heat: pulses & signals

## Ge-NTD detector in EDELWEISS:

$$E \sim 10 \text{ keV}_{ee}$$

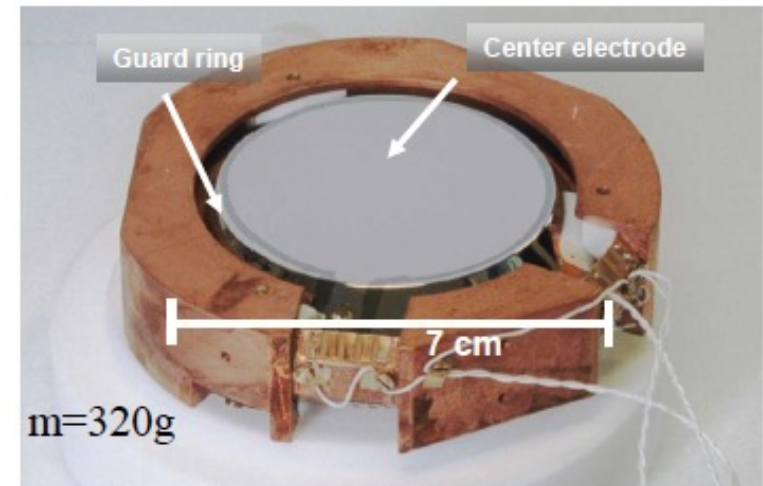
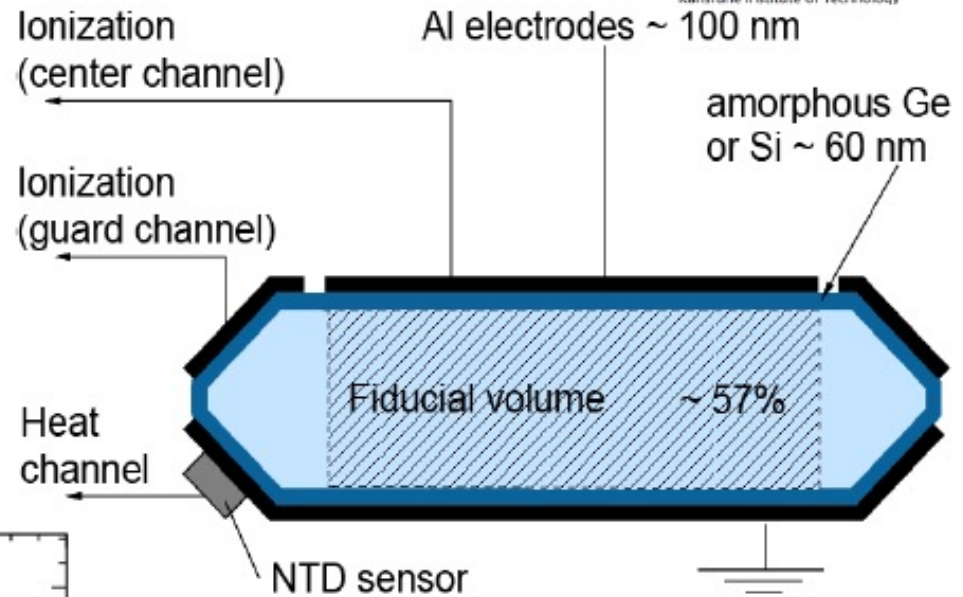
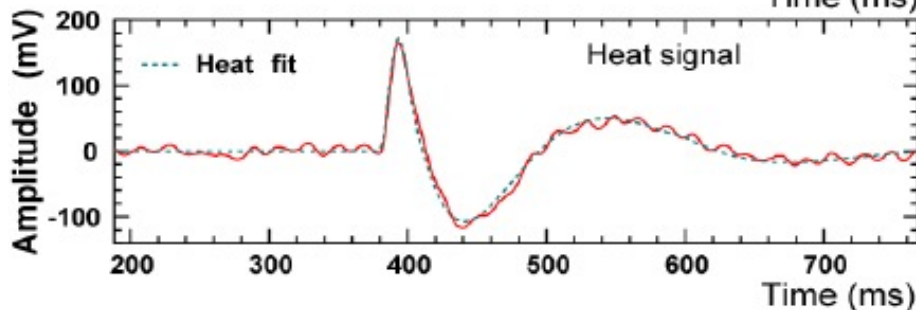
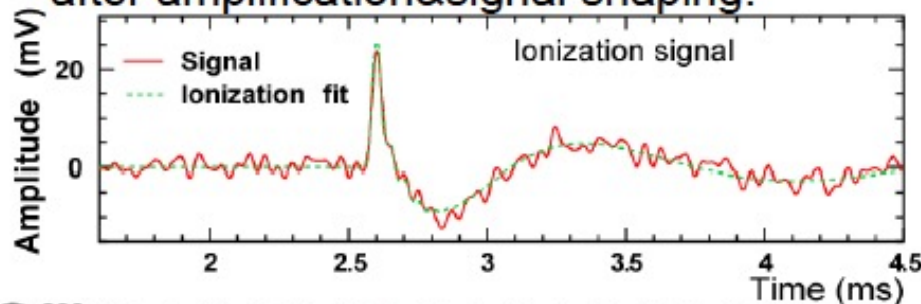
$$\text{heat: } \Delta T = 1.3 \mu\text{K}; \Delta U = 1 \mu\text{V}$$

$$t_{\text{rise}} \sim 10 \mu\text{s} - 10 \text{ms}; t_{\text{fall}} \sim 100 \text{ms}$$

$$\text{ionisation: } \Delta U = 0.5 \text{mV}$$

$$t_{\text{rise}} \sim 100 \text{ns} - 1 \mu\text{s}; t_{\text{fall}} \sim 100 \mu\text{s}$$

## after amplification&signal shaping:





# ionization – phonon signal plane

$^{73}\text{Ge}(n,n'\gamma)$  68.8 keV

13.3 keV

n/γ discrimination

> 99.9%

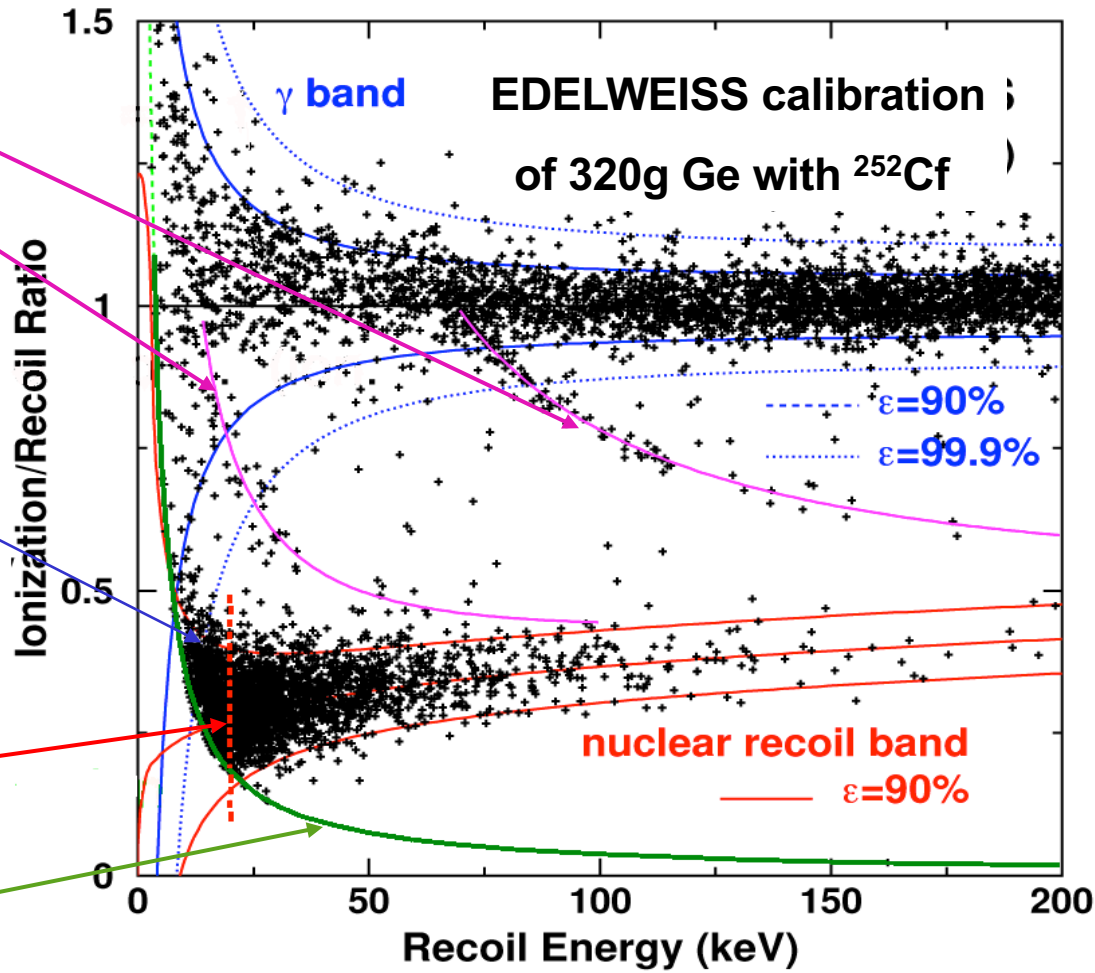
for  $E_r > 15$  keV

Recoil threshold

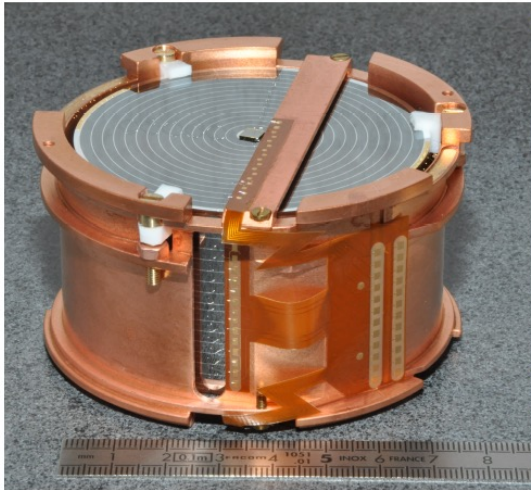
20 keV

Ionization threshold

3.7 keV



# Ex. of instrument : EDELWEISS-III



**36 \* FID-800**

- ✦ **Ge 820 g**
- ✦ High impedance Ge-NTD thermometer (neutron doped Ge crystals)
- ✦ 4 sets of Al electrodes for charge collection
  - Simultaneous measurement of **ionization & heat**
  - Background active rejection



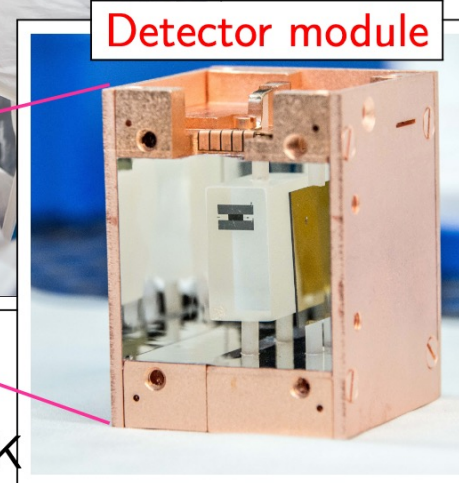
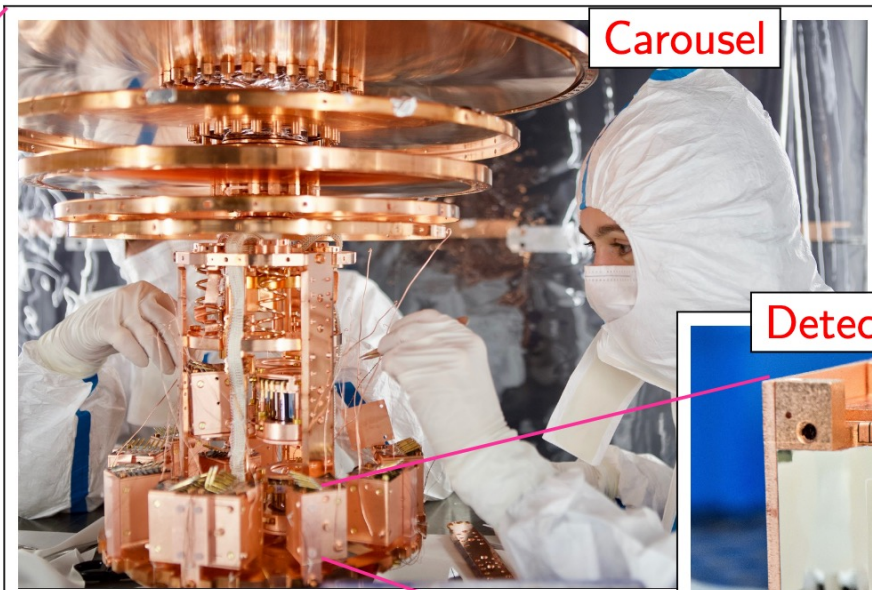
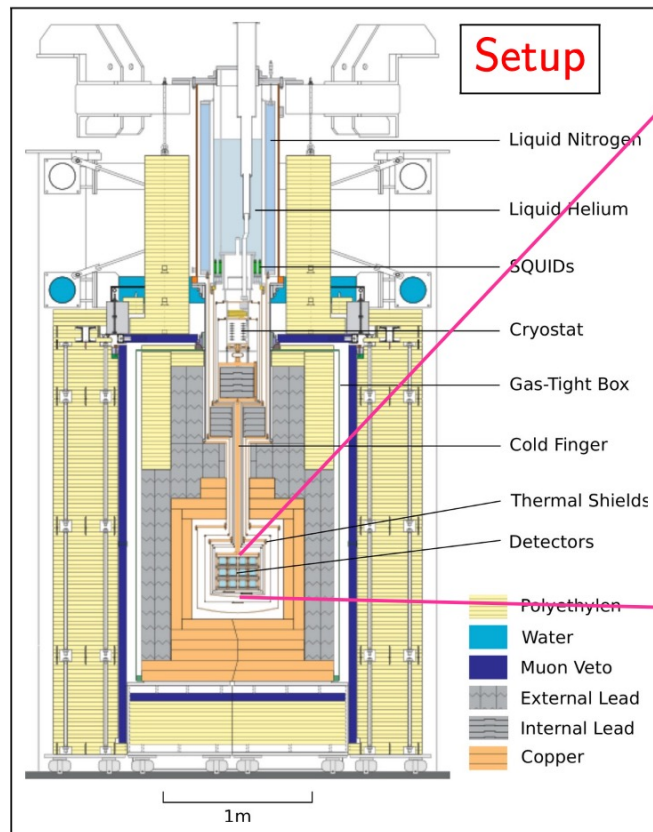
**Running 2013-2023**

- ✦ **10mK Cryostat** + 40 tons of shielding (PE + Pb) @ LSM
- ✦ **3000 coax. cables (6 km)**
- ✦ **350 Si-JFET transistors @ 120K**
- ✦ **36\*2 « Bolometers Boxes » @ 300K**



# The CRESST experiment

- Protected from backgrounds by layers of shielding (PE, Pb, Cu) and an active muon veto

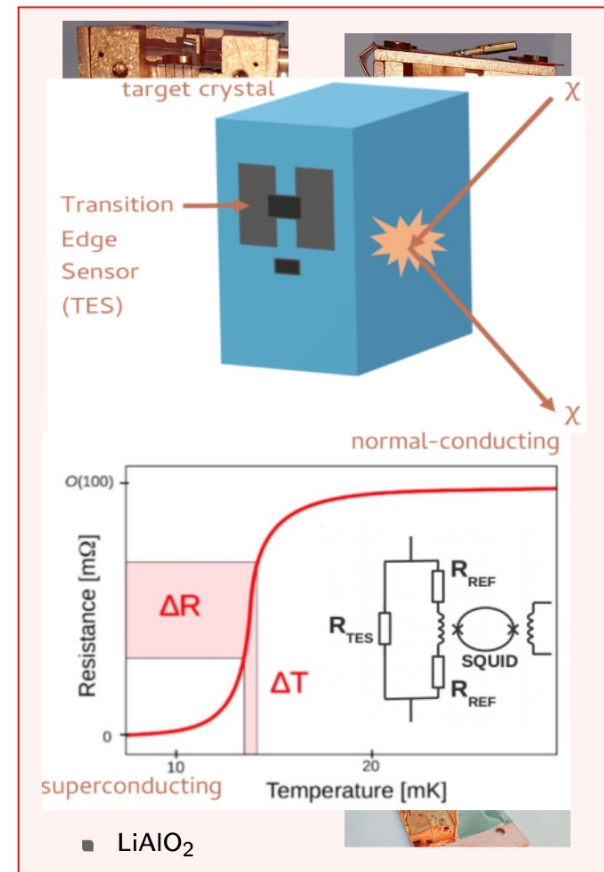


- Detector modules mounted in "carousel" and cooled to  $\sim 10$  mK



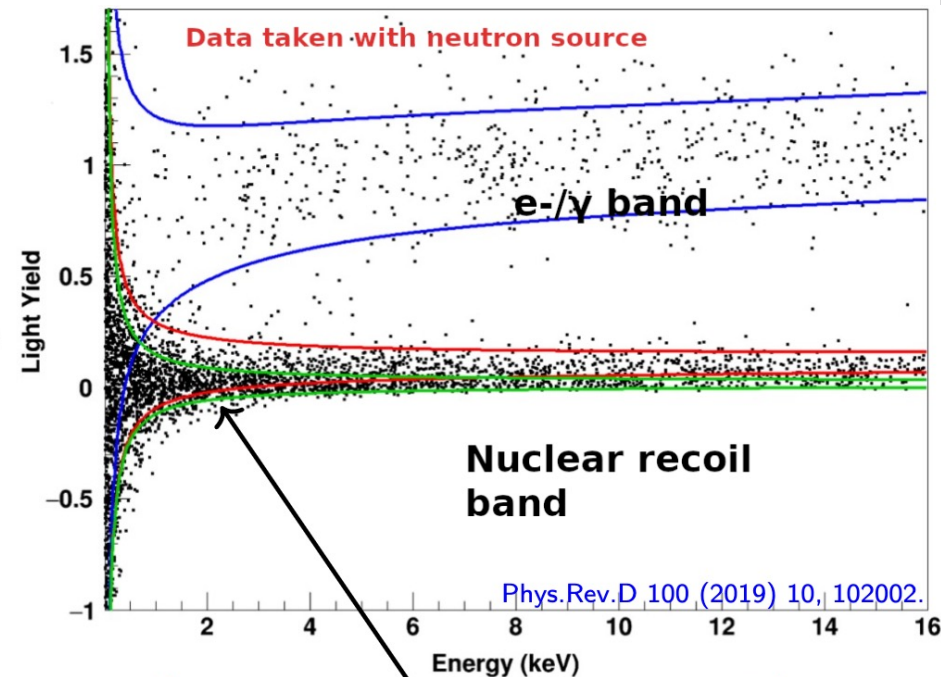
## CRESST-III detectors

- Cryogenic **scintillating** detectors
- Measure phonon and light
- $\text{CaWO}_4$  traditionally used as target material
- **Capable of using range of target materials** ( $\sim 2 \times 2 \times 1 \text{ cm}^3$ ):  $\text{CaWO}_4$  (24 g),  $\text{Al}_2\text{O}_3$  (16 g),  $\text{LiAlO}_2$  (10 g), Si (9 g)
- Thin light detector ( $2 \times 2 \times 0.04 \text{ cm}^3$ ): Si or silicon-on-sapphire (SOS)
- Sensors: W-TES directly evaporated on the crystals
- **Particle interaction**  $\rightarrow$  **energy deposition**  $\rightarrow$  **temperature rise**  $\rightarrow$  **resistance change read out by SQUID**



## CRESST-III detectors

- Cryogenic scintillating detectors
- Measure phonon and light
- $\text{CaWO}_4$  traditionally used as target material
- **Capable of using range of target materials** ( $\sim 2 \times 2 \times 1 \text{ cm}^3$ ):  $\text{CaWO}_4$  (24 g),  $\text{Al}_2\text{O}_3$  (16 g),  $\text{LiAlO}_2$  (10 g), Si (9 g)
- Thin light detector ( $2 \times 2 \times 0.04 \text{ cm}^3$ ): Si or silicon-on-sapphire (SOS)
- **Particle interaction  $\rightarrow$  energy deposition  $\rightarrow$  temperature rise  $\rightarrow$  resistance change read out by SQUID**
- **Seperation between  $e/\gamma$  background and nuclear recoil from two channel measurements**



**Dark matter expected in the nuclear recoil band**

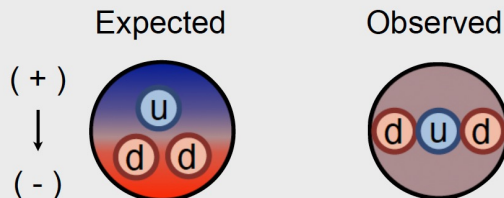
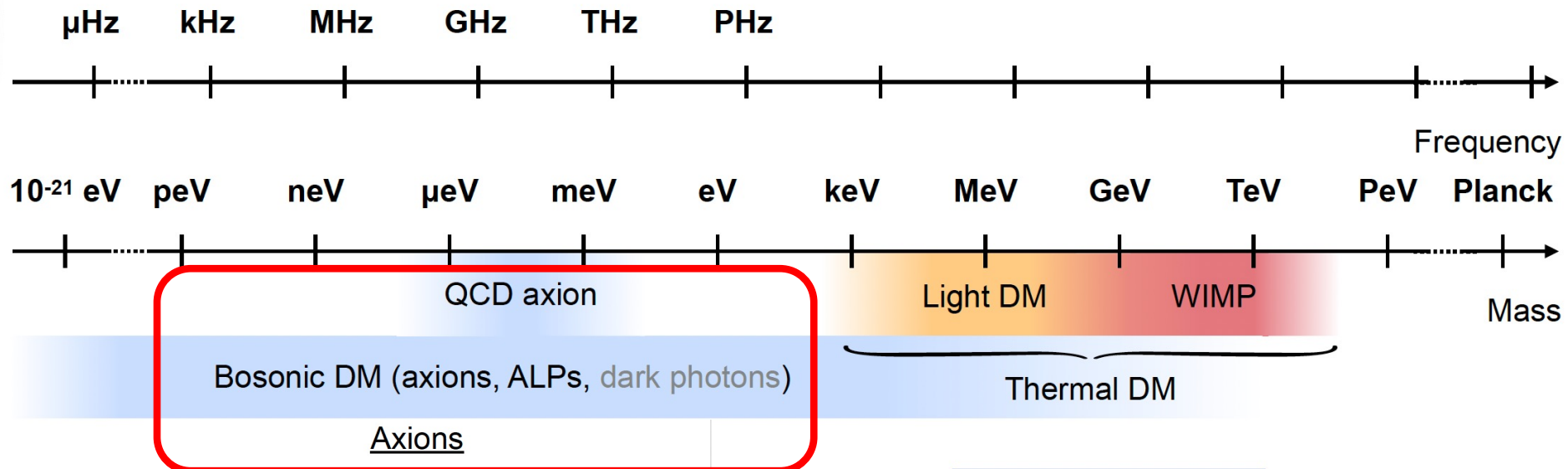
# Dark matter searches

Dark Matter and Axion Searches - Belina von Krosigk



8

## Mass ranges of some beyond SM particles

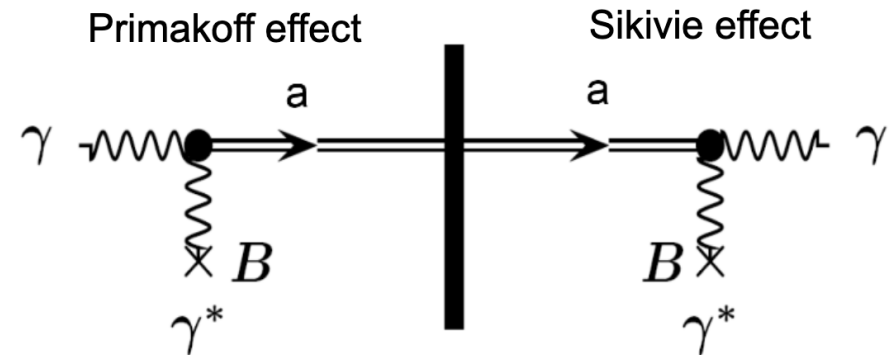


Strong-CP problem:  
Strange absence of measurable neutron  
Electric Dipole Moment (EDM)



## Axions and Axion-like particles (ALPs)

- Proposed as solution to strong CP problem
- Motivated by astrophysical observations:
  - Stellar evolution
  - TeV transparency
- Very weak interaction, good candidate for dark matter
- The main mechanism for detection of light weight axions is through its coupling to photons



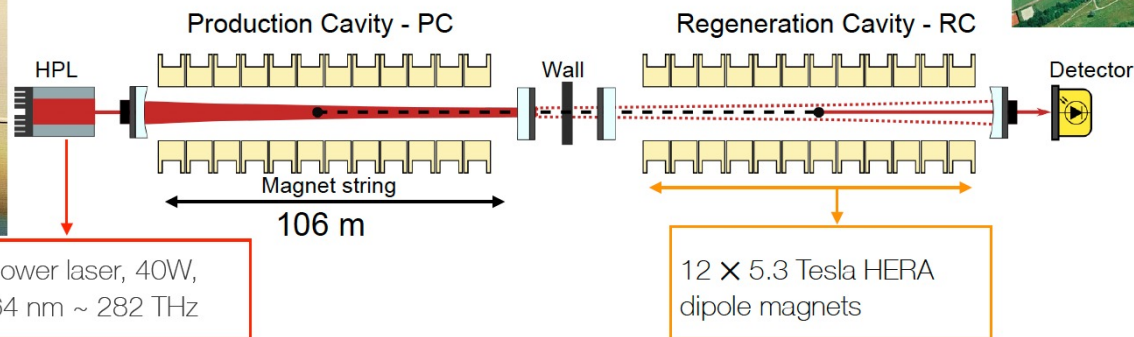
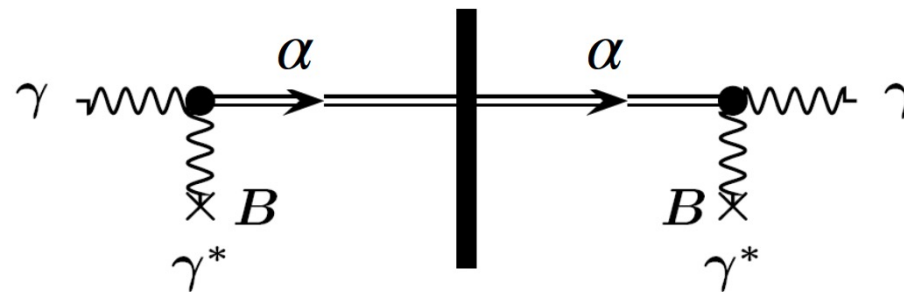
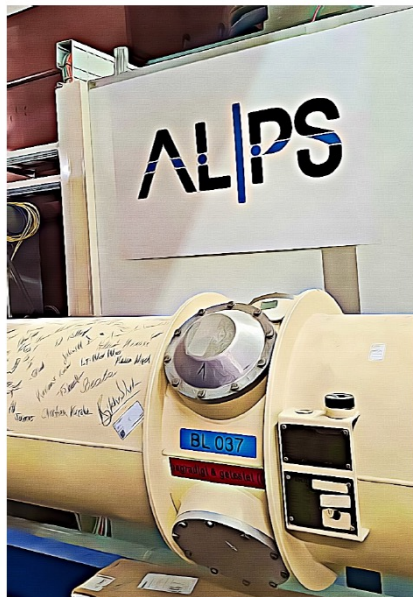
## Light Shining through a Wall (LSW)

Model independent approach,  
independent of dark matter paradigm

# Axions and Axion-like particles (ALPs)

## Any Light Particle Search II

### The axion factory



High power laser, 40W,  
 $\lambda=1064 \text{ nm} \sim 282 \text{ THz}$

12 x 5.3 Tesla HERA  
dipole magnets

$\beta$ : power buildup R  
 $\eta$ : quantum efficien

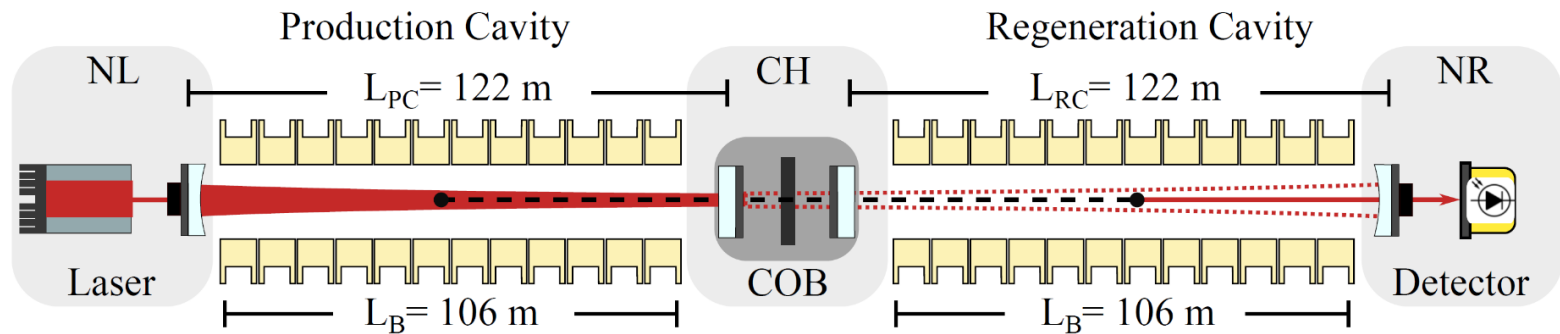
$$n_{\text{signal}} \approx \frac{1 \text{ photon}}{37 \text{ hours}} \cdot \left( \frac{P_{\text{PC}}}{150 \text{ kW}} \right) \left( \frac{\beta_{\text{RC}}}{10,000} \right) \left( \frac{\eta}{0.9} \right) \left( \frac{g_{a\gamma\gamma}}{2 \times 10^{-11} \text{ GeV}^{-1}} \right)^4 \left( \frac{B}{5.3 \text{ T}} \right)^4 \left( \frac{L}{106 \text{ m}} \right)$$



DESY

# Any Light Particle Search II (ALPS II)

Initial Science Run started on 23.05.2023

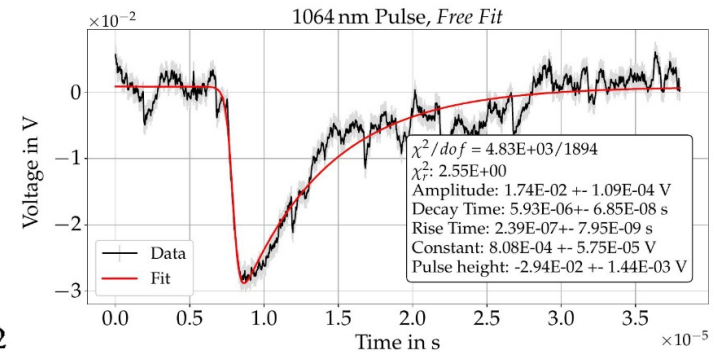
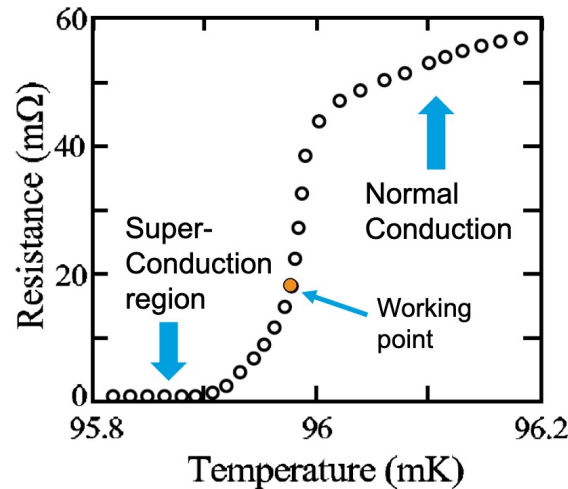
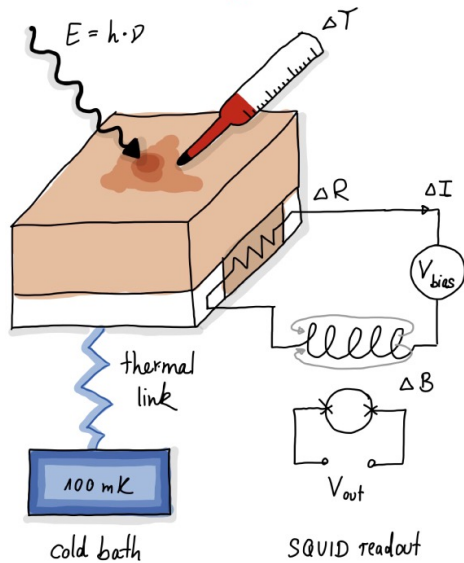


**ALPS II** might produce a rate in the order of 1 reconverted photon per day



# TES Single Photon Detection

## Transition Edge Sensors



Courtesy of Rikhav Shah

K. Irwin, G. Hilton, Transition-edge sensors, in: Cryogenic Particle Detection, Springer Berlin Heidelberg, Berlin, Heidelberg, 2005, pp. 63–150, [http://dx.doi.org/10.1007/10933596\\_3](http://dx.doi.org/10.1007/10933596_3).

- Cryogenic microcalorimeters
- Operated at superconducting transition temperature
- Read-out using Superconducting Quantum Interference Devices (SQUIDs)
- Incident photon leads to temperature increase
- Small temperature increase leads to large variation in resistance
- Change in resistance is measured in changing current
- Signal is proportional to photon energy
- Energy resolution  $\leq 10\%$
- DM signal expected to look like photon

Drawings courtesy of Katharina-Sofie Isleif

DESY. | Direct dark matter searches using ALPS II's TES detector | Christina Schwemmbauer | EPS-HEP Hamburg 2023 | 24/08/2023

Page 15

## Requirements for ALPS II:

- Sensitivity to very low rates (1-2 photons a day)
- Low energy photon detection (1064nm equivalent to 1.16eV)
- Long term stability ( $\sim 20$  days)
- Low background rate:  $< 7.7 \times 10^{-6}$  cps
- $\sim 1$  photon (1064nm-like) every 2 days
- High detection efficiency

# TES as Dark Matter Detector

## Current Challenges

### TES @ ALPS II Status

- Optimized infrastructure (setup, analysis) for signals at 1064 nm → **1.165 eV**
- Limited knowledge about response to other wavelengths

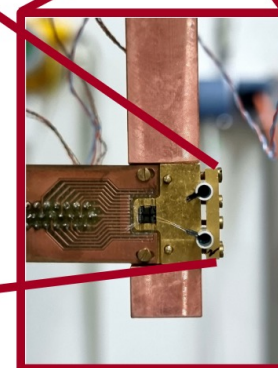
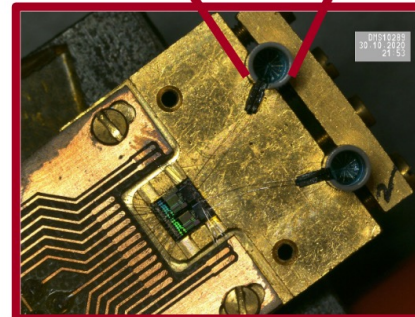
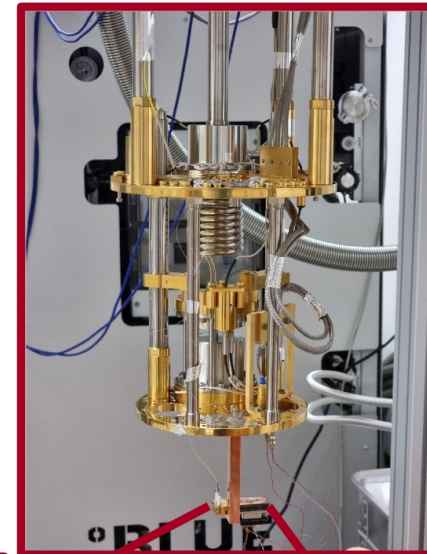
Low background (electronic noise, radioactivity, cosmic backgrounds) → currently:  $6.9 \times 10^{-6} \text{ cps}^1$  (intrinsic background for 1.165 eV signals)

### Challenge/Goal

- Determine TES response at different (lower, sub – eV) energies
- Calibration measurements currently prepared using different wavelengths (880 nm – 2000 nm)

- Further investigate intrinsic backgrounds
- Investigate alternative TES modules with lower noise background

TES chips and module provided by NIST and PTB



<sup>1</sup> R. Shah et al., PoS, EPS-HEP2021, 801 (2022)

## Résumé

- This was a very short and limited snapshot of some of the many ideas and developments on detectors.
- There are many more ideas for sensors and experiments
- Just to mention a few:
  - Kinematic Inductance Detector (KID)
  - Superconductor QUantum Interference Device (SQUID)
  - Nano-dots, nano wires, graphene.....
  - ...





